vegetation parameters cci

CCI+ Vegetation Parameters

Product Validation and Intercomparison Report (CDRP-1)

Jorge Sánchez-Zapero, Fernando Camacho, Enrique Martínez-Sánchez

September 2023

vito remote sensing | UNIVERSITY OF TWENTE. ITC | EOLAB | FastOpt | HYGEOS | Imperial College London | University of Antwerp

Distribution list

Author(s)	:	Jorge Sánchez-Zapero, Fernando Camacho, Enrique Martínez-Sánchez
Reviewer(s)	:	Else Swinnen
Approver(s)	:	Clement Albergel
Issuing authority	:	VITO

Change record

Release	Date	Pages	Description of change	Editor(s)/Reviewer(s)
V1.0	29/09/2023	All	First version	See above
V1.1	17/10/2023	Section 3.6	Addition of section 3.6 including analysis of quality layers to remove outliers.	
V1.2	26/10/2023	All	Naming of VP_CCI dataset made consistent with other documents. Editorial changes.	

Executive summary

CCI+ Vegetation Parameters is part of the ESA Climate Change Initiative. It aims at the identification, development and improvement of algorithms for the consistent retrieval of vegetation ECVs LAI and fAPAR from multi-platform and multi-mission satellite data and interact with the user community to match their requirements. The work plan includes three cycles, in which different data sources are combined, the algorithms' scientific and operational maturity is increased, and user feedback is incorporated.

The Product Validation and Intercomparison Report (PVIR) presents the quality assessment results of the CDRP-1 of VP_CCI LAI and fAPAR products, retrieved from SPOT/VGT and PROBA-V input data (2000-2020) using the OPTISAIL radiative transfer model. The dataset was generated over a latitudinal North-South transect and over a selection of sites for both product intercomparison (LANDVAL) and direct validation (DIRECT V2.1, GBOV, AMMA) purposes. The methodology is described in the product validation plan [VP-CCI_D1.3_PVP_V1.1], in agreement with the CEOS LPV best practices for validation of LAI products. Two main validation approaches are defined: direct validation (i.e., comparison of satellite products with in-situ measurements) and indirect validation (or product intercomparison). Several criteria of performance are evaluated, including completeness, spatial consistency, temporal consistency, error evaluation (Accuracy, Precision and Uncertainty) and conformity test.

This validation exercise, performed over a limited dataset (global sampling of sites and latitudinal transect), demonstrated good overall quality of VP_CCI LAI and fAPAR product. The product completeness was better than other existing reference products because of a better tolerance of OPTISAIL for thin cloud contamination in the retrieval. Reliable values and good spatial consistency are found with CGLS V2 products, except over equatorial areas and some northern regions within CRDP-1 domains. VP_CCI LAI and fAPAR temporal variations are consistent with reference products such as CGLS V2, NASA MOD15A2H C6.1 and VNP15A2H C1 and ground observations from DIRECT V2.1, GBOV V3 and AMMA. The direct validation using DIRECT V2.1, GBOV V3 and AMMA showed slightly worse accuracy and overall uncertainty than other satellite references, except in the comparison with GBOV V3 for non-forest cases where VP_CCI shows the best agreement. The comparison with satellite references shows, as expected, lower values for LAI (VP_CCI provides effective LAI whilst references are true LAI) and good agreement for FAPAR (RMSD=0.09 compared with CGLS V2 and RMSD=0.12 compared with MOD15A2H C6.1 and VNP15A2H C1). VP_CCI provides, in overall, better intra-annual precision than VNP15A2H C1 (i.e., high stability at short time scale) and worse than CGLS V2 (expected as this is a smoothed product). The inter-annual precision of VP_CCI is similar to that found for CGLS V2 and slightly better than VNP15A2H C1.

The main limitations of the VP_CCI products are:

- Stripe line artefacts and some spatial inconsistencies over northern regions (Europe, with abrupt changes showing unexpected high values) and equatorial areas (lower values), probably due to cloud/snow contamination.
- These spatial inconsistencies are related to very noisy profiles observed over EBF and some outliers not identified by the quality flag.

It should be noted that p_chisquare or RETR_LOW_QUALTY additional flags could be partly useful to identify (and filter) most of these outliers as a consequence of more restrictive screening (i.e., worse completeness). In case of χ^2, when the selected threshold turns more restrictive (i.e., greater χ^2), the outlier identification is better, but more valid data is also removed. RETR_LOW_QUALITY is also useful to identify most of the outliers, but the product completeness is considerably worse, removing a high number of useful retrievals as well.

Table of Contents

LIST OF ACRONYMS

AD	Automatic Differentation
AMMA	Analyse Multidisciplinaire de la Mousson Africaine
ANN	Artificial Neural Network
APU	Accuracy, precision, uncertainty
ATBD	Algorithm Theoretical Basis Document
B	mean Bias
BRDF	Bidirectional Reflectance Distribution Function
BRF	Bidirectional Reflectance Factor
CAL/VAL	CALibration/VALidation
CATCHA	Couplage de l'Atmosphère Tropicale et du Cycle Hydrologique
CCI	Climate Change Initiative
CDR	Climate Data Record
CDRP	Climate Data Record Package
CEOS (-LPV)	Committee on Earth Observation Satellites (Land Product Validation subgroup)
CGLS	Copernicus Global Land Service
CI	Clumping Index
CRDP	Climate Research Data Package
CUL	CULtivated
CYC	Project acronym: 'satellite products for change detection and carbon cycle assessment at the regional and global scales'
CYCLOPES	Project acronym: 'satellite products for change detection and carbon cycle assessment at the regional and global scales'
DBF	Deciduous Broadleaf Forest
DIRECT	Database of 3x3 km LAI and fAPAR data for validation
EBF	Evergreen Broadleaf Forest
EOS	Earth Observation Satellite
ESA	*European Space Agency*
ESU	*Elementary Sampling Unit*
*f*APAR	*f*raction of Absorbed Photosynthetically Active Radiation
FCOVER	Fractional Cover
FPAR	Fraction of absorbed Photosynthetically Active Radiation
GBOV	Ground-Based Observations for Validation
GCOS	Global Climate Observing System
GSD	Ground Sampling Distance
HER	HERbaceous
IER	Institut d'Economie Rurale
ILCA	International Livestock Centre for Africa
IUPAC	International Union of Pure and Applied Chemistry
JCGM	Joint Committee for Guides in Metrology
JPSS	Joint Polar Satellite System
LAI	Leaf Area Index
LANDVAL	Land validation sites
LP	Land Product
LPV	Land Product Validation

MAD	Median Absolute Deviation
MAR	Major axis regression
MD	Median Deviation
MODIS	Moderate resolution imaging spectrometer
MSI	Multi-Spectral Instrument
N	Number of samples
NASA	National Aeronautics and Space Administration
NLF	Needle-Leaf Forest
NNT	Neuronal NeTwork
OF	Other Forests
OLIVE	OnLine Validation Exercise
OLS	Ordinary Least Squares
PAR	Photosynthetically Active Radiation
PROBA-V	PRoject for On-Board Autonomy Vegetation instrument
PROSPECT	PROperties of leaf SPECTtra
PUG	Product User Guide
PVASR	Product Validation Algorithm Selection Report
PVP	Product Validation Plan
R	Correlation coefficient
RM	Reference measurement
RMSD	Root Mean Square Deviation
RTM	Radiative transfer model
SAVS	Surface Albedo Validation Sites
SBA	Sparse vegetated and Bare Areas
SCF_QC	Five level confidence score
SHR	SHRublands
SNPP	Suomi National Polar-orbiting Partnership
SPOT	Système Pour l'Observation de la Terre
STD	Standard deviation
TOC	Top Of Canopy
TSGF	Temporal Smoothing Gap Filling
VIIRS	Visible/Infrared Imager Radiometer Suite VNP
VGT	VEGATATION instrument onboard of SPOT4 & 5
VP	Validation Plan
WGCV	Working Group on Calibration and Validation
WMO	World Meteorological Organization

LIST OF FIGURES

LIST OF TABLES

1 Introduction

1.1 Scope of this document

The purpose of this document is to present the validation results of VP_CCI LAI and fAPAR products. The quality assessment is conducted over a climate data record (2000-2020) dataset (CRDP-1) retrieved from SPOT/VGT and PROBA-V input data. The validation dataset was limited to a latitudinal North-South transect and over a selection of sites for both product intercomparison (LANDVAL) and direct validation (DIRECT V2.1, GBOV, AMMA) purposes.
The validation methods and datasets are described in section 2. The validation results are presented in section 3, whilst section 3.6.2 provides the conclusions of this study.

1.2 Related documents

Internal documents

Reference ID	Document
VP-CCI_D2.1_ATBD_V1.3	Algorithm Theoretical Basis Document: fAPAR and LAI, ESA CCI+ Vegetation Parameters http://climate.esa.int/media/documents/VP-CCI_D2.1_ATBD_V1.3.pdf
VP-CCI_D4.2_PUG_V1.2	Product User Guide (PUG) CRDP-1, ESA CCI+ Vegetation Parameters http://climate.esa.int/media/documents/VP-CCI_D4.2_PUG_V1.2.pdf
VP-CCI_D2.4_PVASR_V1.1	Product Validation and Algorithm Selection Report, ESA CCI+ Vegetation Parameters http://climate.esa.int/media/documents/VP-CCI_D2.4_PVASR_V1.1.pdf
VP-CCI_D1.3_PVP_V1.1	Product Validation Plan: fAPAR and LAI, ESA CCI+ Vegetation Parameters http://climate.esa.int/media/documents/VP-CCI_D1.3_PVP_V1.1.pdf

External documents

Reference ID	Document
GCOS-200, 2016	GCOS-200 (2016). The Global Observing System for Climate: Implementation Needs. WMO, Geneva, Switzerland https://library.wmo.int/opac/doc_num.php?explnum_id=3417
JCGM, 2014	JCGM, 2014. International Vocabulary of Metrology–Basic and General Concepts and Associated Terms, Chemistry International -- Newsmagazine for International Union of Pure and Applied Chemistry (IUPAC). Walter de Gruyter GmbH. https://doi.org/10.1515/ci.2008.30.6.21
ATBD-CGLS_PBV_V2	Algorithm Theoretical Basis Document of LAI/fAPAR/FCOVER PROBA-V Collection 1km V2 in the Copernicus Global Land Service. https://land.copernicus.eu/global/sites/cgls.vito.be/files/products/CGLOPS1_ATBD_LAI1km-V2_I1.41.pdf
QAR-CGLS_PBV_V2	Quality Assessment Report of LAI/fAPAR/FCOVER PROBA-V Collection 1km V2 in the Copernicus Global Land Service. https://land.copernicus.eu/global/sites/cgls.vito.be/files/products/CGLOPS1_QAR_LAI1km-PROBAV-V2_I1.40.pdf

ATBD-VIIRS	Algorithm Theoretical Basis Document for VIIRS LAI and FPAR, VNP15 LAI/FPAR ATBD Version 1.1, 17th April 2018. https://lpdaac.usgs.gov/documents/125/VNP15_ATBD.pdf
ATBD-MOD15	MODIS leaf area index (LAI) and fraction of photosynthetically active radiation absorbed by vegetation (FPAR) product (MOD15) – Algorithm Theoretical Basis Document, Version 4.0, 30th April 1999, NASA Goddard Space Flight Center, Greenbelt, MD, 20771. https://modis.gsfc.nasa.gov/data/atbd/atbd_mod15.pdf
ATBD-GBOV-LP3-LP4-LP5	Ground-Based Observations for Validation - Algorithm Theoretical Basis Document - Vegetation Products: LP3 (LAI), LP4 (FAPAR) and LP5 (FCOVER). https://gbov.acri.fr/public/docs/products/2021-09/GBOV-ATBD-LP3-LP4-LP5_v3.0-Vegetation.pdf
CAN_EYE_UG	CAN_EYE V6.4.91 USER MANUAL. Updated October, 10th 2017. https://www6.paca.inrae.fr/can-eye/content/download/3052/30819/version/4/file/CAN_EYE_User_Manual.pdf

1.3 General definitions

Leaf Area Index (LAI) is defined as the total one-sided area of all leaves in the canopy within a defined region, and is a non-dimensional quantity, although units of [m2/m2] are often quoted, as a reminder of its meaning [GCOS-200, 2016]. The selected algorithm in the CCI-Vegetation Parameters project uses a 1-D radiative transfer model, and LAI is uncorrected for potential effects of crown clumping. Its value can be considered as an effective LAI, notably the LAI-parameter of a turbid-medium model of the canopy that would let the model have similar optical properties as the true 3-D structured canopy with true LAI (Pinty et al., 2006). Additional information about the geometrical structure may be required for this correction to obtain true LAI (Nilson, 1971), which involves the estimation of the clumping index, CI, defined as the ratio between the true and effective LAI [see (Fang, 2021) for a review of methods to estimate CI].

Fraction of Absorbed Photosynthetically Active Radiation (fAPAR) is defined as the fraction of Photosynthetically Active Radiation (PAR; solar radiation reaching the surface in the 400-700 nm spectral region) that is absorbed by a vegetation canopy [GCOS-200, 2016]. In contrast to LAI, fAPAR is not only vegetation but also illumination dependent. In the CCI-Vegetation Parameters project we refer to fAPAR as the white-sky value (i.e. assuming that all the incoming radiation is in the form of isotropic diffuse radiation). Total fAPAR is used and no differentiation is made between live leaves, dead foliage and wood.

Uncertainty is a measure to describe the statistically expected distribution of the deviation from the true value. Here, it is given as the physical value, which corresponds to the sigma-parameter of a gaussian distribution.

Accuracy is the degree of the “closeness of the agreement between the result of a measurement and a true value of the measurand” [JCGM, 2014]. Commonly, accuracy represents systematic errors and often is computed as the statistical mean bias, i.e., the difference between the short-term average measured value of a variable and the true value. The short-term average is the average of a sufficient number of successive measurements of the variable under identical conditions, such that the random error is negligible relative to the systematic error. The latter can be introduced by instrument biases or through the choice of remote sensing retrieval schemes [GCOS-200, 2016].

Precision or repeatability is the “closeness of the agreement between the results of successive measurements of the same measurand carried out under the same conditions of measurement” [JCGM, 2014].

Uncertainty is a “parameter, associated with the result of a measurement that characterizes the dispersion of the values that could reasonably be attributed to the measurand” [JCGM, 2014]. Uncertainty includes systematic and random errors.

2 Validation methodology

2.1 Overall validation procedure

The validation procedure, described in the product validation plan [VP-CCI_D1.3_PVP_V1.1], was defined to be consistent with the CEOS LPV LAI validation protocol (Fernandes et al., 2014), which is also suitable for fAPAR products. This protocol was developed thanks to precursor studies on the validation of LAI (Camacho et al., 2013; Fang et al., 2012; Garrigues et al., 2008; Weiss et al., 2007) and the On Line Validation Exercise (OLIVE) tool (Weiss et al., 2014) hosted by CEOS CAL/VAL portal (http://calvalportal.ceos.org/web/olive). Besides, recommendations of the Global Land Service reviewers have been included to complement the CEOS LPV LAI validation protocol. The proposed methodology relies on direct validation and product intercomparison approaches.

- The direct validation is computed against ground data set (DIRECT V2.1) up-scaled according to the CEOS LPV recommendations (Fernandes et al., 2014; Morisette et al., 2006). The confidence in the reference ground-based map derived from empirical transfer functions depends on performances of the transfer functions that should be quantified with appropriate uncertainty metrics. Other existing datasets, such as GBOV and AMMA are used, providing multi-temporal valuable information.
- Intercomparisons with similar remote sensing products (i.e., indirect validation) can determine whether the products behave similarly in space and time on a global scale and allow us to identify differences between products to be investigated in more detail in order to diagnose product anomalies and devise algorithm refinements. The LAND VALidation (LANDVAL) network of sites (Fuster et al., 2020; Sánchez-Zapero et al., 2023, 2020) is used for sampling global conditions in the intercomparison with similar satellite products. The LANDVAL network is composed of 720 sites, of which 521 sites are from Surface Albedo Validation Sites (SAVS 1.0) (Loew et al., 2016). The LANDVAL sampling is complemented with 20 desert calibration sites (Lacherade et al., 2013) and additional sites in order to cover under-sampled regions and biome types. To allow comparison between the products, the same temporal and spatial supports are used. These analyses are achieved per aggregated land cover class based on the 8 generic classes: Evergreen Broadleaf Forest (EBF, 9.6% of LANDVAL sites), Deciduous Broadleaf Forest (DBF, 7.5%), Needle-Leaf Forest (NLF, 11.3%), Other Forests (OF, 8.8%), Cultivated (19.5%), Herbaceous (21.3%), Shrublands (8.2%) and Sparse and Bare areas (SBA, 13.8%).

The following criteria are analysed: product completeness, spatial consistency, temporal consistency and error evaluation, which involves Accuracy, Precision and Uncertainty (APU). In addition, the conformity test matching the GCOS uncertainty requirements is also performed.

2.1.1 Product Completeness

Completeness corresponds to the absence of spatial and temporal gaps in the data. Missing data are mainly due to cloud or snow contamination, poor atmospheric conditions or technical problems during the acquisition of the images and is generally considered by users as a severe limitation of a given product. It is therefore mandatory to document the completeness of the product (i.e., the distribution in space and time of missing data).

- Global maps of missing values for the period under study are displayed.
- Distribution of gaps as a function of the season is also analysed.

2.1.2 Spatial consistency

Spatial consistency refers to the realism and repeatability of the spatial distribution of retrievals over the globe.

A first qualitative check of the realism and repeatability of spatial distribution of retrievals and the absence of strange patterns or artefacts (e.g., missing values, stripes, unrealistic low values, etc.) can be achieved through systematic visual analysis of all global maps based on the expert knowledge of the scientist.

The spatial consistency can be quantitatively assessed by comparing the spatial distribution of a reference validated product with the product biophysical maps under study. Two products are considered spatially consistent when the residuals are within uncertainty requirements of the variable. The residual (ε) is estimated assuming a linear trend between two products ($Y = a X + b + \varepsilon$), then the residual can be written as $\varepsilon = Y - a X - b$, which represent the remaining discrepancies regarding the general trend between both products. In this way, systematic trends are not considered, depicting more clearly patterns associated to the spatial distribution of retrievals.

- The methodology for visual analysis includes the visualization of zoom over sub-continental areas, selected tiles or areas of interest at full resolution, and the visualization of animations of global maps at a reduced (1/4 pixels) resolution.
- Global maps (over the whole transect) and histograms of residuals, at a reduced (1/4 pixels) resolution, between the product under study and reference products are analysed in order to identify regions showing spatial inconsistencies for further analysis (e.g., temporal profiles).

2.1.3 Temporal consistency

The realism of the temporal variations and the precision of the products were assessed over the 720-site LANDVAL network plus additional sites with availability of ground measurements (i.e., DIRECT V2.1, GBOV V3, AMMA).

- The temporal variations of the product under study are qualitatively analysed as compared to reference products and available ground measurements.

2.1.4 Error evaluation

Accuracy, Precision and Uncertainty (APU) are evaluated by several metrics (Table 1) reporting the goodness of fit between the products and the corresponding reference dataset.

Commonly, accuracy represents systematic errors and often is computed as the statistical mean bias (B). Precision represents the dispersion of product retrievals around their expected value and can be estimated by the standard deviation (STD) of the difference between retrieved satellite product and the corresponding reference estimates. Uncertainty includes systematic and random errors and can be estimated by the Root Mean Square Deviation (RMSD). In addition to these metrics, other statistics are useful to evaluate the goodness of fit between two datasets including linear model fits. For this purpose, Major Axis Regression (MAR) is computed instead of Ordinary Least Squares (OLS) because it is specifically formulated to handle error in both of the x and y variables (Harper, 2014). In case of LAI, CEOS LPV recommends RMSD as the overall performance statistic to evaluate the accuracy, due to limitation in the temporal availability of ground datasets (Fernandes et al., 2014). It should be noted that strong and/or multiple outliers affect the classical metrics described above (i.e. B and STD): in such cases using the median deviation (MD) instead of the mean bias to estimate systematic error and the median absolute deviation (MAD) as a measure of precision is more suitable.

Note that two aspects of the precision should be also evaluated: inter-annual and intra-annual precision (Fernandes et al., 2014).

- Scatterplots and validation metrics (Table 2) versus references are produced.
- Histograms of product values per main biome type are evaluated over LANDVAL sites. The analysis is complemented with violin plots of Bias per biome.

- **Intra-annual precision** (smoothness) corresponds to temporal noise assumed to have no serial correlation within a season. In this case, the anomaly of a variable from the linear estimate based on its neighbours can be used as an indication of intra-annual precision. It can be characterized (Weiss et al., 2007) as follows: for each triplet of consecutive observations, the absolute value of the difference between the center P(dn+1) and the corresponding linear interpolation between the two extremes P(dn) and P(dn+2) is computed:

$$\delta = \left| P(d_{n+1}) - P(d_n) - \frac{P(d_n) - P(d_{n+2})}{d_n - d_{n+2}} (d_n - d_{n+1}) \right| \quad \text{Eq. 1}$$

  The distribution of the intra-annual precision is analysed, and the median δ value is used as a quantitative indicator of the inter-annual precision (Fernandes et al., 2014; Wang et al., 2019). Hence, the lower median of δ values, the higher the inter-annual precision.
- Anomalies of an upper and lower percentile of variable are indicators of **inter-annual precision**, i.e. ,dispersion of variable values from year to year (Fernandes et al., 2014). It can be assessed providing a box-plot of anomalies for a given product between consecutive years per bins, and its median values. Note that cultivated sites are not considered in this analysis due to the non-natural variability in this land cover type due to agricultural practices (e.g., crop rotation). In addition, Evergreen Broadleaf Forest sites are neither considered in the analysis since they are typically affected by cloud coverage for most of the products, and values are filled in case of products using gap-filling techniques.

Table 1: Validation metrics for product validation

Statistics	Comment
N	Number of samples. Indicative of the power of the validation
B	Mean Bias. Difference between average values of x and y. Indicative of accuracy and offset.
MD	Median deviation between x and y. Best practice reporting the accuracy.
STD	Standard deviation of the pair differences. Indicates precision.
MAD	Median absolute deviation between x and y. Best practice reporting the precision.
RMSD	Root Mean Square Deviation. RMSD is the square root of the average of squared errors between x and y.
MAR	Slope and offset of the Major Axis Regression linear fit. Indicates some possible bias
R	Correlation coefficient. Indicates descriptive power of the linear accuracy test. Pearson coefficient is used.

2.1.5 Summary of validation procedure

Table 2 summarizes the validation criteria used for the quality assessment of the products under study.

It should be noted that the validation is mainly focused on 2012-2015 period as it covers the transition SPOT/VGT to PROBA-V. In case of VP_CCI, SPOT/VGT input data is used until 13th October 2013, both SPOT/VGT and PROBA-V data sources are used from mid-October 2013 to early June 2014, and PROBA-V is used from early June 2014 onwards. The period is extended to the whole climate data record (2000-2020) for some analysis (spatial consistency, direct validation). The algorithm selection exercise [VP-CCI_D2.4_PVASR_V1.] demonstrated almost identical validation results for SPOT/VGT and PROBA-V periods.

Table 2: Summary of validation methodology of VP_CCI product.

Quality Criteria	Reference	Coverage /period	Results
Product completeness	CGLS V2 (non-filled) VNP15A2H C1	LANDVAL /2012-2015	- Distribution of gaps (maps, temporal variations).
Spatial consistency	Expert knowledge	TRANSECT /2000-2020	-Visual inspection of maps
	CGLS V2	TRANSECT /2012-2015	-Distribution of residuals.
Temporal consistency	CGLS V2 VNP15A2H C1	LANDVAL /2012-2015	-Qualitative inspection of temporal variations.
	DIRECT V2.1 CGLS V2 MOD15A2H C6.1	DIRECT SITES /2000-2020	-Qualitative inspection of the realism of the temporal variations.
	GBOV V3 CGLS V2 VNP15A2H C1	GBOV SITES /2013-2020	-Qualitative inspection of the realism of the temporal variations.
	AMMA CGLS V2 MOD15A2H C6.1	AMMA SITES /2005-2016	-Qualitative inspection of the realism of the temporal variations.
Error evaluation (direct validation)	DIRECT V2.1	DIRECT SITES /2000-2020	- Scatterplots and validation metrics. Conformity test. -Analysis for CGLS V2 & MOD15A2H C6.1 for benchmarking
	GBOV V3	GBOV SITES /2013-2020	- Scatterplots and validation metrics. Conformity test. Analysis per biome types. -Analysis for CGLS V2 & VNP15A2H C1for benchmarking
	AMMA	AMMA SITES /2005-2016	- Scatterplots and validation metrics. Conformity test. -Analysis for CGLS V2 & MOD15A2H C6.1 for benchmarking
Error evaluation (product intercomparison)	CGLS V2 VNP15A2H C1 MOD15A2H C6.1	LANDVAL /2012-2015	- Overall scatterplots and validation metrics. Conformity test. - Analysis per biome type: PDFs of retrievals, violin plots of bias, scatterplots and validation metrics. -Intra-annual precision (Histograms of the smoothness. Median δ values). -Inter-annual precision (median absolute anomaly of 95th percentile and 5th percentile).

Satellite products must be compared over a similar spatial support area and temporal support period. To allow comparison between the products in case of the error evaluation, the same temporal (10-days, using the closest date) and spatial (3km^2, i. e., 3x3 pixels in case of CGLS and CCI products and 6x6 pixels in case of MOD15A2H C6.1 and VNP15A2H C1) supports are used. Reference NASA products (e.g., MOD15A2H C6.1 and VNP15A2H C1) are re-sampled on the Plate Carrée projection over 1/112^o which is the CCI and CGLS grid.

2.2 Satellite products

This section provides an overview of the retrieval algorithms of the satellite products used in this exercise. Table 3 summarizes the quality flag information of the different products which is used to discard pixels flagged as low quality, out of range or invalid.

Table 3: Summary of quality flags used to remove pixels with suboptimal quality of each satellite product.

Product	Quality Flag (LSB = bit 0)
CCI VP_CCI	Bit 8 (RETR_UNTRUSTED) of invcode
CGLS Collection 1km V2	Bit 0 (Land/Sea: Sea) Bit 5 (Input status: All reflectance data out of range or invalid) Bits 6,7,8 (LAI/FAPAR/FCover status: Out of range) (*) Bit 2 (Filled: filled) (*) Only used in product completeness quality criteria.
NASA MOD15A2H C6.1	Bits 5,6,7 of FparLai_QC, which correspond to SCF_QC or five-level confidence score: -2 Main (RT) method failed due to bad geometry, empirical algorithm used. -3 Main (RT) method failed due to problems other than level 2. -4 Pixel not produced at all, value could not be retrieved).
NASA VNP15A2H C1	Bits 0,1,2 of FparLai_QC, which correspond to SCF_QC or five-level confidence score: -2 Main (RT) method failed due to bad geometry, empirical algorithm used -3 Main (RT) method failed due to problems other level 2. -4 Pixel not produced at all, value could not be retrieved).

2.2.1 Evaluated dataset: VP_CCI

VP_CCI LAI and fAPAR products were derived based on OPTISAIL radiative transfer model [VP-CCI_D2.1_ATBD_V1.]. OPTISAIL is an optimisation framework built around the models SAIL4H (Verhoef et al., 2007), PROSPECT-D (Féret et al., 2017), TARTES (Skiles and Painter, 2019), an empirical soil model with a semi-empirical moisture effect, and a cloud contamination model. They directly simulate Top Of Canopy (TOC) reflectances for given sets of spectrally invariant parameters (e.g., LAI, leaf pigments etc.) and scene geometries at given bands. In order to retrieve these parameters for observed TOC reflectance data, an inversion is made for each pixel. During cycle 1 of this project, repeatedly cloud-contaminated data was encountered, which was not flagged as such. Therefore, the cloud contamination model of OptiSAIL was activated, which simulates the effect of variable amounts of thin clouds per observation. This significantly reduces the number of outlier retrievals. The inversion in OptiSAIL minimises a cost function with data and prior term. It uses gradient information which is efficiently provided by adjoint code of the models. These adjoint codes are obtained by Automatic Differentiation (AD), which allows for quick adaption of the whole system to changes in the models. OptiSAIL includes an algorithm to model the effects of residual cloud contamination after atmospheric correction; this option has been used. The model is described with further references and demonstrated (Blessing and Giering, 2021). All outputs for the CRDP-1 are on the same 1 km regular lat-lon grid as the TOC reflectance data used for input [VP-CCI_D4.2_PUG_V1.].

The product validation is performed over a subset of the climate data record (2000-2020 period) based on SPOT/VGT and PROBA-V (CRDP-1). The validation dataset was generated over a globally distributed selection of sites and a latitudinal transect (see Figure 1) distributed as 10^o x 10^o tiles plus one additional European site. Figure 1 illustrates the sampling strategy for the validation. It consists in two approaches:

- A selection of sites for product intercomparison (LANDVAL) and direct validation (DIRECT V2.1, GBOV, AMMA).
- A latitudinal transect for the evaluation of the spatial consistency and qualitative visual inspection of the reliability of the products. It should be noted that the latitudinal transect used for validation is half (10º longitude) than the transect provided in the CDRP-1 (20º longitude) (see PUG [VP-CCI_D4.2_PUG_V1.]).

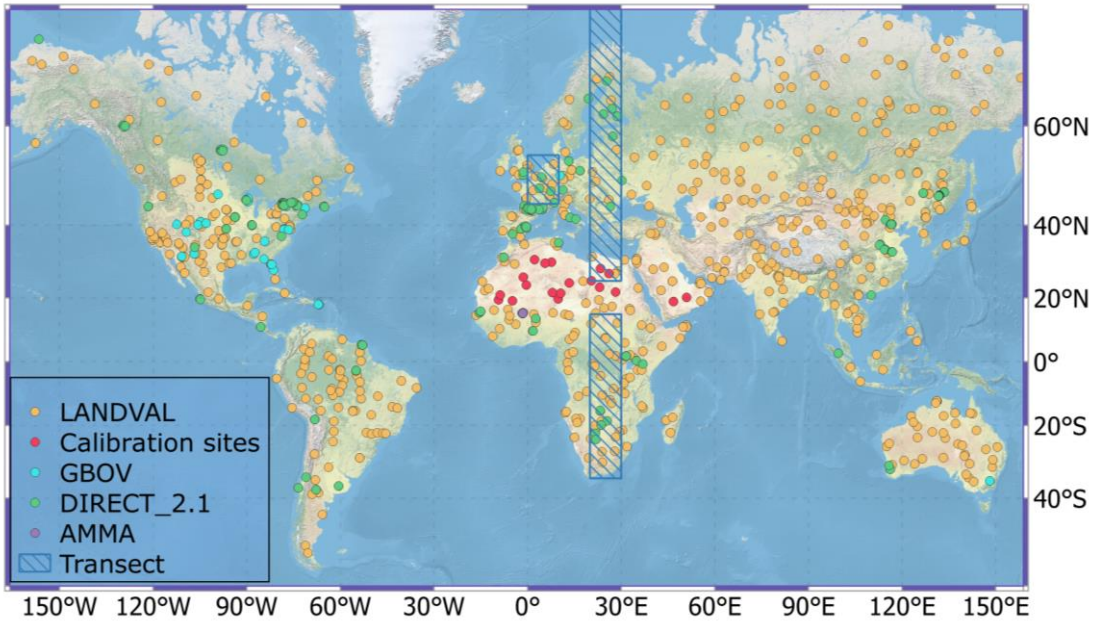

Figure 1: Validation sampling strategy: A) selected sites from LANDVAL, Calibration Sites, GBOV, DIRECT_2.1 and AMMA. B) Latitudinal Transect (see blue rectangles)

The tile products include the layers listed in Table 4. The site products contain the same thematic products as the tile products and additional layers (see PUG [VP-CCI_D4.2_PUG_V1.] for more details).

Table 4: Thematic products included in the tile and site dataset (8 layers).

Parameter	Meaning
LAI	SAIL effective Leaf Area Index
fAPAR	fraction of Absorbed Photosynthetically Active Radiation using diffuse ASTM-G0173
LAI_ERR	LAI standard error
fAPAR_ERR	fAPAR standard error
LAI_fAPAR_correl	LAI fAPAR standard correlation
n_bands_used	number of bands used
p_chisquare	Probability of Chi-square statistics; low values mark bad correspondence of model and data
Invcode	Inversion code

2.2.2 Reference satellite products

Different satellite products from different services (CGLS, NASA) are used for product intercomparison with VP_CCI fAPAR and LAI products. It should be noted that reference satellite products provide actual LAI products whereas VP_CCI provides effective LAI retrievals. Table 5 summarizes the main characteristics of existing LAI and fAPAR products.

Table 5: Characteristics of the existing LAI/FAPAR global remote sensing reference products. ANN and RTM stands for "Artificial Neural Network", and "Radiative Transfer Model", respectively. GSD stands for "Ground Sampling Distance"

Product	Satellite /Sensor	GSD	Frequency /compositing	Temporal availability	Algorithm	Clumping	Reference
CGLS Collection 1km V2	SPOT/VGT PROBA/VGT	1 km	10 days /variable	1999-2014 2014-2020	ANN trained with CYC and MOD + gap filling & smoothing	Weighted of CYC and MOD	(Verger et al., 2023) [ATBD-CGLS_PBV_V2]
NASA MOD15A2H C6.1	TERRA /MODIS	500 m	8 days /8 days	2000-present	Inversion RTM 3D	Plant, canopy & landscape	(Knyazikhin et al., 1998) [ATBD-MOD15]
NASA VNP15A2H C1	SNPP /VIIRS	500 m	8 days /8 days	2012-present	Inversion RTM 3D	Plant, canopy & landscape	(Knyazikhin et al., 1998) [ATBD-VIIRS]

2.2.2.1 CGLS Collection 1km V2

The retrieval algorithm (Verger et al., 2023) [ATBD-CGLS_PBV_V2] was initially defined for the estimation of LAI, FAPAR (and FCOVER) from the VEGETATION series of observations and was also applied to daily top-of-canopy reflectance provided by the PROBA-V sensor. As the neural network (NNT) algorithm was trained with SPOT/VGT observations, two specific adaptations are applied to achieve good consistency when applied to PROBA-V data. First, a spectral conversion is applied on the actual PROBA-V TOC reflectances to get SPOT/VGT-like TOC reflectances values. Second, PROBA-V NNT outputs are rescaled with regard to SPOT/VGT NNT output using a polynomial function fitted over BELMANIP2.1 sites. The CGLS V2 algorithm aims providing improved products as compared to CGLS V1 (Baret et al., 2013), although derived from the same sensors observations, with smoother retrievals and no missing values. CGLS V2 products have the same temporal sampling frequency of 10 days as CGLS V1. Similarly to CGLS V1, CGLS V2 capitalizes on the development and validation of already existing products: Carbon cYcle and Change in Land Observational Products from an Ensemble of Satellites (CYCLOPES) version 3.1 and MODIS collection 5, and the use of neural networks (Baret et al., 2013; Verger et al., 2008). The basic underlying assumption is that a strong link exists between VEGETATION observations and the fused product resulting from CYCLOPES and MODIS products. Products are associated with quality assessment flags as well as quantified uncertainties.

The algorithm starts from the daily PROBA-V top-of-canopy reflectance products. The output is the instantaneous first guess of the three variables. Then, a temporal smoothing and gap filling (TSGF) method is applied, using several techniques including the Savitzky-Golay filter, a climatology (Verger et al., 2013) or interpolation methods to smooth the time profile and fill the gaps.

The CGLS PROBA-V Collection 1 km V2 products were validated over the period October 2013–October 2014 [QAR-CGLS_PBV_V2], and the quality stability was systematically checked every year. The reports are available on the CGLS website (https://land.copernicus.eu/global/products/lai). The products displayed better spatial coverage (no gaps) and smoother profiles than CGLS V1 and MODIS C5 products. Specifically, over evergreen broadleaf forests, the CGLS V2 presented smooth trajectories with high values and very limited seasonality while the CGLS V1 showed unexpectedly low LAI and fAPAR values and seasonality and noise due to permanent clouds. The accuracy assessment over a limited number of concomitant ground-based measurements (<15) showed RMSD values of 0.79 and 0.12 for LAI and fAPAR, respectively.

More recently, the quality of CGLS V2 was assessed with due attention to consistency and improvements with CGLS V1 (Verger et al., 2023). CGLS V2 products are consistent with V1 at the global scale and meet CGLS and GCOS uncertainty requirements in 90% of cases for LAI, and 80% for fAPAR. CGLS V2 showed a similar accuracy as CGLS V1 for LAI and slight improvements for fAPAR as

evaluated over the limited ground measurements available (DIRECT V2). In addition, CGLS V2 highly improves V1 in terms of product completeness and does not show any missing data thanks to climatological gap filling that ensures product retrieval even when scarce or no observation are available during a long period. CGLS V2 and V1 time series showed high temporal consistency in most of the situations. V2 corrects the inconsistencies identified in V1 at very high Northern latitudes (artefacts introduced by the Bidirectional Reflectance Distribution Function (BRDF) model in extreme illumination conditions) and for evergreen broadleaf forest (noise and discontinuities in V1 due to cloud cover). Additionally, V2 improves both the inter- and intra-annual precision.

2.2.2.2 NASA MOD15A2H C6.1

TERRA MODIS C6.1 LAI and fAPAR products (MOD15A2H) are available at a spatial resolution of 500 m over a sinusoidal grid and a step of eight days since 2000 at https://ladsweb.modaps.eosdis.nasa.gov.

The algorithm retrieves LAI and FAPAR values given sun and view directions, Bidirectional Reflectance Factor (BRF) for each spectral band, uncertainties (i.e., relative stabilized precision, (Wang et al., 2001)) in input BRFs, and land cover classes based on an 8-biome classification map (Myneni et al., 2002; Yang et al., 2006). The operational LAI/fAPAR algorithm consists of a main algorithm that is based on 3D radiative transfer equation and a backup algorithm. By describing the photon transfer process, this algorithm links surface spectral BRFs to both structural and spectral parameters of the vegetation canopy and soil (Asrar and Myneni, 1991; Ross, 1981). Given atmosphere corrected BRFs and their uncertainties, the algorithm finds candidates of LAI and fAPAR by comparing observed and modeled BRFs that are stored in biome type specific Look-Up-Tables. All canopy/soil patterns for which observed and modeled BRFs differ within biome-specified thresholds of uncertainties (e.g., 30% and 15% for red and near-infrared bands, respectively, for forest biomes) are considered candidate solutions and the mean values of LAI and fAPAR from these solutions are reported as outputs. The mean and dispersion of LAI/fAPAR candidates are reported as retrieval and its reliability, respectively. The law of energy conservation (reflectance, transmittance and absorbance sum up to unity) and the theory of spectral invariance are two important features of this main algorithm [ATBD-MOD15].

The main algorithm may fail to localize a solution if uncertainties of input BRFs are larger than threshold values or due to deficiencies of the RT model that result in incorrect simulated BRFs. In such cases, a backup empirical method based on relations between NDVI and LAI/fAPAR (Knyazikhin et al., 1998; Myneni and Williams, 1994) is utilized to output LAI/fAPAR with relatively poor quality (called the backup algorithm). It should be noted that pixels computed by this backup solution are discarded from the analysis.

The consistency between of previous collections C5 and C6 was analysed (Nestola et al., 2017; Yan et al., 2016a) without finding spatial differences due to resolution changes with an RMSD between both versions of 0.091 for fAPAR (Yan et al., 2016a). The accuracy assessment performed over 45 fAPAR ground measurements showed an overestimation of both C5 and C6 fAPAR products over sparsely vegetated areas (Yan et al., 2016b). Comparisons with SPOT/VGT Collection 1km V1 products showed similar spatial distributions at a global scale (Yan et al., 2016b), and temporal comparisons for the 2001–2004 period showed that the products properly captured the seasonality of different biomes, except in evergreen broadleaf forests.

The improvements of C6.1 respect to C6 are:

- The Version 6.1 Level-1B products have been improved by undergoing various calibration changes that include: changes to the response-versus-scan angle approach that affects reflectance bands for Aqua and Terra MODIS, corrections to adjust for the optical crosstalk in Terra MODIS infrared bands, and corrections to the Terra MODIS forward look-up table update for the period 2012 - 2017.
- A polarization correction has been applied to the L1B Reflective Solar Bands.

2.2.2.3 NASA VNP15A2H C1

As Terra and Aqua MODIS sensors will likely be terminated (Terra and Aqua MODIS have far exceeded their design life, 6 years, and have a strong chance of operating successfully into the early 2020s), the Visible/Infrared Imager Radiometer Suite (VIIRS) instrument onboard the Suomi National Polar-orbiting Partnership (SNPP) and Joint Polar Satellite System (JPSS) has inherited the scientific roles of MODIS (Justice et al., 2013). The first VIIRS sensor onboard the SNPP platform was successfully launched in October 2011. In this context, the NASA SNPP VIIRS LAI/fAPAR product (https://viirsland.gsfc.nasa.gov/Products/NASA/LAI_FparESDR.html) (VNP15) should ensure the continuity with the MODIS LAI/fAPAR product (MxD15). The VIIRS LAI/fAPAR algorithm [ATBD-VIIRS] has benefitted from the heritage of the MODIS operational algorithm.
The validation approach for VIIRS LAI/fAPAR is similar to that of MODIS Collection 6. The VIIRS subsets and the Earth Observation Satellite (EOS) Core Validation Sites as well as the BELMANIP2 sites are used to achieve the goal of CEOS level 2 validation stage. LAI and fAPAR retrievals from VIIRS and MODIS were found consistent at different spatial (i.e., global and site) and temporal (i.e., 8-day, seasonal and annual) scales (Xu et al., 2018; Yan et al., 2018), with mean discrepancies (mean differences of −0.006 ± 0.013 for LAI and −0.002 ± 0.002 for fAPAR) meeting the stability requirement for long-term LAI/fAPAR Earth System Data Records from multi-sensors as suggested by the GCOS. Relative uncertainties (RMSD) of VIIRS LAI and fAPAR products, assessed through comparisons to ground measurements, of 0.60 (42.2%) and 0.10 (24.4%), respectively were reported (Xu et al., 2018). Comparison of VIIRS LAI/fAPAR (VNP15A2H) versus GBOV ground data over North America sites (Brown et al., 2020) showed similar performance than MODIS Collection 6 (MOD15A2H), with RMSD = 0.81 to 0.89 for LAI, and RMSD = 0.12 for fAPAR.

2.3 Reference ground datasets

2.3.1 CEOS WGCV LPV DIRECT V2.1

Ground references of high quality are needed to validate satellite-based products. The DIRECT V2.1 database hosted at the CEOS cal/val portal (https://calvalportal.ceos.org/lpv-direct-v2.1) compiles LAI and fAPAR averaged values over a 3 km x 3 km area. The ground data was upscaled using high spatial resolution imagery following CEOS WGCV LPV LAI good practices to properly account for the spatial heterogeneity of the site. Ground measurements including in the first version (DIRECT) were resulting from several international activities including VALERI, BigFoot, SAFARI-2000, CCRS, Boston University and ESA campaigns compiled by S. Garrigues (Garrigues et al., 2008), and later ingested in the CEOS WGCV LPV OLIVE tool (Weiss et al., 2014) for accuracy assessment. F. Camacho reviewed DIRECT to remove those sites without understory measurements (Camacho et al., 2013) and after that expanded the database with ImagineS sites (Camacho et al., 2021). DIRECT V2.1 is the last update including 44 new sites from China (Fang et al., 2019; Song et al., 2021) and 2 sites from ESA FRM4Veg (Brown et al., 2021a).

The CEOS WGCV LPV DIRECT V2.1 database constitutes a major effort of the international community to provide ground reference for the validation of LAI and FAPAR ECVs, with a total of 176 sites around the world (7 main biome types) and 280 LAI values, 128 FAPAR and 122 FCOVER values covering the period from 2000 to 2021.

2.3.2 The Ground-Based Observations for Validation (GBOV)

As part of the Copernicus Global Land Service, the Ground-Based Observations for Validation (GBOV) service (https://land.copernicus.eu/global/gbov) aims at facilitating the use of observations from operational ground-based monitoring networks and their comparison to Earth Observation products. In case of LAI and FAPAR, the GBOV service performs the implementation and maintenance of a database for the distribution of Reference Measurements (RMs) and the corresponding Land Products (LPs) (i.e., upscaled maps). Currently, GBOV provides multi-temporal Land Products over 27 sites.
The current version (V3) of GBOV LP algorithm [ATBD-GBOV-LP3-LP4-LP5] takes as input the Reference Measurements (RMs) collected over a given site, in addition to a series of high spatial resolution images. Calibration functions are then derived between RM and Radiative Transfer Model (RTM)-based (PROSAIL) retrievals, enabling high spatial resolution maps of each RM to be produced.
The use of calibrated RTM-based retrievals (GBOV V3) as opposed to vegetation index-based multi temporal transfer functions in previous version (GBOV V2) enables the impact of non-canopy factors that perturb the vegetation index-biophysical variable relationship to be reduced. For example, as viewing and illumination angles are an explicit input, seasonal variations in sun-sensor geometry can be better accounted for, whilst the variety of soil spectra used in the RTM simulations helps reduce the impact of the soil background (Brown et al., 2021b). To maintain computational efficiency, a hybrid method using artificial neural networks (ANNs) trained with RTM simulations was selected as opposed to a pure inversion approach.
As a summary, the main changes of V3 algorithm respect to V2 are:

- A new upscaling method has been implemented, using an RTM-based retrieval approach as opposed to vegetation index-based multitemporal transfer functions. In the new method, RMs are used to establish calibration functions, which enable biases in the raw RTM-based retrievals to be corrected for (Brown et al., 2020);
- A footprint matching procedure has been implemented in which RMs are related to the mean of a variable window of Landsat Operational Land Imager (OLI)/Sentinel-2 Multi-Spectral Instrument (MSI) pixels, whose size depends on the Elementary Sampling Unit (ESU) measurement footprint at the site in question (Brown et al., 2020);
- To improve temporal consistency, the constraint for relating RMs to high spatial resolution imagery has been reduced from ± 7 days to ± 1 day (Brown et al., 2021b);
- In the case of LAI LPs (i.e., LP3), RMs (i.e., RM7) derived according to Wilson approach (Wilson, 1963) is now adopted, as it has been shown to provide more stable estimates under canopies with different leaf angle distributions when compared to Miller's (Miller, 1967) integral (Leblanc and Fournier, 2014).

A limitation of this dataset is that the calibration is not performed per site, therefore over forest sites with different level of clumping a bias is expected by using a generic calibration function. The use of PROSAIL model in the RTM-based retrieval approach should favour satellite products based on 1-D RTM models. Furthermore, there is a limitation for sparse canopies where large fraction of missing values is observed in GBOV LP.

2.3.3 AMMA – Cycle Atmosphérique et Cycle Hydrologique (CATCH) system

AMMA – Cycle Atmosphérique et Cycle Hydrologique (CATCH) observing system has collected a data set composed of LAI, fAPAR and clumping index in the Sahelian rangelands of *Gourma* region in Mali over the 2005-2017 period. Currently, the dataset is available only for the 2005-2016 period.
The measures were carried out at the sites previously installed in 1984 and monitored till 1994 by the International Livestock Centre for Africa (ILCA) and by the *Institut d'Economie Rurale* (IER, Bamako) (Hiernaux et al., 2009a, 2009b), and reactivated by the AMMA–CATCH observing system during the AMMA project (Redelsperger et al., 2006). These 1 km x 1 km sites were chosen within large and

relatively homogeneous areas to sample the main vegetation types and canopies encountered within the super-site.

The variables were derived from the acquisition and the processing of hemispherical photographs taken along 1 km linear sampling transects for four herbaceous canopies and one millet field. Also, an inundated forest site was measured but it was limited to 0.5 km due to the difficulties associated with the field work in such an environment. At each sampling date, 100 or 50 hemispherical photographs were acquired at 1 km for herbaceous or 0.5 km for forest sites, respectively, that means a picture taken every 10 m. At the forest site, photographs were acquired both in the upward and downward directions to sample the forest canopy and the herbaceous understory. When the forest floor was inundated, only the herbaceous vegetation component above the water surface was considered.

The collected hemispherical pictures were analysed using the image processing software CAN-EYE V [CAN_EYE_UG] and the estimated mean vegetation variables at the 1 km scale were computed by averaging all the 100 or 50 measurements acquired along the sampling transect for the herbaceous and forest canopy, respectively.

Generally, hemispherical photographs were taken approximately every 10 days during the growing seasons for the herbaceous canopies, whereas at the *Kelma* forest site, the monitoring took place approximately every 10 days during the leafy period, i.e., from July to January, and every month during the dry season.

3 Results

3.1 Product completeness

Figure 2 shows the temporal evolution of missing values of VP_CCI (green), CGLS V2 (pink and purple for SPOT/VGT and PROBA-V) and VNP15A2H C1 for 2012-2015 period. It should be noted that, as CGLS V2 are gap-filled products (i.e., no gaps), only those CGLS V2 pixels non gap-filled according to its quality flag were used in this computation.

The maps of the percentage of missing values over LANDVAL sites are displayed in Figure 3.

The main conclusions are:

- All products show the expected temporal trend of missing data over LANDVAL sites, with higher fraction of missing data in wintertime of northern hemisphere. However, VP_CCI shows considerably lower fraction of missing data (maximum value typically around 30% in January) than CGLS V2 (maximum value around 45%) and VNP15A2H C1 (around 55%) products.
- The maps of missing values (Figure 3) shows that VP_CCI provides low percentage of missing data than CGLS V2 non-filled pixels over areas typically affected by cloud coverage (equatorial belt and northern latitudes), which could be indicative of less restrictive cloud screening approach and, in consequence, more contamination in retrieving product values. VNP15A2H C1 does not provide over desert targets as is biome (Myneni et al., 2002; Yang et al., 2006).
- When VP_CCI quality flags are used to remove pixels with suboptimal quality (see dashed green lines in Figure 2), similar missing values are found than for all pixels (continuous green lines). This is indicative of a low restrictive quality flag.

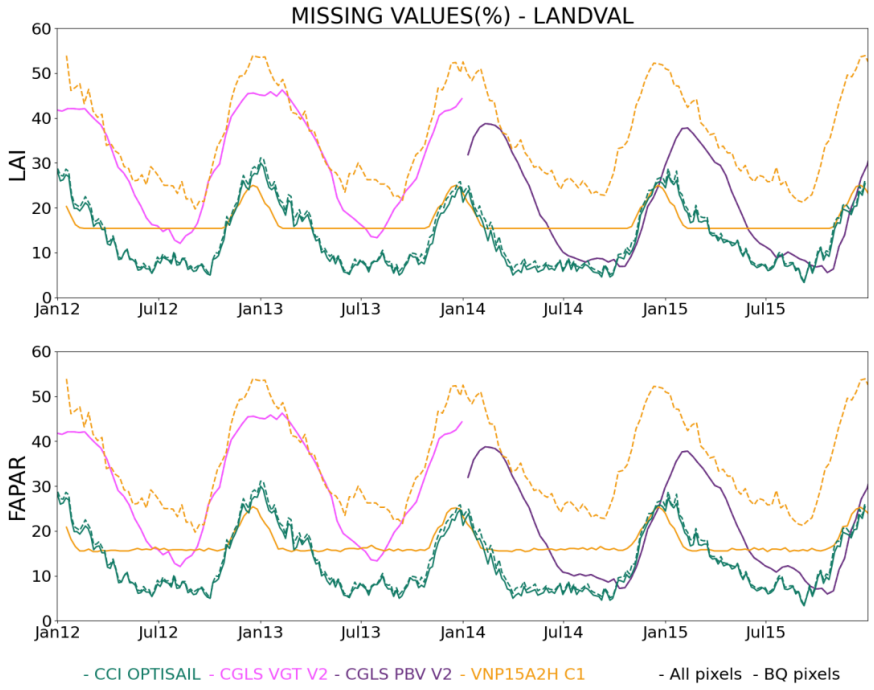

Figure 2: Temporal variation of the percentage of missing values (computed over LANDVAL sites) for VP_CCI (CCI OPTISAIL) (green), CGLS V2 non-filled (pink and purple for SPOT/VGT and PROBA-V) and VNP15A2H C1 (yellow) during 2012-2015. The computation of gaps was performed considering all pixels (continuous lines) and best quality using quality flags (dashed lines).

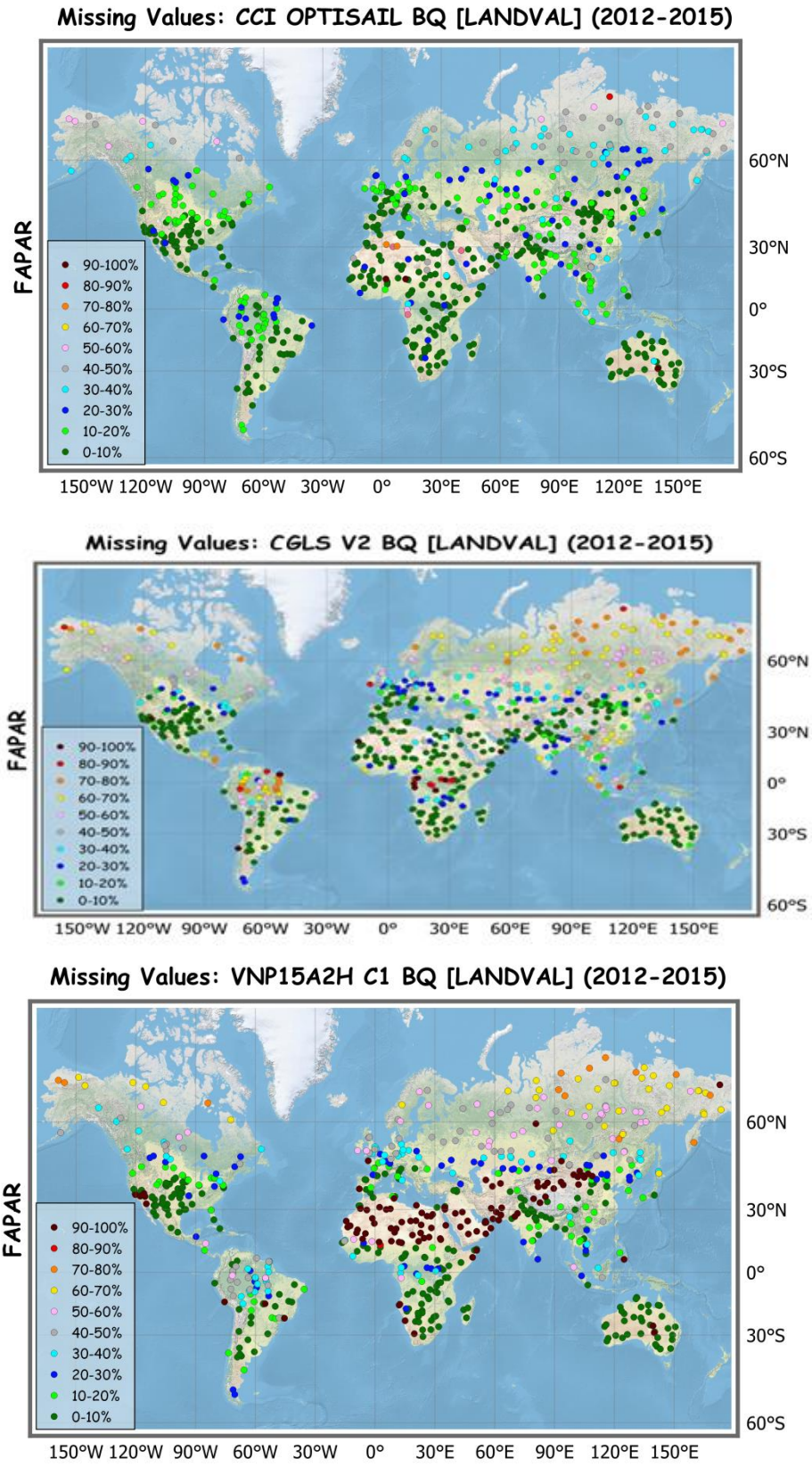

Figure 3: Maps of missing values (computed over LANDVAL sites, best quality pixels) for VP_CCI (CCI OPTISAIL) (top), CGLS V2 non-filled (middle) and VNP15A2H C1 (bottom) during 2012-2015.

3.2 Spatial consistency

3.2.1 Visual inspection of maps

The physical values of VP_CCI products are given in LAI and fAPAR layers. The spatial consistency was visually checked a with animations over the validation transect plus one European tile for the two variables. Figure 4 and Figure 5 show some examples of the global distributions of LAI and fAPAR for 2015 (based on PROBA-V) and 2012 (based on SPOT/VGT) year at 3 months of temporal frequency.

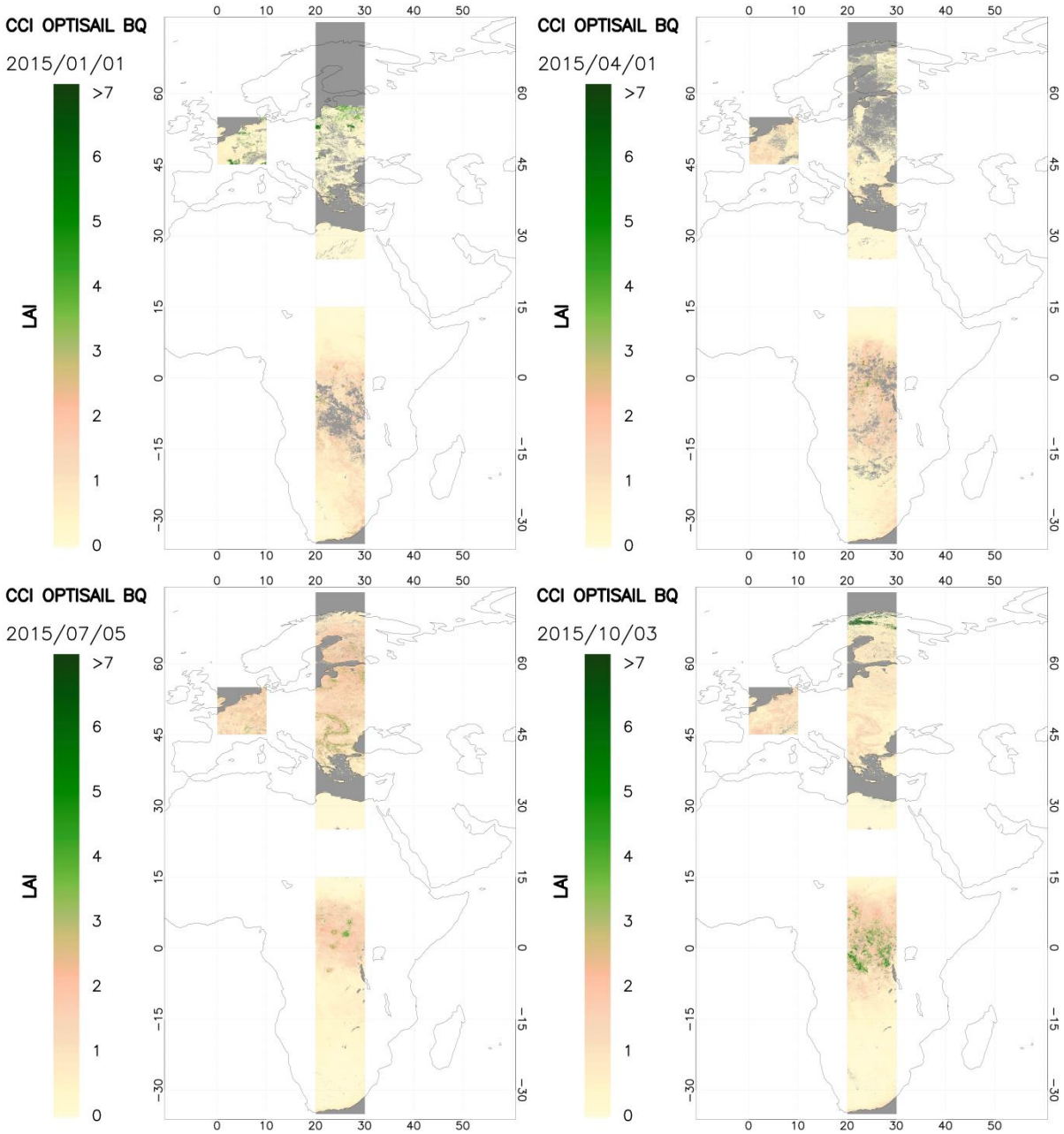

Figure 4: Maps over the validation transect of OPTISAIL LAI products (best quality pixels) in early January, April, July and October 2015. Grey values correspond to filled values (e.g., over oceans and seas) or low quality pixels.

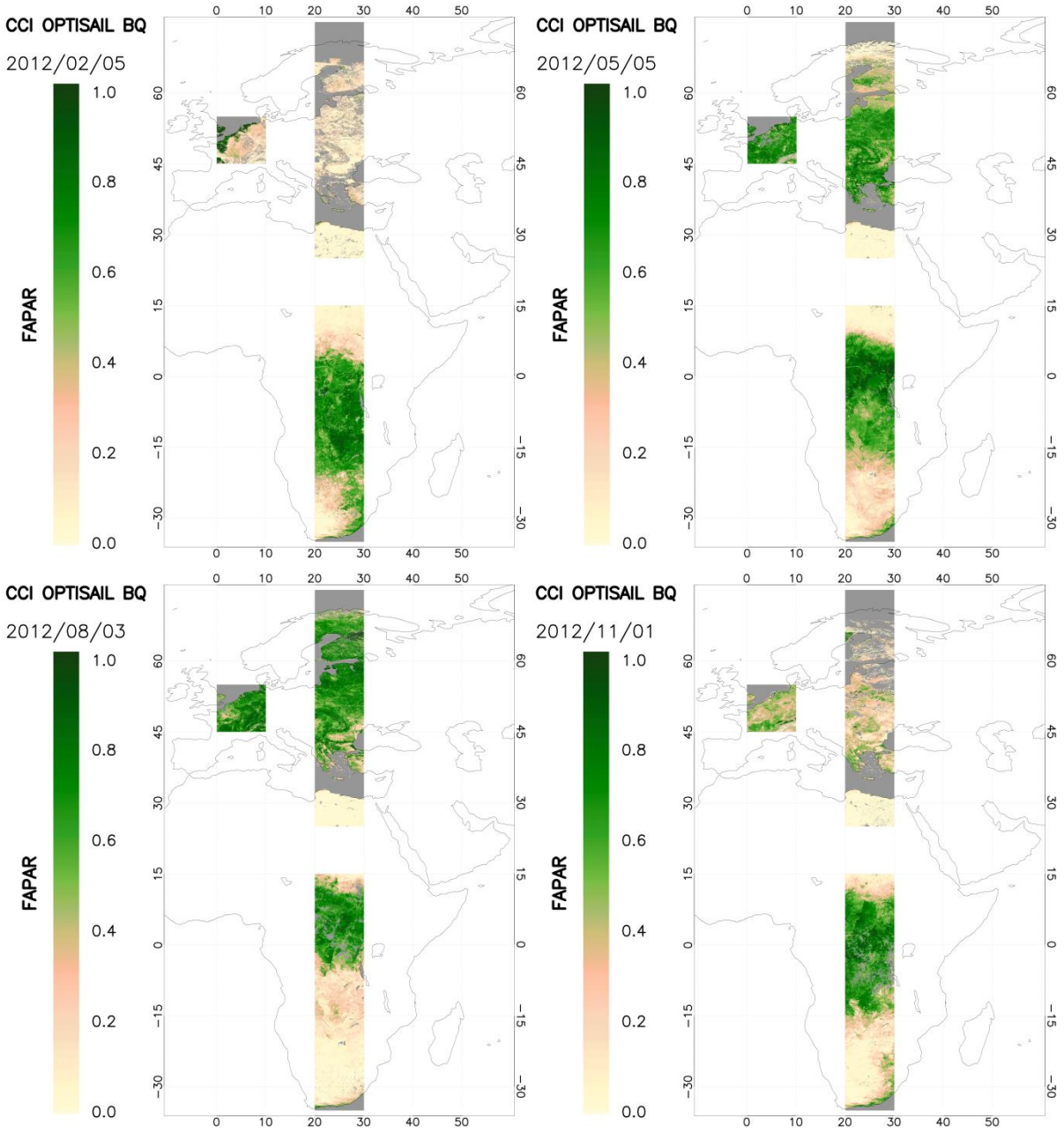

Figure 5: Maps over the validation transect of VP_CCI (CCI OPTISAIL) fAPAR products (best quality pixels) in early February, May, August and November 2012. Grey values correspond to filled values (e.g., over oceans and seas) or low quality pixels.

The main conclusions for the visual inspection of the maps over the transect (Figure 4 and Figure 5) are:

- Reliable spatial distributions for both variables are generally found over most areas covered by this analysis.
- However, some spatial inconsistencies are found:
    - Some unrealistic high values are commonly found over northern regions typically in winter (e.g., some pixels in South France in 2015.01.01 for LAI, or in North France in 2012.02.05 for fAPAR). These values could be related to cloud and/or snow contamination.

- Remarkably good completeness is observed over equatorial areas but unrealistic low values are found over large areas, mainly for LAI (LAI < 2 over equatorial forests), which could be explained by cloud contamination.

In order to better understand the spatial inconsistencies observed over northern and equatorial areas, the maps at full resolution over the tiles X18Y02 [45°N - 55°N; 0°E - 10°E] and X20Y07 [5°S - 5°N; 20°E - 30°E] are displayed and presented for six consecutive dates in Figure 6 (tile X18Y02 for LAI), Figure 7 (tile X18Y02 for fAPAR), Figure 8 (tile X20Y07for LAI) and Figure 9 (tile X20Y07 for fAPAR).

Main conclusions are:

- For X18Y02 some unexpected high values are found, showing abrupt changes, which can observed at local scale (e.g., transition from 2014.01.21 to 2014.01.31 at North-East in Figure 6 for LAI) or over large areas (e.g., transition from 2014.12.22 to 2014.12.27 over almost the whole tile in Figure 7 for fAPAR).
- For X20Y07, too much variation is observed between consecutive dates, mainly for LAI (Figure 8), which is not expected over these areas mainly dominated by EBF.
- Some stripes are found in both cases: northern latitudes in winter and equatorial areas.

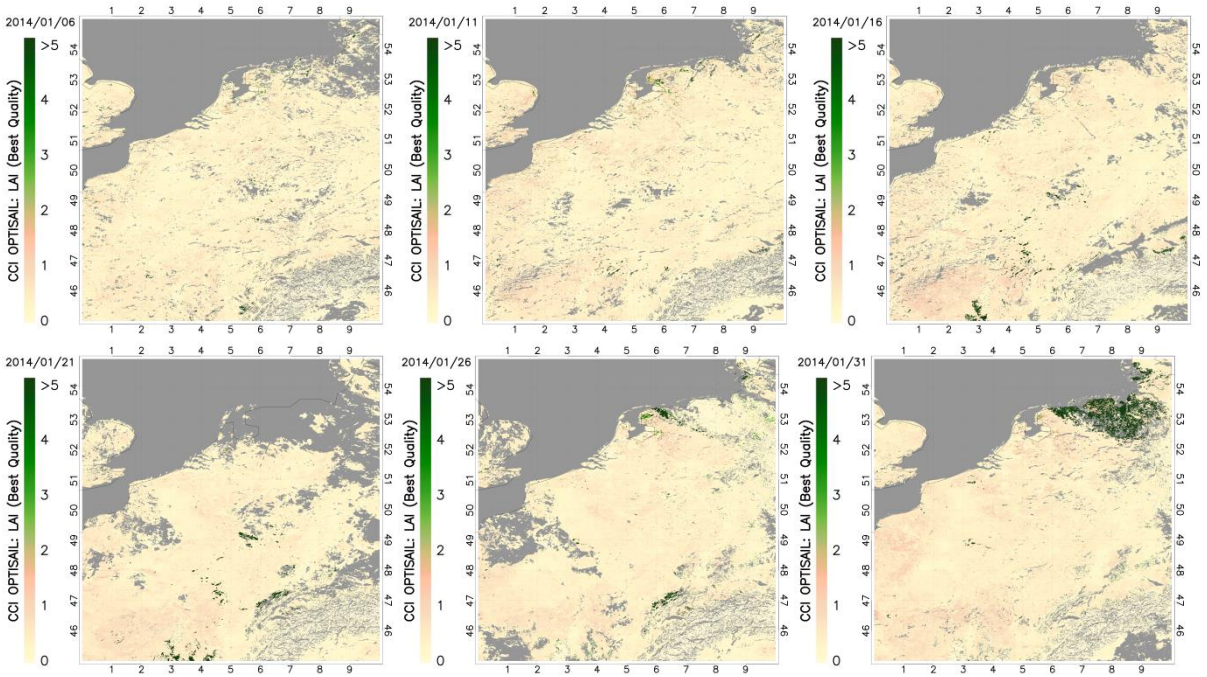

Figure 6: Maps over X18Y02 tile of VP_CCI (CCI OPTISAIL) LAI products (best quality pixels) for six consecutive dates starting in early January 2014.

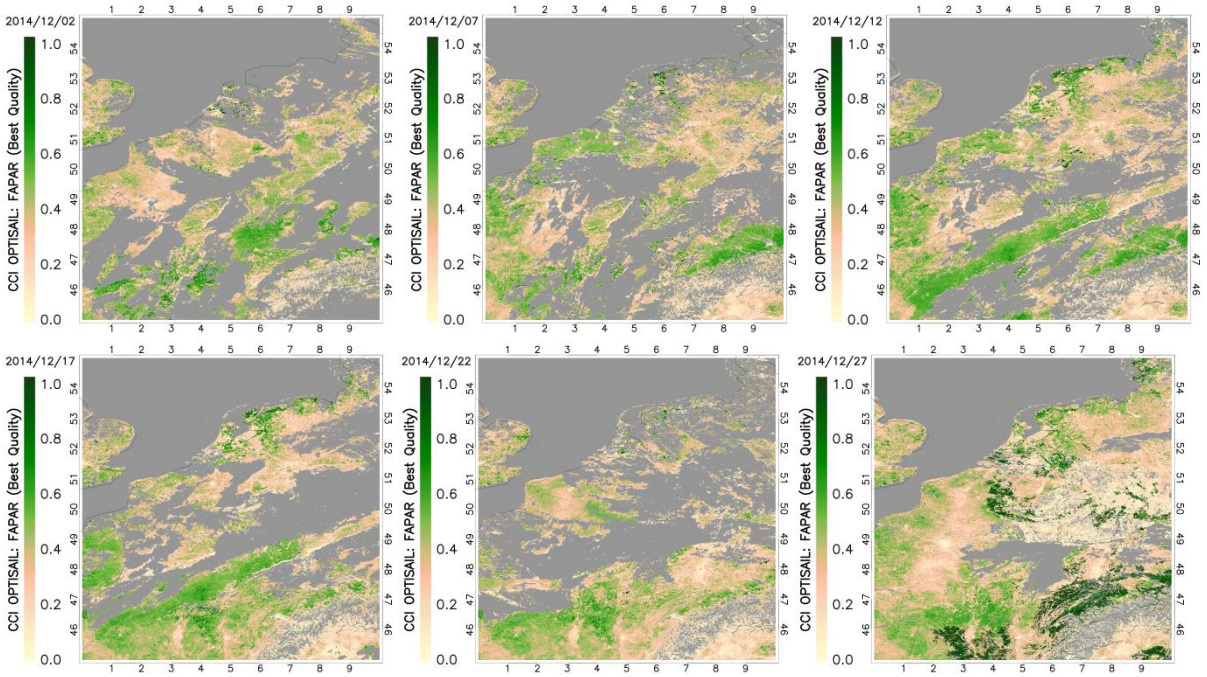

Figure 7: Maps over X18Y02 tile of VP_CCI (CCI OPTISAIL) fAPAR products (best quality pixels) for six consecutive dates starting in early December 2014.

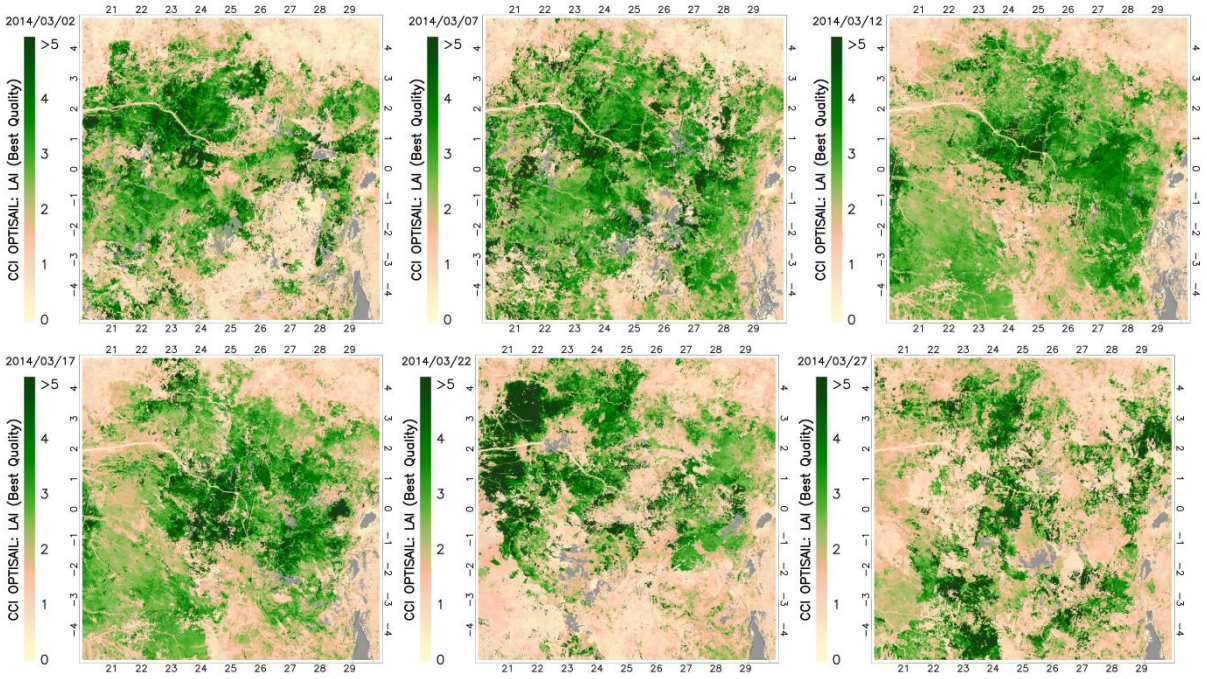

Figure 8: Maps over X20Y07 tile of VP_CCI (CCI OPTISAIL) LAI products (best quality pixels) for six consecutive dates starting in early March 2014.

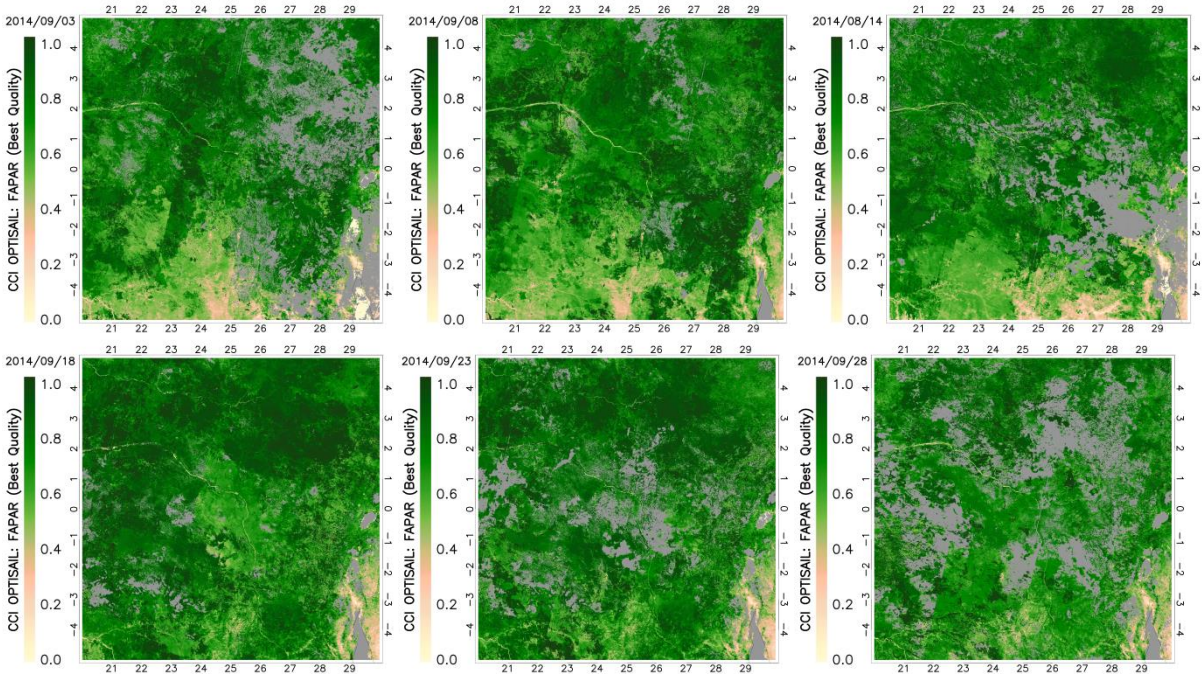

Figure 9: Maps over X18Y02 tile of VP_CCI (CCI OPTISAIL) fAPAR products (best quality pixels) At full resolution for six consecutive dates starting in early September 2014.

3.2.2 Analysis of residuals

In this section, the spatial distribution of residuals between VP_CCI and CGLS V2 LAI and fAPAR is evaluated. Maps of residuals for one year of data (four examples per year) are presented in Figure 10 and Figure 11. Table 6 shows the linear equations used to compute the residuals between VP_CCI and CGLS V2. These equations are based on the Major Axis Regression (MAR) linear trends, which are computed using LANDVAL sites. It should be noted that, in case of fAPAR, residuals are similar to differences (MAR close to 1:1 line).

Table 6: Summary of validation methodology

	MAR relationship VP_CCI and CGLS V2
LAI	Y=-0.02+0.48x
fAPAR	Y=-0.03+1.05x

Main findings from the spatial consistency between VP_CCI and CGLS V2 LAI and fAPAR products are:

- For LAI (Figure 10), both products are spatially consistent over large areas, with most of residuals between ±0.5 LAI. Larger spatial inconsistencies typically are found over equatorial areas.
- Similarly, for fAPAR (Figure 11), both products are spatially consistent in overall, with most of residuals between ±0.1 fAPAR. Larger spatial inconsistencies are observed over equatorial areas and Europe.

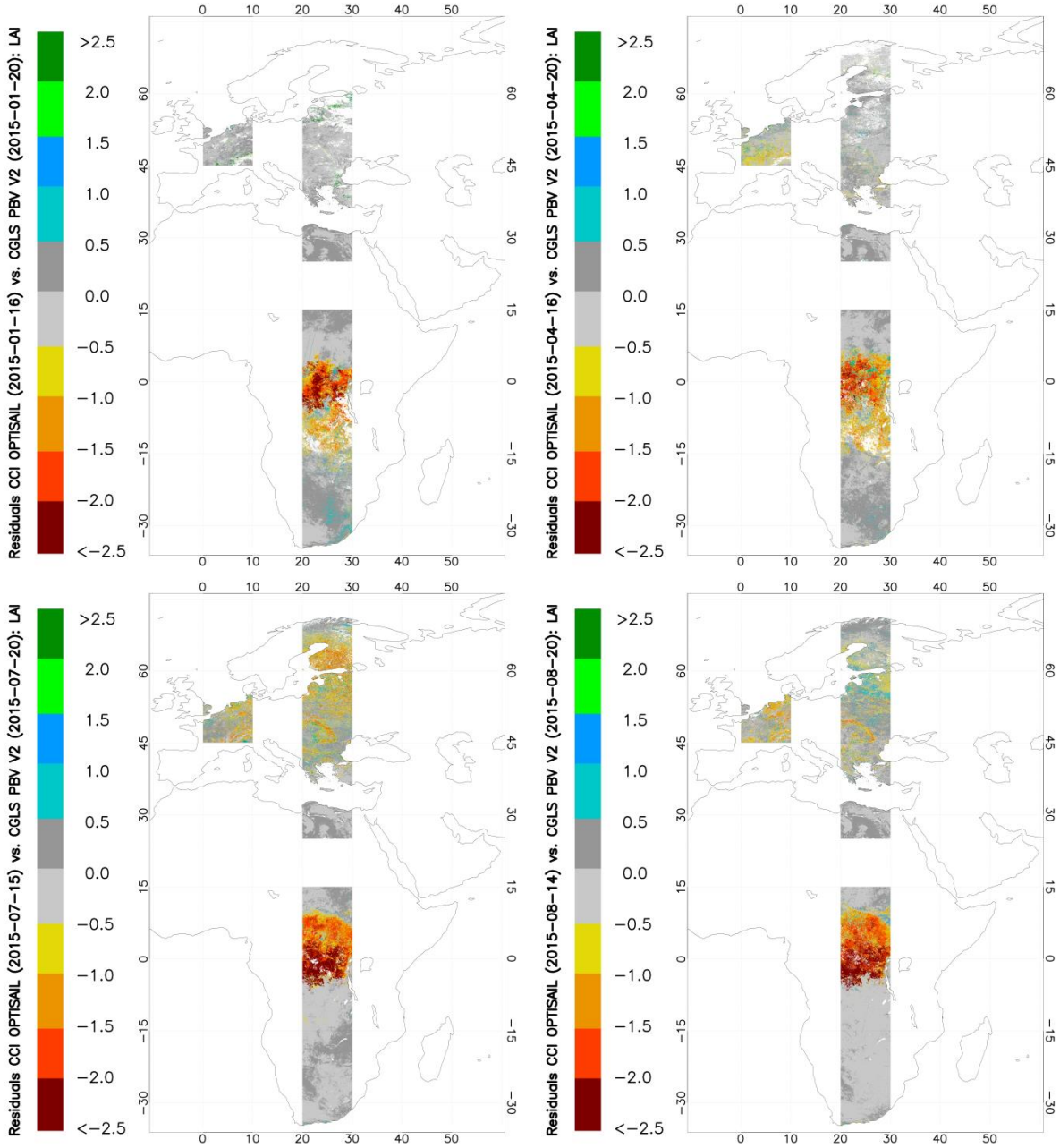

Figure 10: Maps of residual between VP_CCI (CCI_OPTISAIL) and CLGS V2 LAI products (best quality pixels) over the validation transect in mid-January, April, July and October 2015.

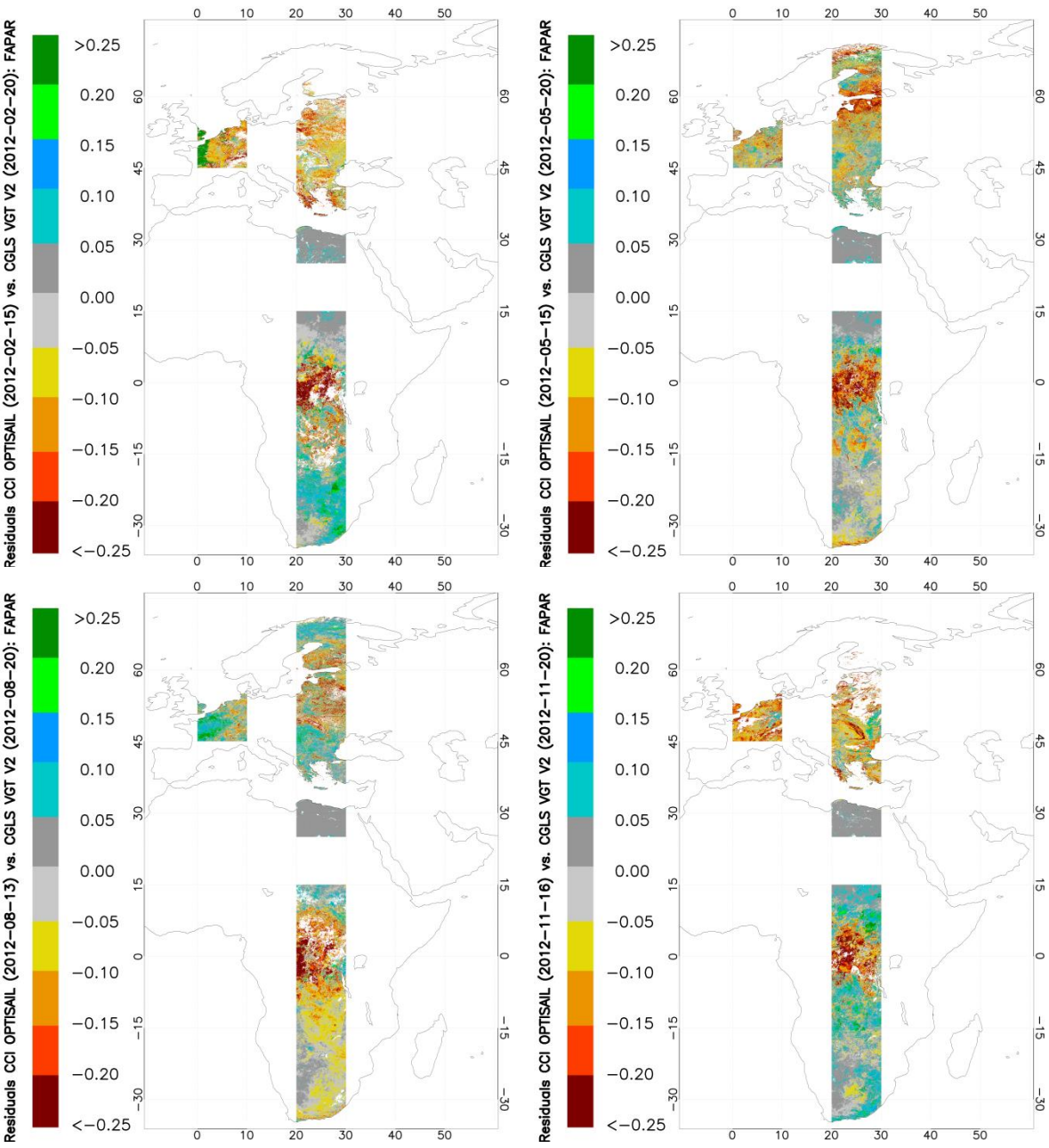

Figure 11: Maps of residual between VP_CCI (CCI OPTISAIL) and CLGS V2 fAPAR products (best quality pixels) over the validation transect in mid-February, May, August and November 2012.

3.3 Temporal consistency

This section examines the consistency of VP_CCI temporal variations as compared to the reference products (CGLS V2, VNP15A2H C1) and multi-temporal ground data from GBOV V3 and AMMA (when available). Temporal profiles were displayed over the 720 LANDVAL sites and the additional sites with ground data availability. From Figure 12 to Figure 18, two examples are selected to illustrate the LAI and fAPAR typical variations for each biome type: EBF, DBF, NLF, croplands, herbaceous, shrublands and sparse and bare areas.

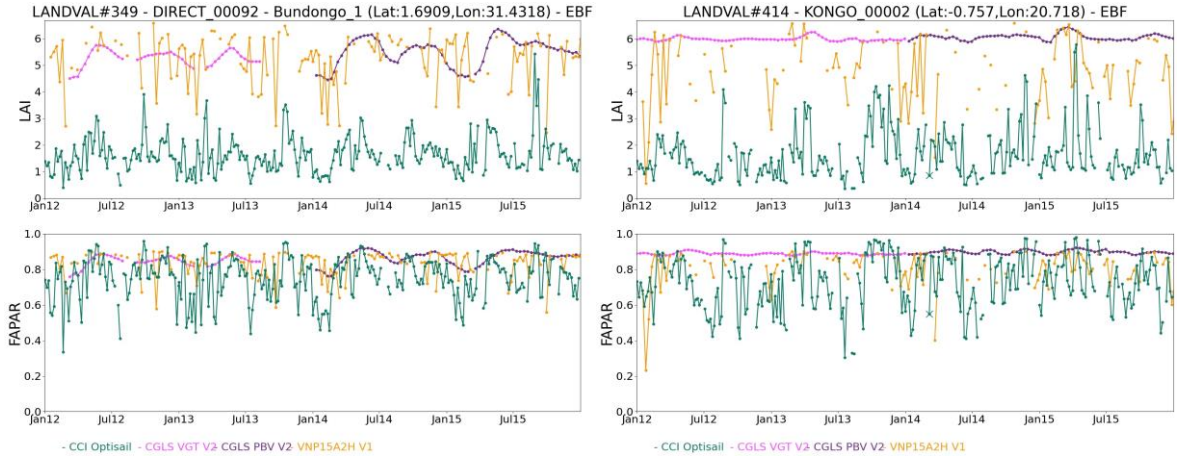

Figure 12: Temporal profiles over two selected Evergreen Broadleaved Forest sites of VP_CCI (CCI OPTISAIL) (green), CGLS (pink for SPOT/VGT and purple for PROBA-V) and VNP15A2H C6.1 (yellow). Note: VP_CCI provides effective LAI values, hence lower value than CGLS and VNP15A2Hthat represent actual LAI are expected.

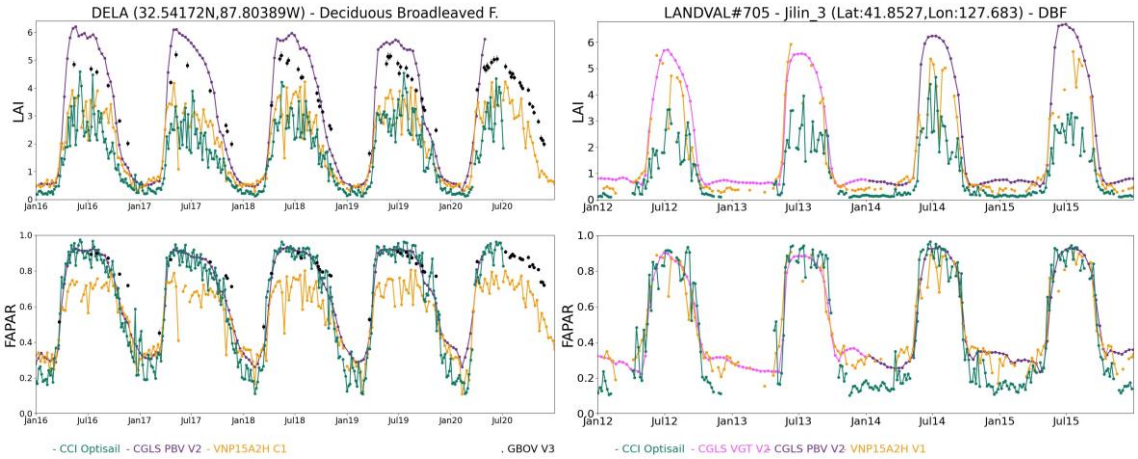

Figure 13: As in Figure 12 but for Deciduous Broadleaved Forest.

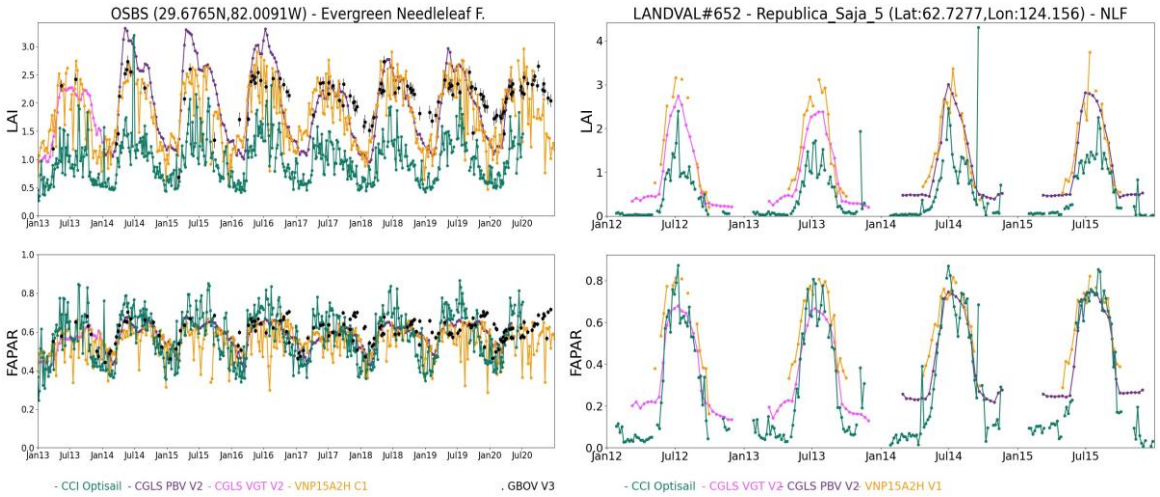

Figure 14: As in Figure 12 but for Needle-Leaf Forest.

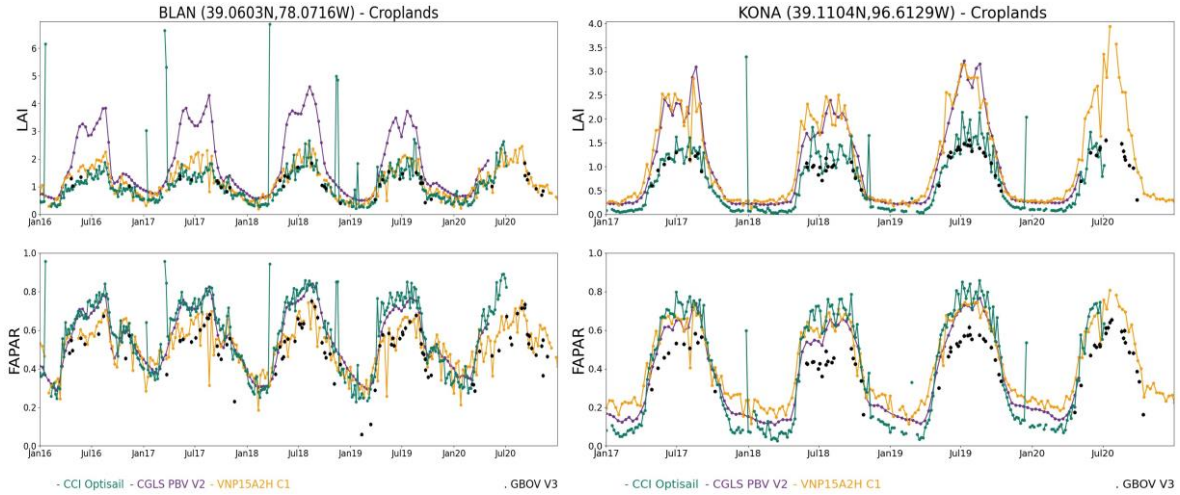

Figure 15: As in Figure 12 but for Croplands.

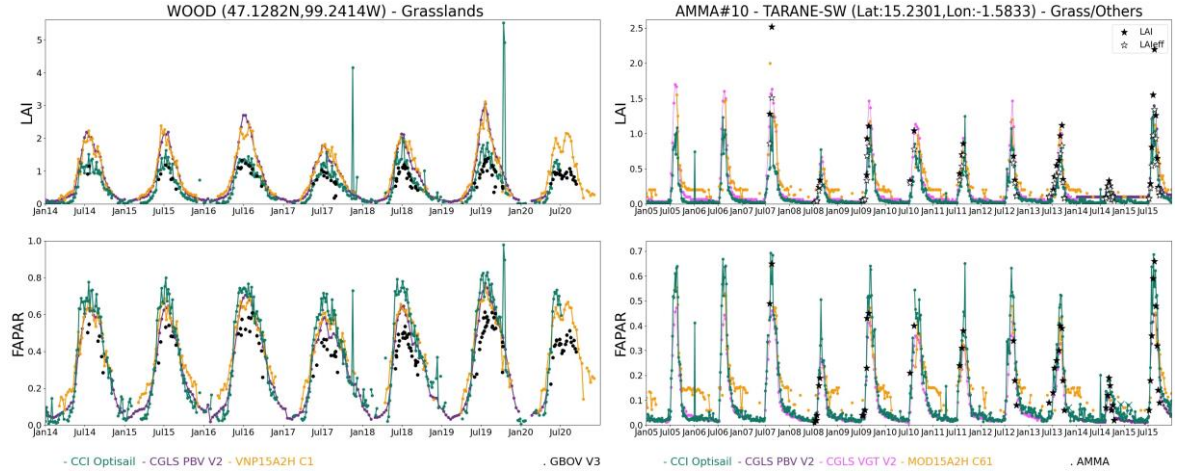

Figure 16: As in Figure 12 but for Herbaceous.

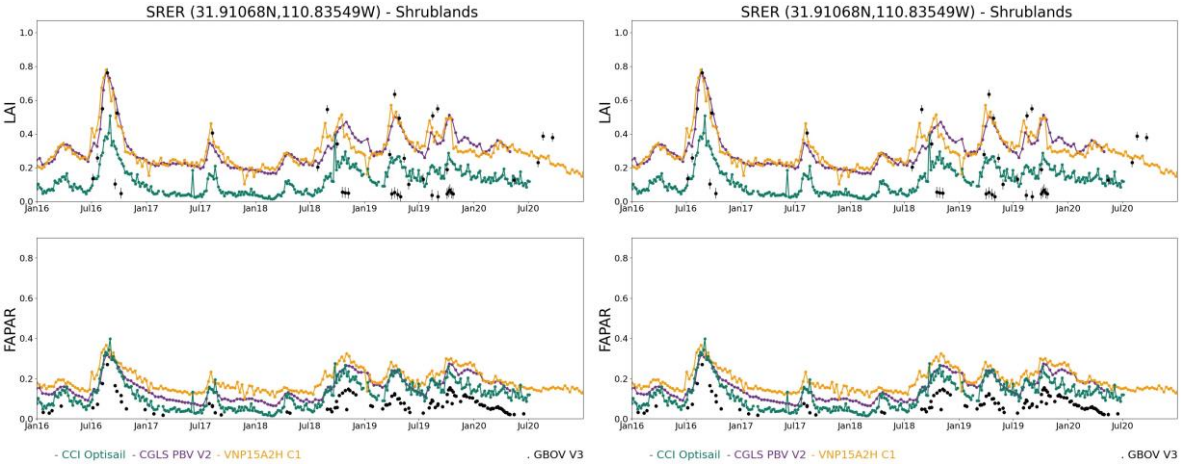

Figure 17: As in Figure 12 but for Shrublands.

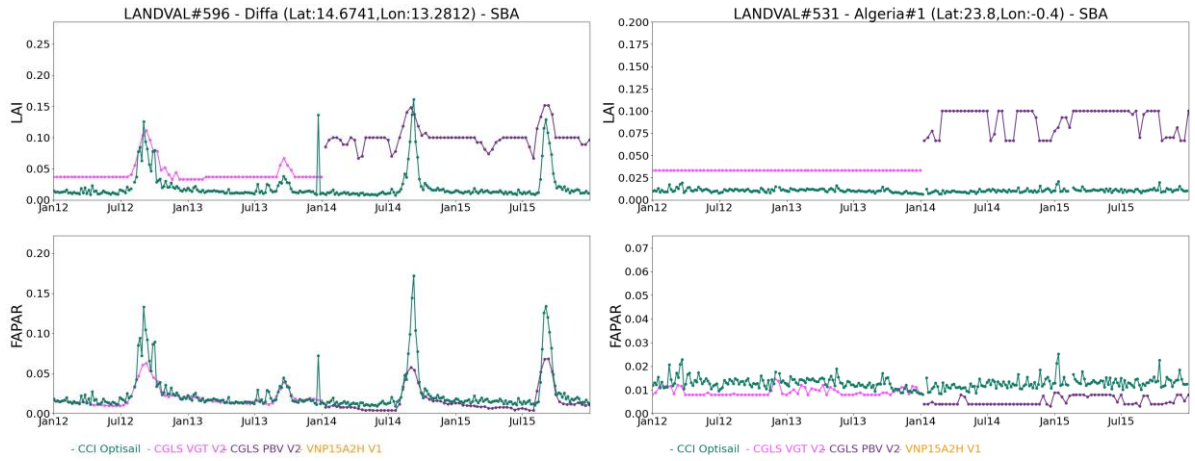

Figure 18: As in Figure 12 but for Sparse and Bare Areas.

Main conclusions from the visual inspection of temporal trajectories are:

- For EBF (Figure 12), the temporal trajectories of VP_CCI show very low fraction of missing values but showing noisy profiles probably due to a little restrictive cloud screening. This noise is related to spatial inconsistencies observed in section 3.2. The temporal trajectories of CGLS V2 are very smooth and present very low seasonality, as expected due to smoothing techniques applied in the temporal composites (Verger et al., 2023).
- For DBF (Figure 13), VP_CCI shows similar temporal trajectories than other products and GBOV V2 multi-temporal ground observations. For LAI, VP_CCI shows lower magnitude of values than references due to different definitions (LAIeff vs LAI). Remarkably good agreement is found, in terms of magnitude of values, between VP_CCI, CGLS V2 and GBOV for higher fAPAR values.
- VP_CCI shows, again, similar temporal trajectories than reference products and multi-temporal GBOV V3 ground data for NLF (Figure 14). Some outliers are found for some cases located at northern latitudes (e.g., LANDVAL #652 in Figure 14) in wintertime which could be attributed to cloud or snow contamination.
- Similarly, for croplands (Figure 15), herbaceous (Figure 16) and shrublands (Figure 17), VP_CCI shows same seasonality and temporal trends than reference satellite products and ground data. Some outliers are found, again, for several observations typically during wintertime.
- VP_CCI provides very low or almost zero values for sparse vegetated (Figure 18-left) and bare areas (Figure 18-right). In case of CGLS V2 some bias is observed in the transition from SPOT/VGT (2013) to PROBA-V (2014) whilst for VP_CCI remarkably good continuity is observed when using different input data (SPOT/VGT and PROBA-V). VNP15A2H C1 does not provide valid values over desert targets as heritages biome dependency from MODIS operational algorithm (Myneni et al., 2002; Yang et al., 2006).
- The outliers seem to be related to some of the spatial inconsistencies observed in the visual inspection of maps (unrealistic high values, see section 3.2.1).

3.4 Error evaluation (direct validation)

3.4.1 Comparison with DIRECT V2.1

Figure 19, Figure 20 and Figure 21 show the scatter-plots between VP_CCI, CGLS V2 and MOD15A2H C6.1 products versus DIRECT V2.1 LAI, effective LAI and fAPAR ground-based reference maps.

Concomitant 'best quality' samples between all satellite products under study are used, and comparison was performed at 3km^2 (i.e., average values of 3x3 pixels in case of VP_CCI and CGLS V2 and 6x6 in case of MOD15A2H C6.1).

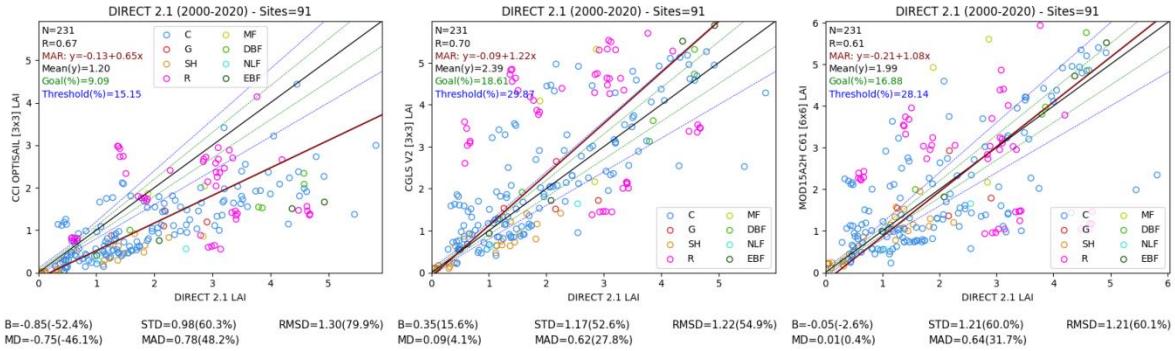

Figure 19: Scatter-plots between VP_CCI (CCI OPTISAIL), CGLS V2 and MOD15A2H C6.1 LAI products versus DIRECT V2.1 LAI ground-based maps. 'C' stands for cultivated, 'G' for grasslands, 'SH' for shrublands, 'R' for rice, 'MF' for mixed forests, 'DBF' for deciduous broadleaved forests, 'NLF' for needle-leaf forests and 'EBF' for evergreen broadleaved forests. Green and blue lines stand for goal and threshold levels, respectively. Note: VP_CCI provides effective LAI values.

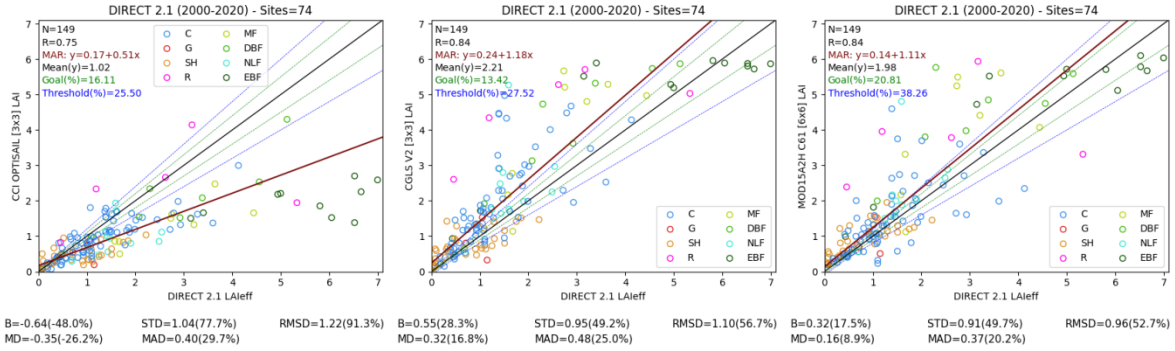

Figure 20: As in Figure 19 but comparing with DIRECT V2.1 effective LAI. Note: VP_CCI provides effective LAI values.

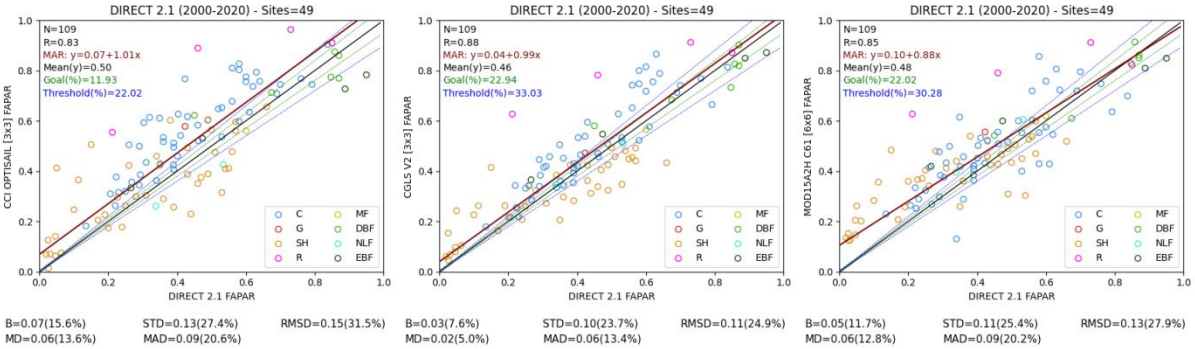

Figure 21: As in Figure 19 but for fAPAR products.

Main conclusions for LAI (Figure 19 and Figure 20) are:

- VP_CCI shows systematically lower values than DIRECT V2.1 LAI (Figure 19) and effective LAI (Figure 20) with large negative mean bias of -0.9 (-52%) and -0.6 (-48%) and overall uncertainties (RMSD) of 1.3 and 1.2 (around 90%), respectively. The overestimation is mainly observed for higher values, with slope of 0.5 even when comparing with effective LAI.

- As expected, higher number of VP_CCI cases is within goal (16%) and threshold (26%) GCOS uncertainty requirements when comparing with effective LAI than when comparing with true LAI values (9% and 15%).
- Both CGLS V2 and MOD15A2H C6.1 satellite references show improved accuracy (mean bias) and lower uncertainty (RMSD=1.2, around 50-60% in relative terms, when comparing with true LAI ground-based maps). CGLS tends to slightly overestimate DIRECT V2.1 high values (slope=1.22), whilst MOD15A2H C6.1 show mean bias close to zero.
- CGLS V2 and MOD15A2H C6.1 show higher number of samples within goal (19% and 17% for CGLS V2 and MOD15A2H C6.1) and threshold level (30% and 28%) than VP_CCI.

For fAPAR (Figure 21):

- VP_CCI shows systematic positive bias of 0.07 compared with DIRECT V2.1, with linear relationship (slope around 1) and overall uncertainty (RMSD) of 0.15.
- CGLS V2 shows the best agreement (mean bias of 0.03, RMSD of 0.11). MOD15A2H C6.1 also shows better overall agreement (B=0.05, RMSD=0.13) than VP_CCI, but with a clear tendency to overestimate low fAPAR values over sparsely vegetated areas (D'Odorico et al., 2014).
- As for LAI, VP_CCI provides lower number of samples within optimal (12%) and threshold (22%) GCOS uncertainty requirements than CGLS V2 (23% and 33%) and MOD15A2H C6.1 (22% and 30%).

3.4.2 Comparison with GBOV V3

Figure 22 and Figure 23 show the scatterplots between VP_CCI, CGLS V2 and VNP15A2H C1 LAI and fAPAR products versus GOBV V3 LAI and fAPAR ground-based reference maps. Concomitant 'best quality' samples between the three satellite products under study are used, and comparison was also performed at 3km^2 (i.e., average values of 3x3 pixels for VP_CCI and CGLS V2 and 6x6 pixels in case of VNP15A2H C1). It should be noted that, in case of LAI, the results are presented for forest and for non-forest sites due to the different level of clumping. Therefore, larger discrepancies due to the different definition (effective LAI in case of VP_CCI and actual LAI in case of GBOV V3) are expected in those sites with higher clumping (i.e., over forests).

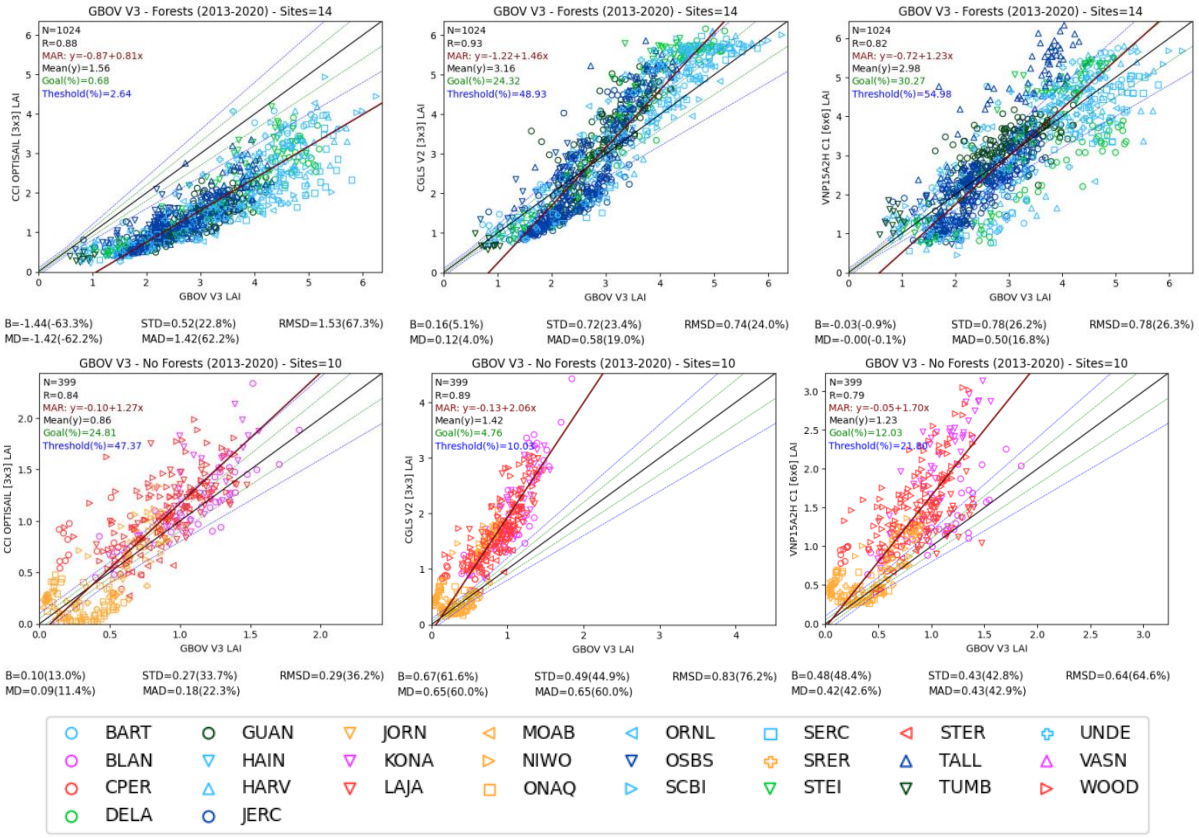

Figure 22: Scatterplots between VP_CCI (CCI OPTISAIL), CGLS V2 and VNP15A2H C1 LAI products versus GBOV V3 LAI ground-based maps. Forest sites are presented at the top (dark and light green represent EBF and DBF, dark and light blue represent NLF and mixed forests) and non-forest sites at the bottom side (purple, red and orange represent croplands, grasslands and shrublands). Green and blue lines stand for goal and threshold levels, respectively. Note: VP_CCI provides effective LAI values.

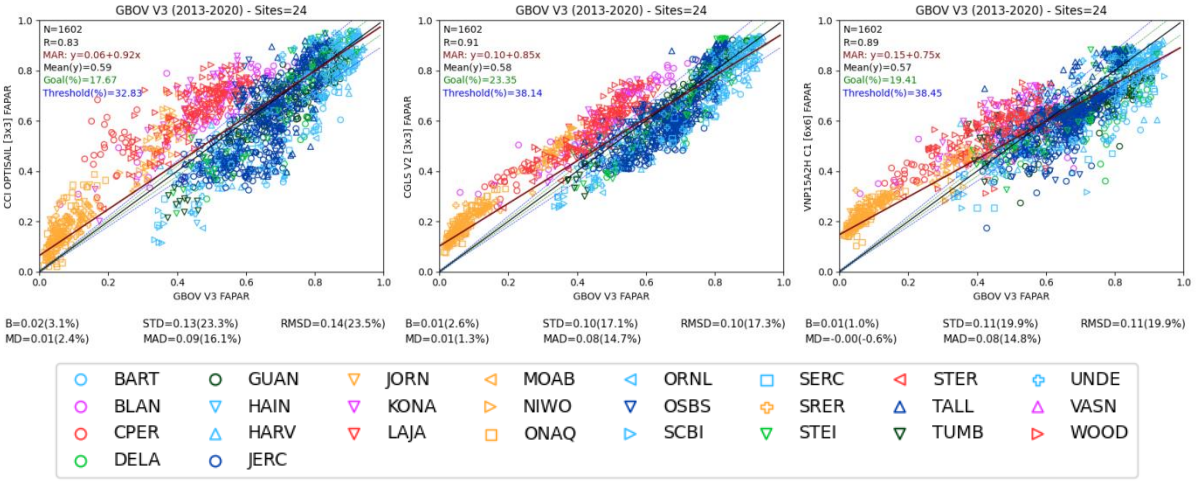

Figure 23: Scatterplots between VP_CCI (CCI OPTISAIL), CGLS V2 and VNP15A2H C1 fAPAR products versus GBOV V3 fAPAR ground-based maps. Dark and light green represent EBF and DBF, dark and light blue represent NLF and mixed forests, and purple, red and orange stand for croplands, grasslands and shrublands. Green and blue lines stand for goal and threshold levels, respectively.

Main conclusions for LAI are:

- For forest sites (Figure 22, top side) VP_CCI shows, as expected, lower values than GBOV V3 due to different definitions (LAIeff vs LAI true). CGLS V2 shows a tendency to overestimate higher values and the opposite trend for lower values, with overall uncertainty (RMSD) of 0.74. VNP15A2H C1 shows mean bias close to zero, but large scattering, with RMSD of 0.78.
- For non-forest sites (Figure 22, bottom side) VP_CCI shows the best agreement with RMSD of 0.29 and slight positive bias of 0.1 (slope of 1.27). Both CGLS V2 and VNP15A2H C1 show large bias in comparison with GBOV V3, with slopes of the linear regression of 2 and 1.7 respectively.
- For non-forest sites, VP_CCI shows the higher number of samples within GCOS uncertainty requirements with 25% and 47% of cases within optimal and threshold level.

Main conclusions for fAPAR are:

- VP_CCI tends to provide higher values than GBOV V3 for non-forest sites and the opposite trend for forest cases, with mean bias of 0.02 (3%) and overall uncertainty (RMSD) of 0.14.
- Both satellite references provide better results, with RMSD of 0.1 (CGLS V2) and 0.11 (VNP15A2H C1) and low scattering (STD).
- VP_CCI provides slightly lower number of cases within goal (18%) and threshold (33%) GCOS uncertainty requirements than CGLS V2 (23% and 38%) and VNP15A2H C1 (19% and 38%).

It should be noted that all satellite products show a clear tendency to overestimate GBOV V3 LAI and fAPAR ground-based maps for non-forest cases and could be, partly, due to GBOV V3 uncertainties.

3.4.3 Comparison with AMMA

Figure 24, Figure 25 and Figure 26 show the scatterplots between VP_CCI, CGLS V2 and MOD15A2H C6.1 products versus AMMA LAI, LAIeff and fAPAR ground data. Concomitant 'best quality' samples between both satellite products under study are used, and comparison was performed at 1km^2 of spatial support, as AMMA ground measurements are provided over transects of around 1km.

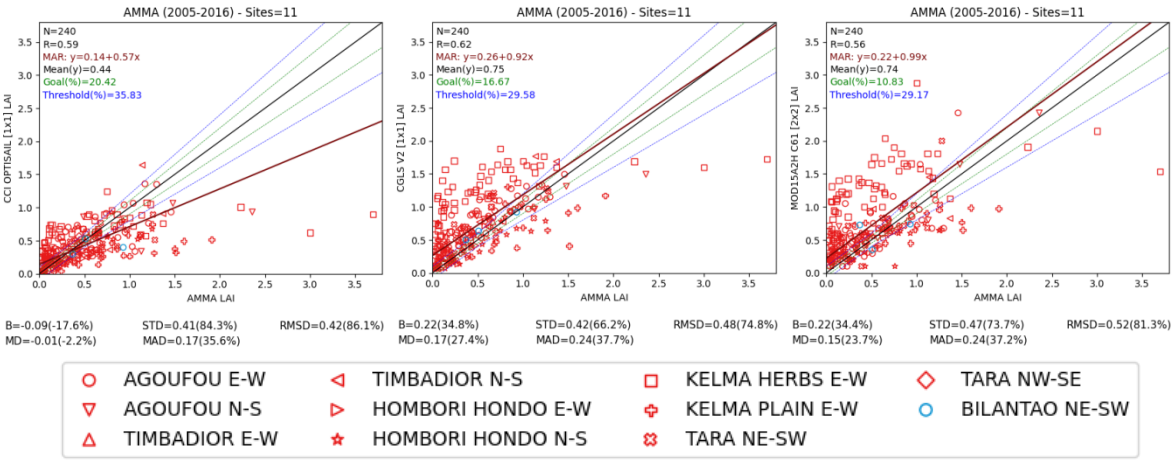

Figure 24: Scatterplots between VP_CCI (CCI OPTISAIL), CGLS V2 and MOD15A2H C6.1 LAI products versus AMMA LAI ground data. Green and blue lines stand for goal and threshold levels, respectively. Green markers stand for Forests sites, blue for Croplands sites and red for Grassland or other sites. Note: VP_CCI provides effective LAI values.

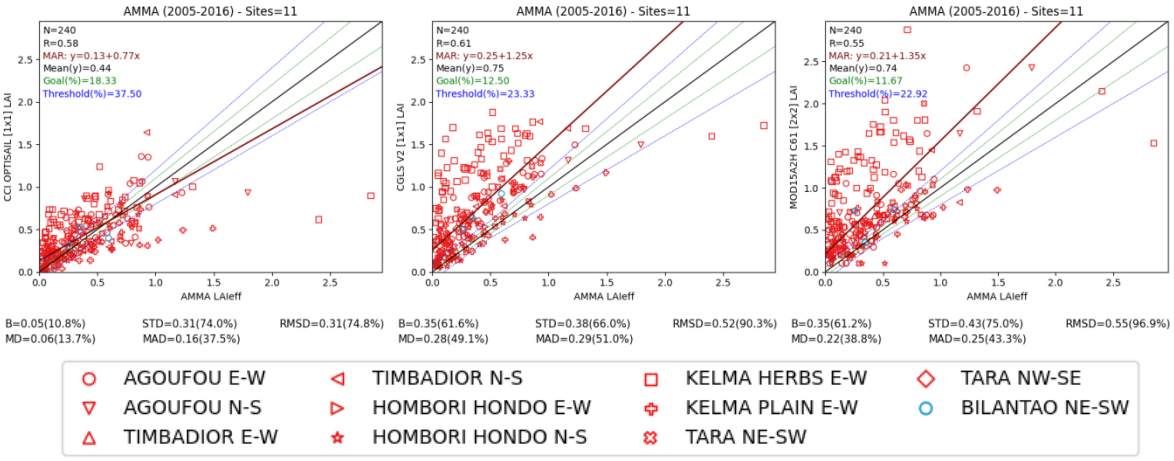

Figure 25: Scatterplots between VP_CCI (CCI OPTISAIL), CGLS V2 and MOD15A2H C6.1 LAI products versus AMMA LAIeff ground data. Green and blue lines stand for goal and threshold levels, respectively. Green markers stand for Forests sites, blue for Croplands sites and red for Grassland or other sites. Note: VP_CCI provides effective LAI values.

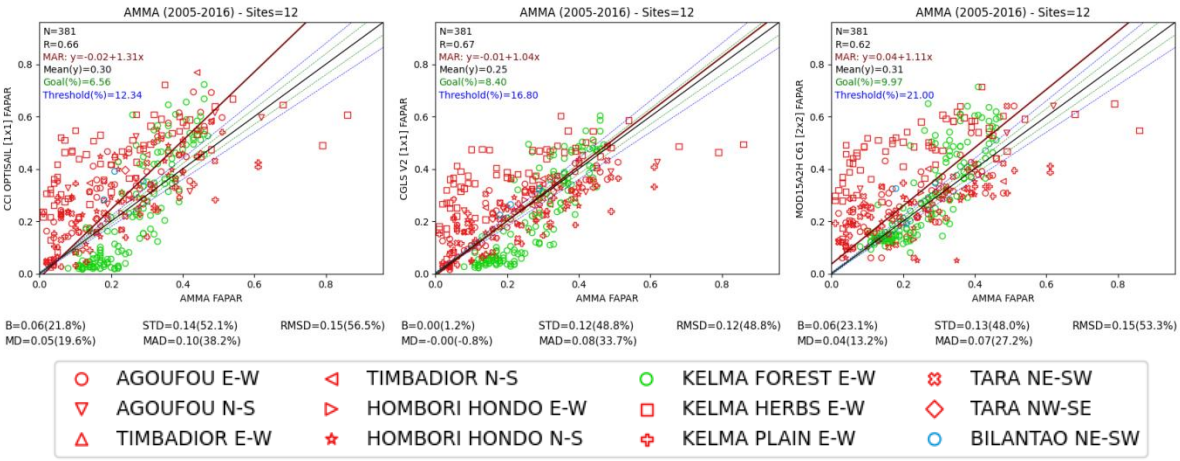

Figure 26: Scatterplots between VP_CCI (CCI OPTISAIL), CGLS V2 and MOD15A2H C6.1 fAPAR products versus AMMA fAPAR ground data. Green and blue lines stand for goal and threshold levels, respectively. Green markers stand for Forests sites, blue for Croplands sites and red for Grassland or other sites.

In case of LAI products (see Figure 24 and Figure 25 for comparisons with LAIeff and LAI true ground data):

- VP_CCI shows, as expected, better agreement with LAIeff ground data (B=0.05, RMSD=0.31) than LAI true (B=-0.09, RMSD=0.42). For the comparison with LAIeff, 18% and 38% of VP_CCI cases are within optimal and threshold GCOS uncertainty levels.
- Both CGLS V2 and MOD15 A2H C6.1 show same bias compared with AMMA LAI measurements (B=0.22), sowing CGLS V2 slightly improved uncertainty (RMSD of 0.48 vs 0.52). The overall uncertainty of reference dataset compared with AMMA LAI is similar to that found when comparing VP_CCI with AMM LAIeff (RMSD around 75%).

In case of fAPAR:

- VP_CCI shows a tendency to provide higher values than AMMA ground measurements (B=0.06, slope=1.3), with overall uncertainty (RMSD) of 0.15.

- CGLS V2 shows the best agreement (B~0, RMSD=0.12) and MOD15A2H C6.1 shows similar validation metrics (B=0.06, RMSD=0.15) than VP_CCI.
- VP_CCI also provides slightly lower percentage of cases within goal (7%) and target (12%) GCOS uncertainty requirements than CGLS V2 (8% and 17%) and MOD15A2H C6.1 (10% and 21%).

3.5 Error evaluation (product intercomparison)

3.5.1 Overall analysis

The overall consistency between VP_CCI and other satellite products (CGLS V2, MOD15A2H C6.1 and VNP15A2H C1) is evaluated over best quality retrievals of LANDVAL sites during 2012-2015. Figure 27 and Figure 28 show the scatter-plots between pair of products for LAI and fAPAR respectively.

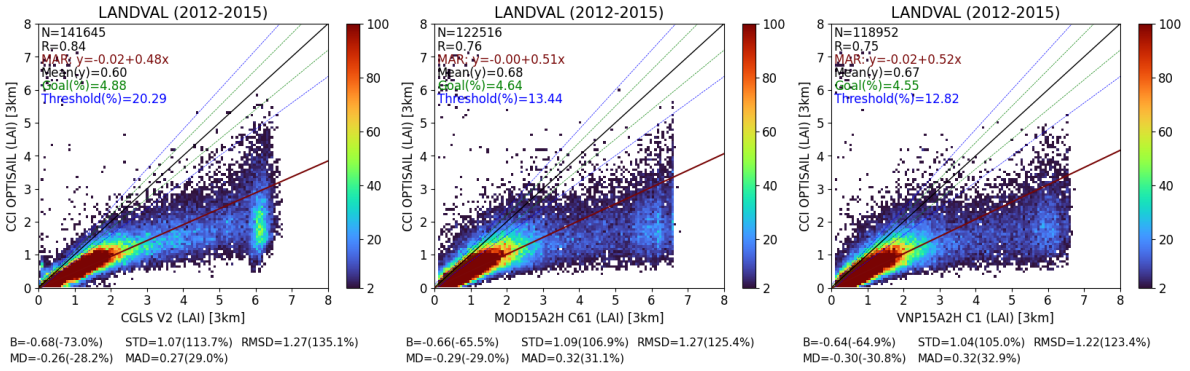

Figure 27: Scatter-plots between pair of satellite LAI products (colorbar represents density of points). Computation over best quality retrievals over LANDVAL sites for 2012-2015 period. From left to right: VP_CCI (CCI OPTISAIL) versus CGLS V2, VP_CCI (CCI OPTISAIL) versus MOD15A2H C6.1 and VP_CCI (CCI OPTISAIL) versus VNP15A2H C1. Green and blue lines stand for goal and threshold levels, respectively. Note: VP_CCI provides effective LAI values.

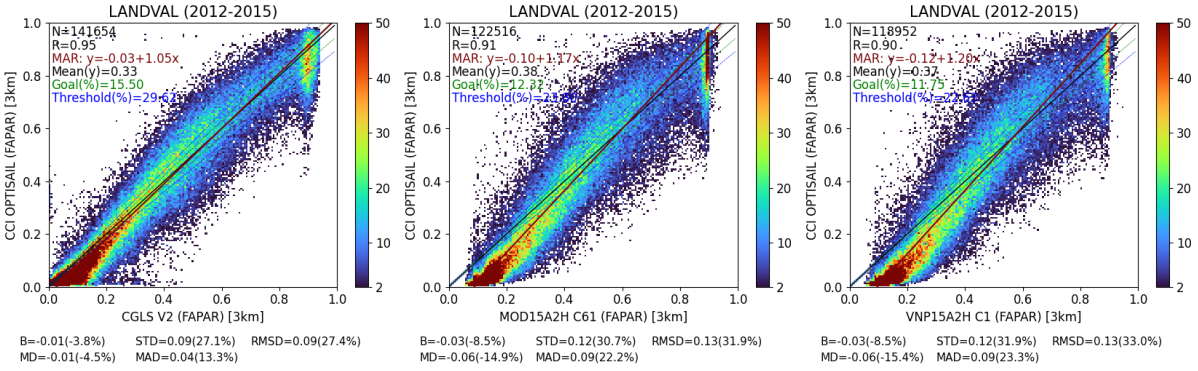

Figure 28: As in Figure 27 for fAPAR products.

For LAI (Figure 27), the main results are:

- VP_CCI shows, as expected, large differences (lower values) with CGLS V2, MOD15A2H C6.1 and VNP15A2H C1 due to the different LAI definitions (true LAI values in case of CGLS and NASA products and effective LAI in case of VP_CCI).
- Considering that the average clumping index is typically about 0.6 (Chen et al., 2005), the LAIeff values of VP_CCI can be considered reliable in comparison with satellite references, as

slopes of the MAR of around 0.5 are found in comparison with CGLS V2 and MOD15A2H C6.1 and VNP15A2H C1.

For fAPAR (Figure 28), the main results are:

- The comparison of VP_CCI vs. CGLS V2 shows the better agreement (RMSD = 0.09). VP_CCI typically tends to provide slightly lower values than CGLS (mean bias of -4%), mainly observed for the lower (fAPAR<0.2) and higher (fAPAR>0.8, typically dominated by EBF cases where CGLS V2 uses gap-filling techniques) values.
- The comparison of VP_CCI vs. NASA MOD15A2H C6.1 and VNP15A2H C1 products shows worse overall agreement (RMSD=0.13) than the comparison with CGLS V2. VP_CCI tends to provide lower values than NASA products for low fAPAR ranges, which is expected due to the well-known tendency of MODIS based products to overestimate fAPAR for the lowest value ranges (D'Odorico et al., 2014; Fuster et al., 2020).

3.5.2 Analysis per biome type

This section presents the overall spatio-temporal consistency between VP_CCI and reference CGLS V2 and VNP15A2H C1 products per biome type. Figure 29 and Figure 30 show the histograms of LAI and fAPAR retrievals, and the violin-plots of the bias of VP_CCI with references per main biome type. Additionally, the scatterplots (with their associated statistics) per biome type are available in Annex I (VP_CCI versus PBV 300m V1) and Annex II (VP_CCI versus VNP15A2H C1).

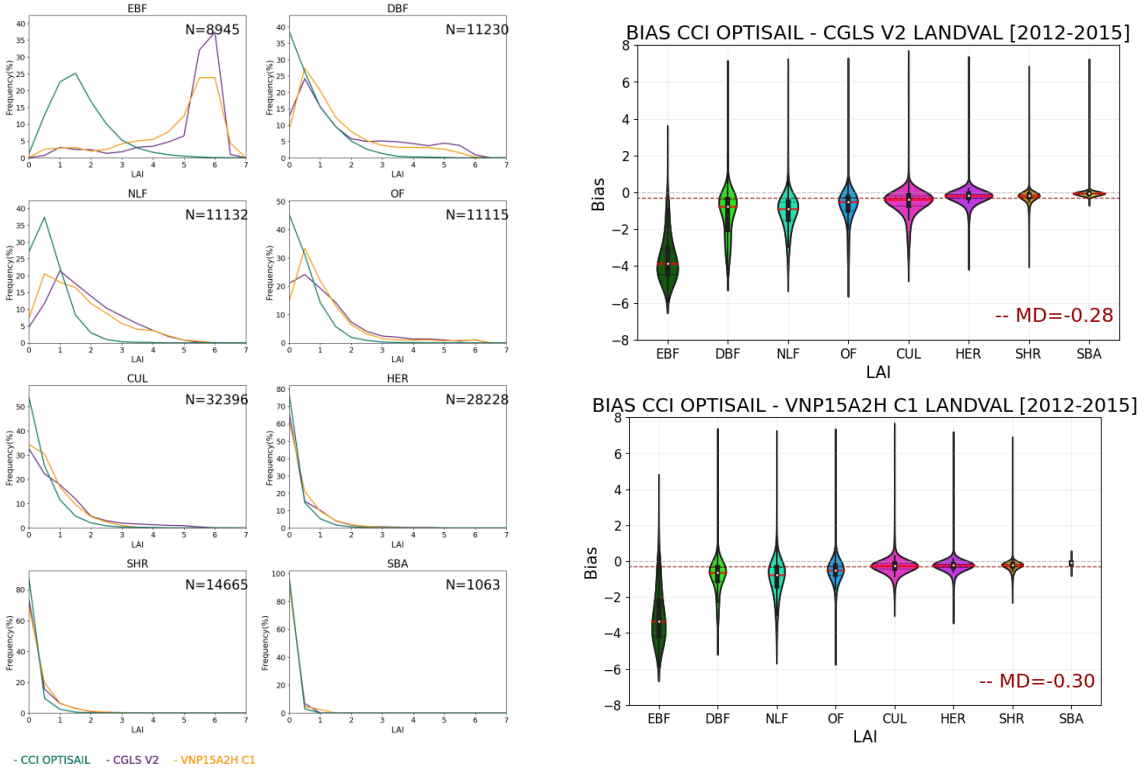

Figure 29: Left: Distribution of LAI values for VP_CCI (CCI OPTISAIL), CGLS V2 and VNP15A2H C1 products per main biome type for 2012-2015 period. Right: Violin-plots of the bias between VP_CCI and reference CGLS V2 (top) and VNP15A2H C1 (bottom) products per biome type. In the violin-plots, red horizontal bars indicate median values, horizontal dashed black lines stretch from first and third quartile of the data, and vertical black lines stretch from the lower and upper adjacent value. The biases are expressed in absolute values. Note: VP_CCI provides effective LAI values.

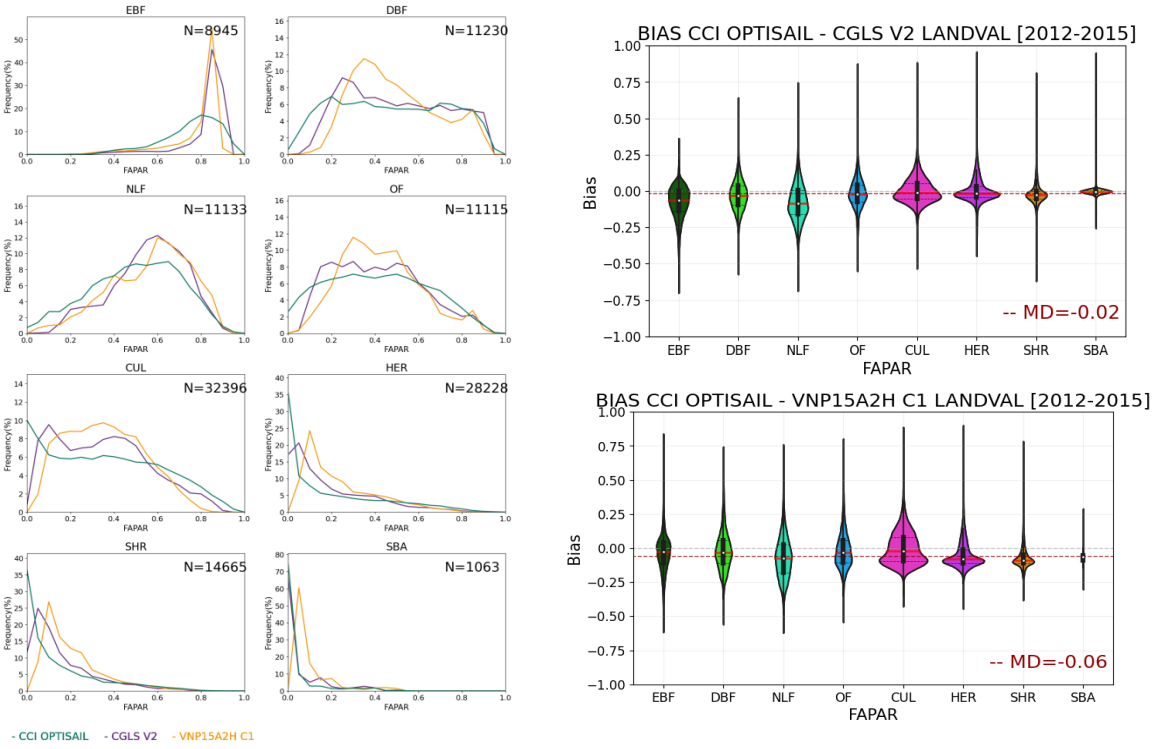

Figure 30: As in Figure 29 for fAPAR products.

For LAI (Figure 29):

- VP_CCI provides typically lower values than CGLS V2 and VNP15A2H C1 for forest sites, as expected due to clumping index mainly impacts in dense canopies.
- Similar distributions of LAI retrievals are found between VP_CCI and both reference products for non-forest sites, except for cultivated.

For fAPAR (Figure 30):

- VP_CCI provides similar distribution of retrievals than references for most biome types, except for EBF where large discrepancies are found (OTISAIL shifted towards lower values).
- The main discrepancies are found for EBF (RMSD of 0.12 and 0.15 in the comparison with CGLS V2 and VNP15A2H C1) and NLF (RMSD of 0.14 and 0.17), probably due to a more conservative cloud screening reference satellite datasets as these biomes are most affected by cloud coverage (located typically over equatorial and northern areas).
- The tendency of VNP15A2H C1 to provide higher values than VP_CCI and CGLS V2 for sparse or low vegetated biomes (HER, SHR, SBA) is clearly observed in the histograms of values, which is similar to previous NASA collection products based on MODIS (D'Odorico et al., 2014; Fuster et al., 2020).
- VP_CCI also shows a tendency to provide high frequencies for fAPAR values close to zero in CUL, HER, and SBA, which is not observed in reference satellite datasets.

3.5.3 Intra-annual precision

The histograms of the intra-annual precision (δ, the so-called smoothness) for OPTISAIL, CGLS V2 and VNP15A2H C1 are presented in Figure 31 for LAI (left side) and fAPAR (right). The computation is

performed over LANDVAL sites for 2012-2015 and median δ values are provided as indicative of the intra-annual precision of the products.

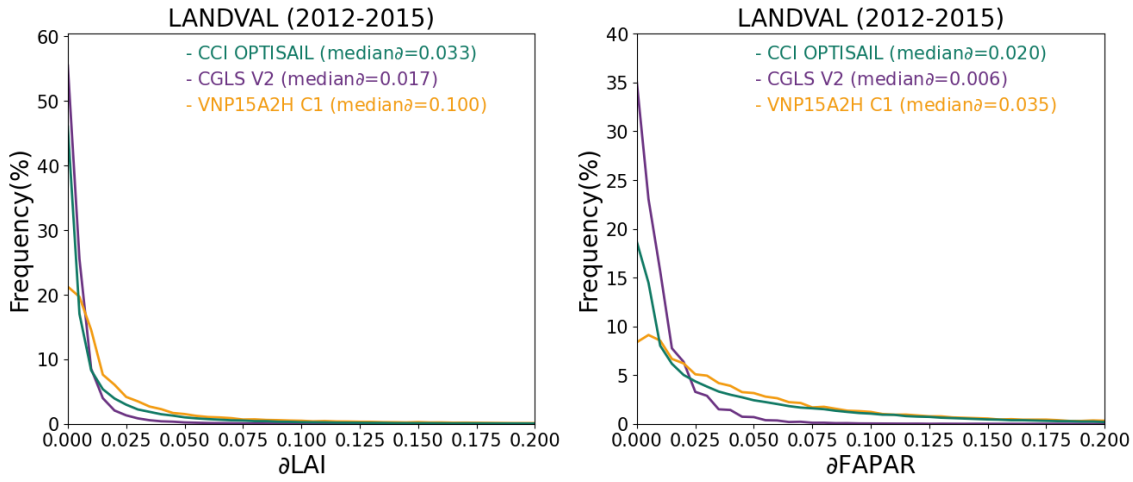

Figure 31: Histograms of delta function (smoothness) for VP_CCI (CCI OPTISAIL) (green), CGLS V2 (purple) and VNP15A2H C1 (yellow) LAI (left) and fAPAR (right) products over LANDVAL sites during the 2012-2015 period.

The main conclusions are:

- CGLS V2 shows, as expected, lower δ values as this product uses smoothing techniques in the algorithm (Verger et al., 2023), which was clearly observed in the temporal consistency analysis.
- VP_CCI provides, in overall, lower δ values than VNP15A2H C1, which is translated in higher precision at short time scale.

3.5.4 Inter-annual precision

To investigate the inter-annual precision of VP_CCI, CGLS V2 and VNP15A2H C1, violin plots per bin value of absolute inter-annual anomalies for the 2012-2015 period (i.e., year 2012 vs. 2013, 2013 vs. 2014 and 2014 vs. 2015) of the products under study were computed using the upper 95th and lower 5th percentiles over LANDVAL sites. Figure 32 and Figure 33 show the inter-annual precision for LAI and fAPAR products. The median of the absolute anomaly is proposed as overall indicator of inter-annual precision.

Main conclusions are:

- All products show similar inter-annual precision.
- For LAI, VP_CCI shows slightly better inter-annual precision (4.7%) than the other products: CGLS V2 (6%) and VNP15A2H C1 (7.8%).
- For fAPAR, VP_CCI (6.1%) shows slightly worse inter-annual than CGLS V2 (5.3%) but better than VNP15A2H C1 (7.5%).

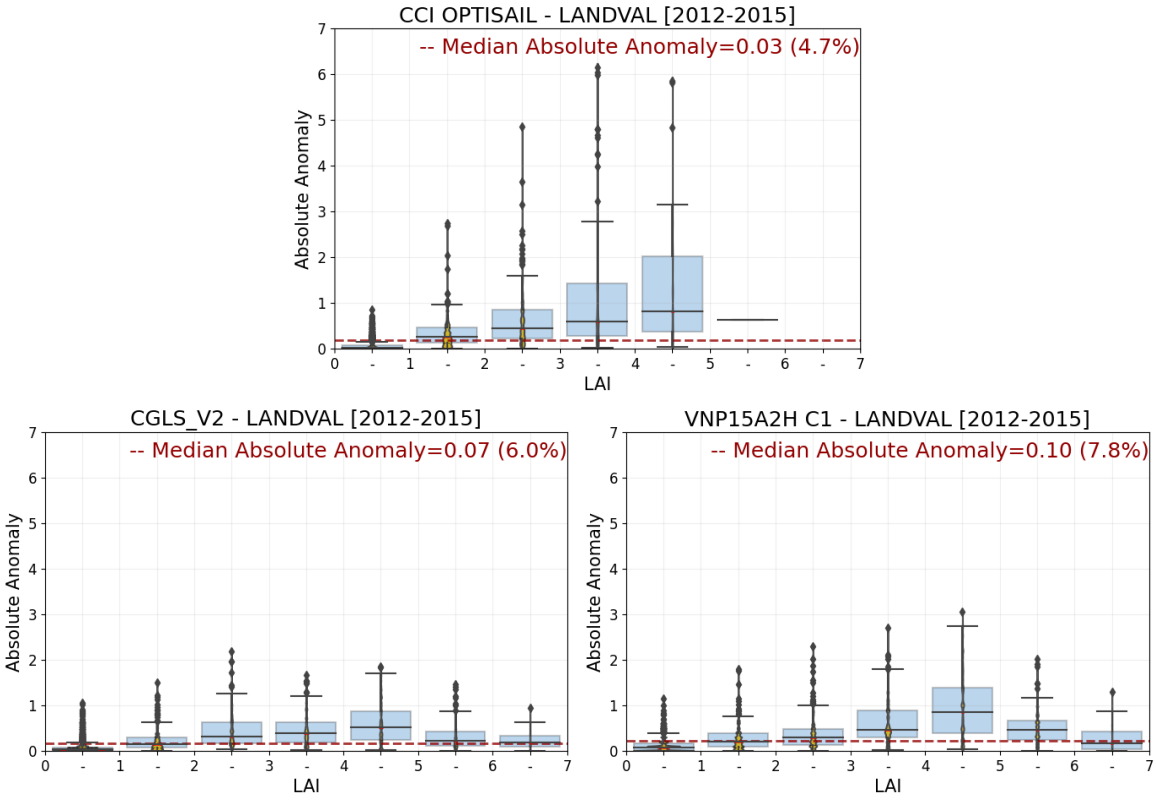

Figure 32: Violin plots of inter-annual absolute anomalies of VP_CCI (CCI OPTISAIL) (top), CGLS V2 (bottom-left) and VNP15A2H C1 (bottom-right) for 2012-2015 period per bin LAI value. Black bars in each box indicate median values and the dashed red line corresponds to the median absolute anomaly including all LAI ranges.

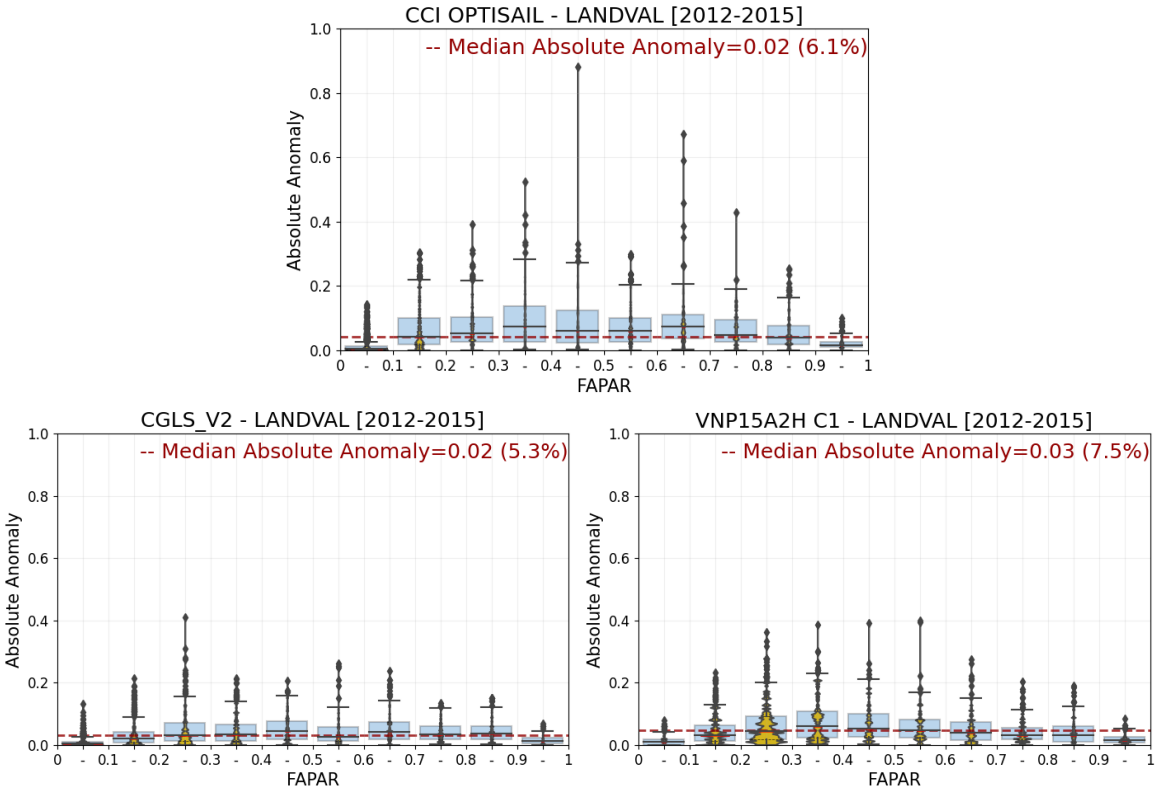

Figure 33: As in Figure 32 for fAPAR.

3.6 Quality layers analysis

In order to identify and remove the unexpected high values observed in the visual inspection of maps (see section 3.2.1) and analysis of temporal trajectories (see outliers in section 3.3), two indicators have been analyzed in addition to the recommended best quality pixels (i.e., RETR_UNTRUSTED of invcode, see Table 3):

- **p_chisquare** (χ^2: probability of Chi-square statistics). This parameter is provided as an additional layer in the product. It ranges from 0 to 1, where low values mark bad correspondence of model and data. Different χ^2 thresholds (χ^2<0.1, χ^2<0.5 or χ^2<0.8) have been investigated to remove outliers.
- **RETR_LOW_QUALITY.** This flag is included in the bit 9 of **Invcode** (inversion code) layer.

3.6.1 Impact on product completeness

Figure 34 shows the temporal evolution of missing values of VP_CCI best quality pixels (green) and the effect of including additional flags: pixels with χ^2<0.1 (purple), χ^2<0.5 (yellow), χ^2<0.8 (pink) or RETR_LOW_QUALITY (red) were removed.

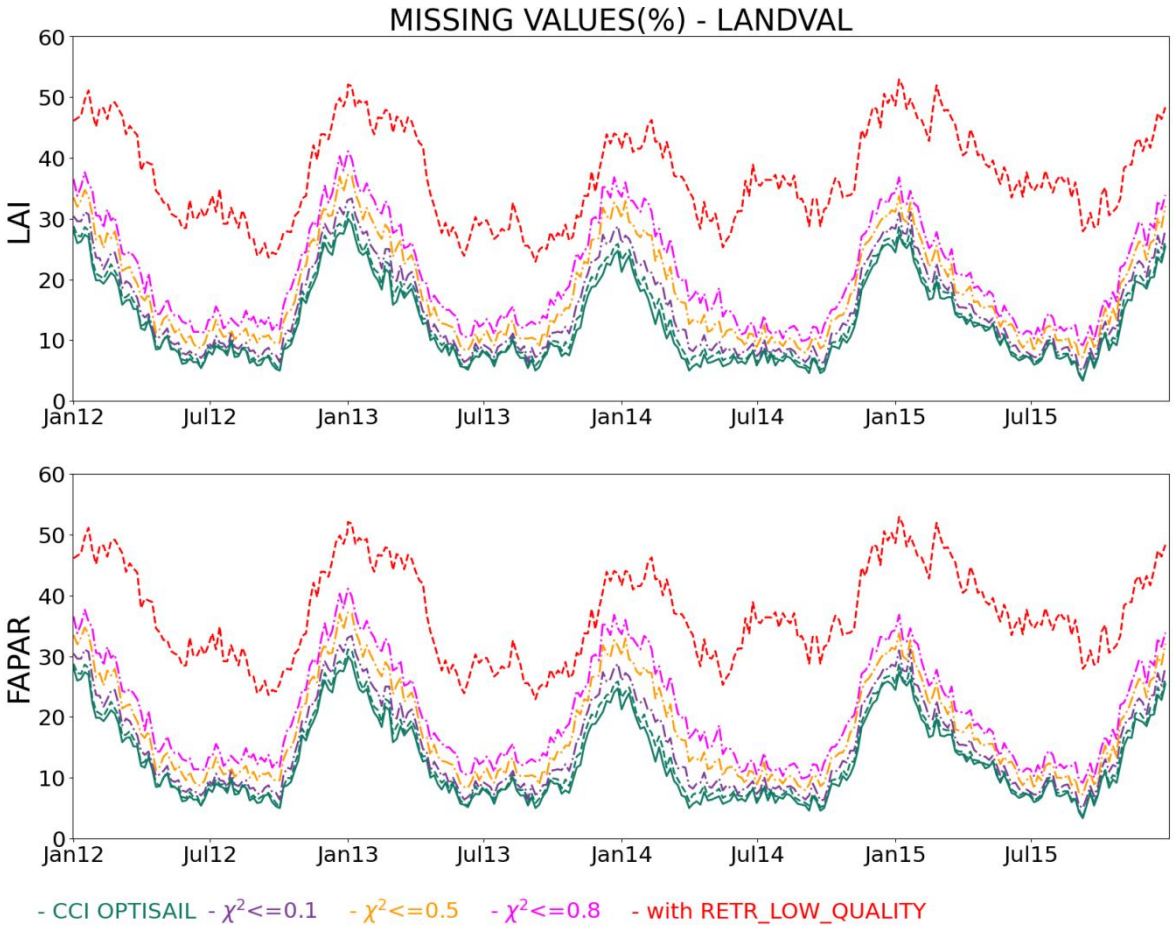

Figure 34: Temporal variation of the percentage of missing values (computed over LANDVAL sites) for VP_CCI (CCI OPTISAIL) considering best quality pixels (green) and including additional flags: pixels with χ^2<0.1 (purple), χ^2<0.5 (yellow), χ^2<0.8 (pink) or RETR_LOW_QUALITY (red) were removed.

The main conclusions are:

- The impact of including χ^2 additional flag is significantly lower in the product completeness compared with RETR_LOW_QUALITY, with an increase of the maximum value of missing data from 31% to 41% in case of the most restrictive threshold (χ^2<0.8).
- The use of RETR_LOW_QUALITY has a major impact on the product completeness, with an increase of the maximum values of missing data from 31% to 53% in January and displaying a larger increase of missing data around July (from 15% to 35%). The use of this flag will imply to have even lower completeness than other existing products.

3.6.2 Impact on spatial consistency

This sub-section analyses the impact of using the additional quality layers on the removal of spatial inconsistencies (i.e., unexpected high values). Maps of the X18Y02 tile are displayed for different dates: two for winter-time (2014.01.16 in Figure 35 and 2014.01.31 in Figure 36) and two for spring (2014.05.31 in Figure 37) and summer (2014.07.10 in Figure 38).

Main findings from the visual investigation of these maps are:

- For winter time (2014.01.16 in Figure 35 and 2014.01.31 in Figure 36), RETR_LOW_QUALITY seems to be more effective to remove unexpected high values than χ^2 (all thresholds). When using χ^2, the higher threshold the better removal.
- However, the use of RETR_LOW_QUALITY should be used with caution in spring (2014.05.31 in Figure 37) and summer (2014.07.10 in Figure 38), as it removes most of reliable observations.

Best quality (RETR_UNTRUSTED)

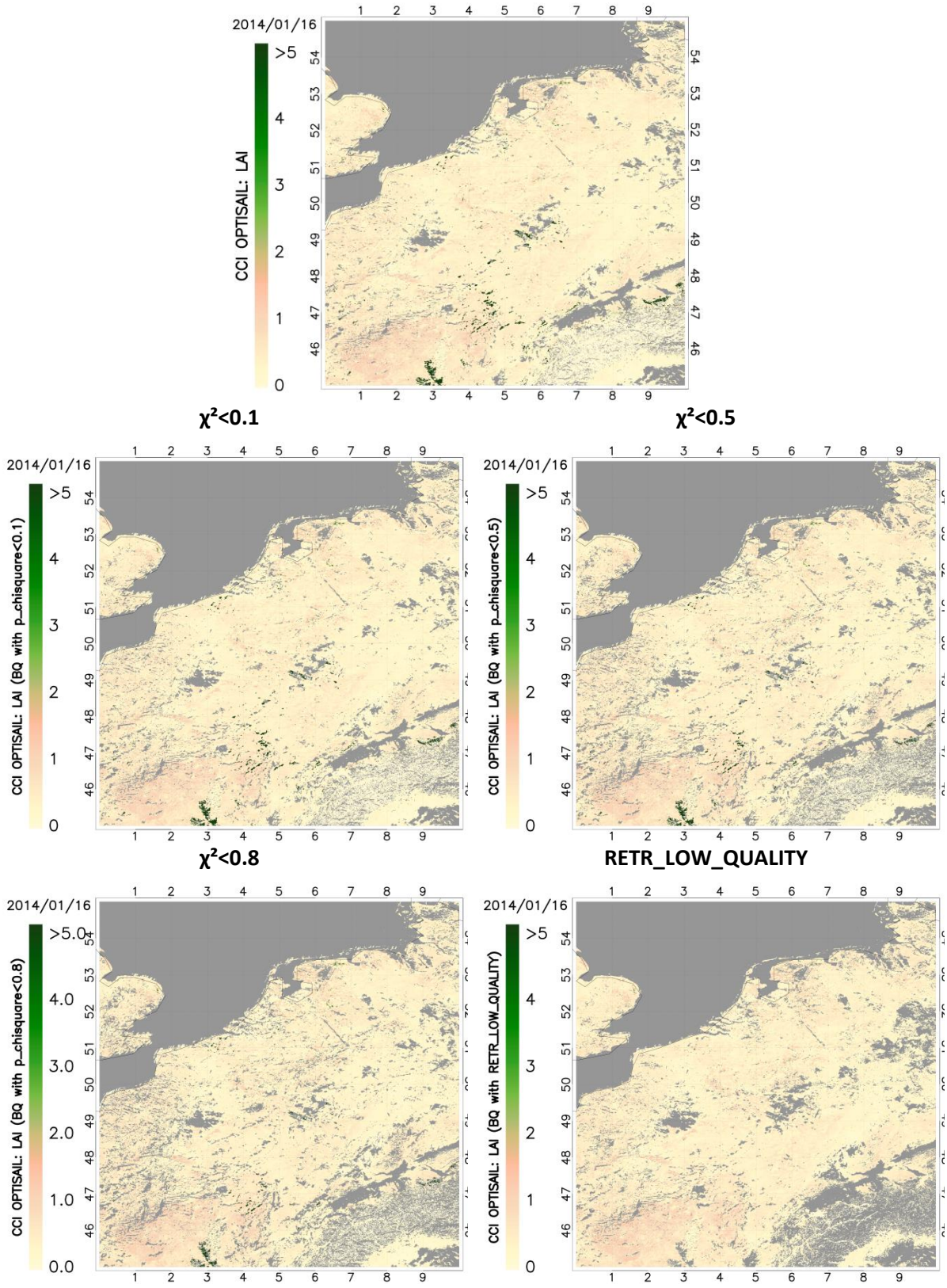

Figure 35: Maps over X18Y02 tile (2014.01.16) of VP_CCI (CCI OPTISAIL) LAI products best quality pixels (Top) and including additional flags: pixels with χ^2<0.1 (middle-left), χ^2<0.5 (middle-right), χ^2<0.8 (bottom-left) or RETR_LOW_QUALITY (bottom-right) were removed.

Best quality (RETR_UNTRUSTED)

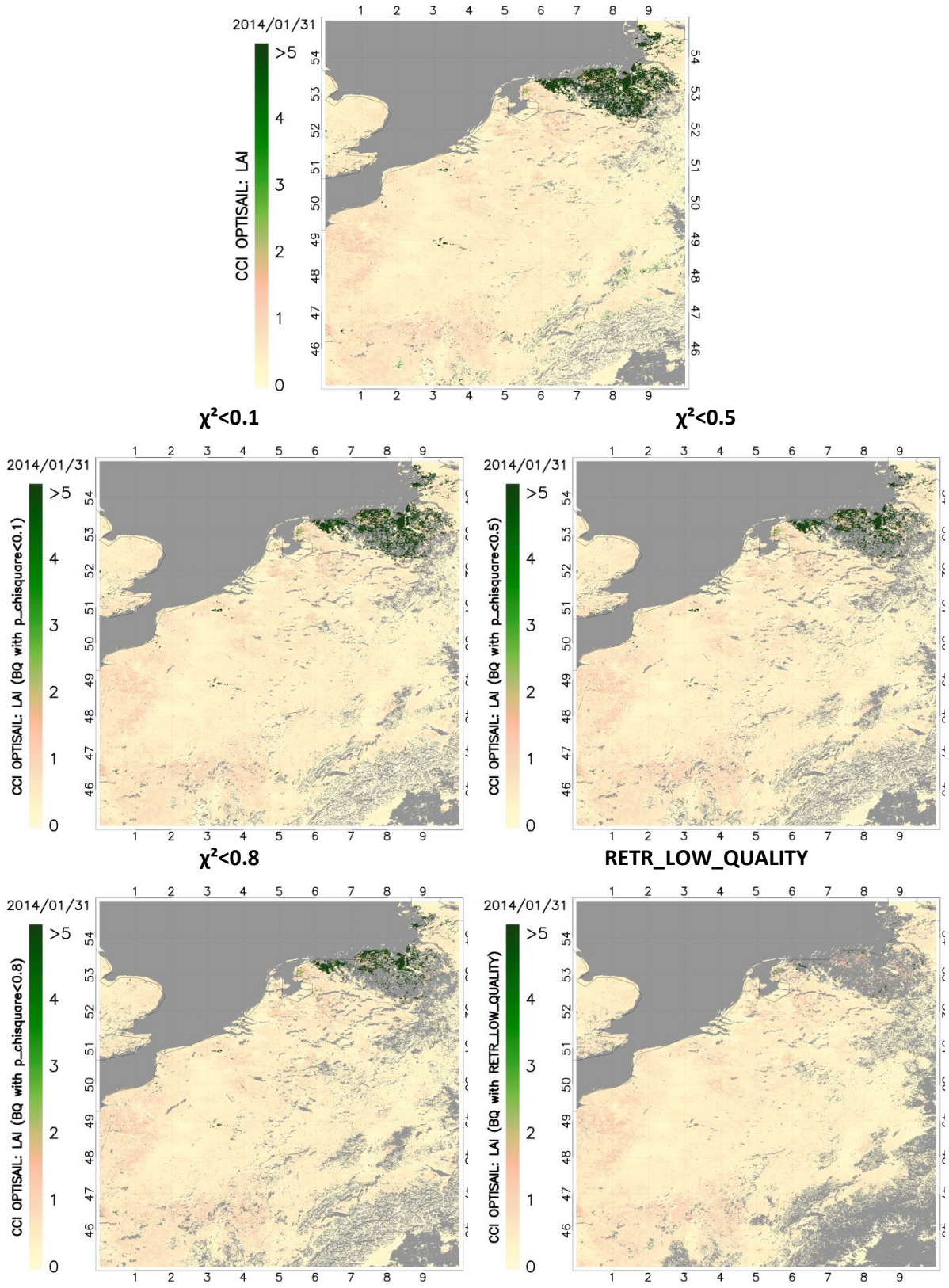

Figure 36: Maps over X18Y02 tile (2014.01.31) of VP_CCI (CCI OPTISAIL) LAI products best quality pixels (Top) and including additional flags: pixels with χ^2<0.1 (middle-left), χ^2<0.5 (middle-right), χ^2<0.8 (bottom-left) or RETR_LOW_QUALITY (bottom-right) were removed.

Best quality (RETR_UNTRUSTED)

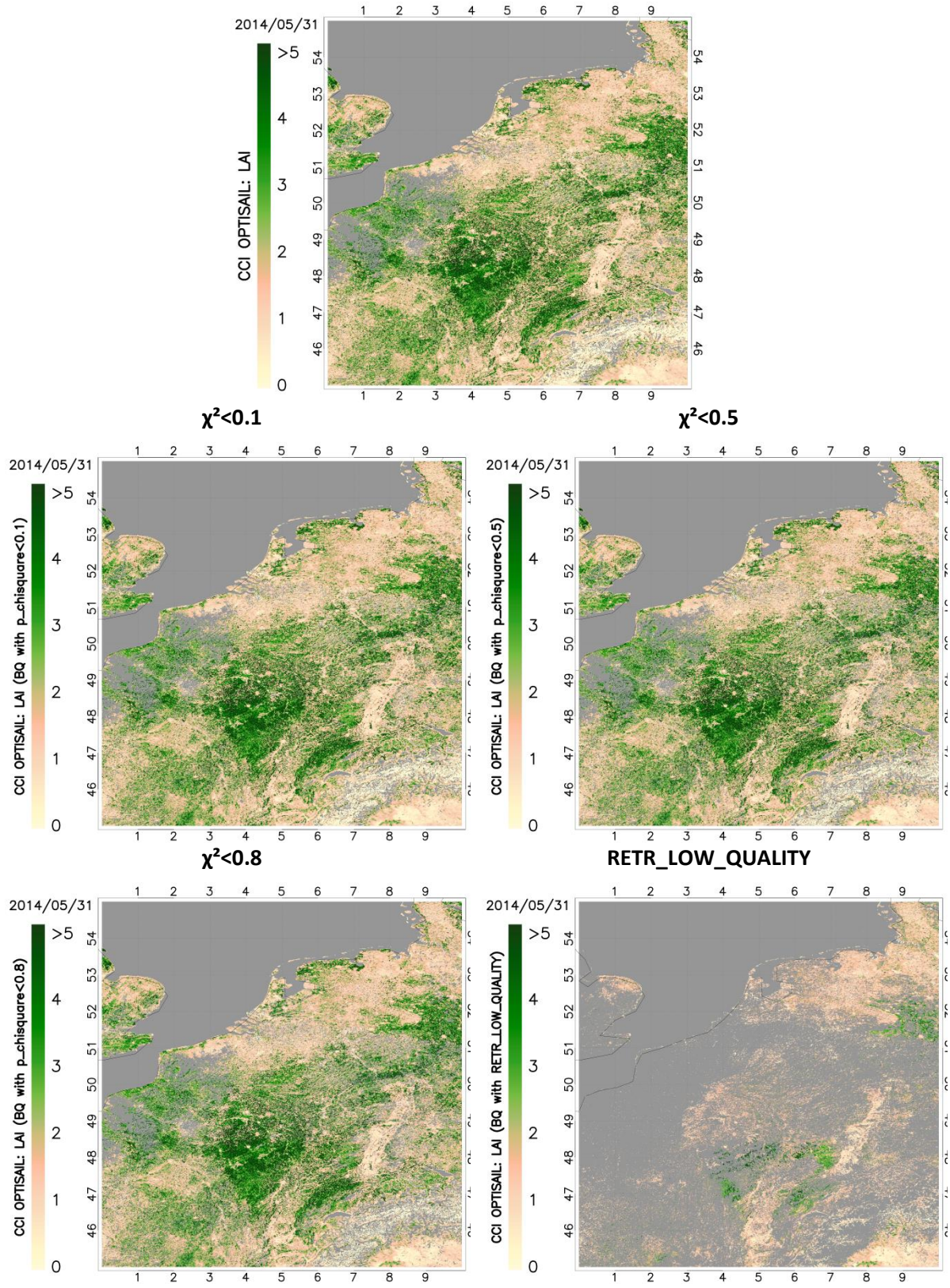

Figure 37: Maps over X18Y02 tile (2014.05.31) of VP_CCI (CCI OPTISAIL) LAI products best quality pixels (Top) and including additional flags: pixels with χ^2<0.1 (middle-left), χ^2<0.5 (middle-right), χ^2<0.8 (bottom-left) or RETR_LOW_QUALITY (bottom-right) were removed.

Best quality (RETR_UNTRUSTED)

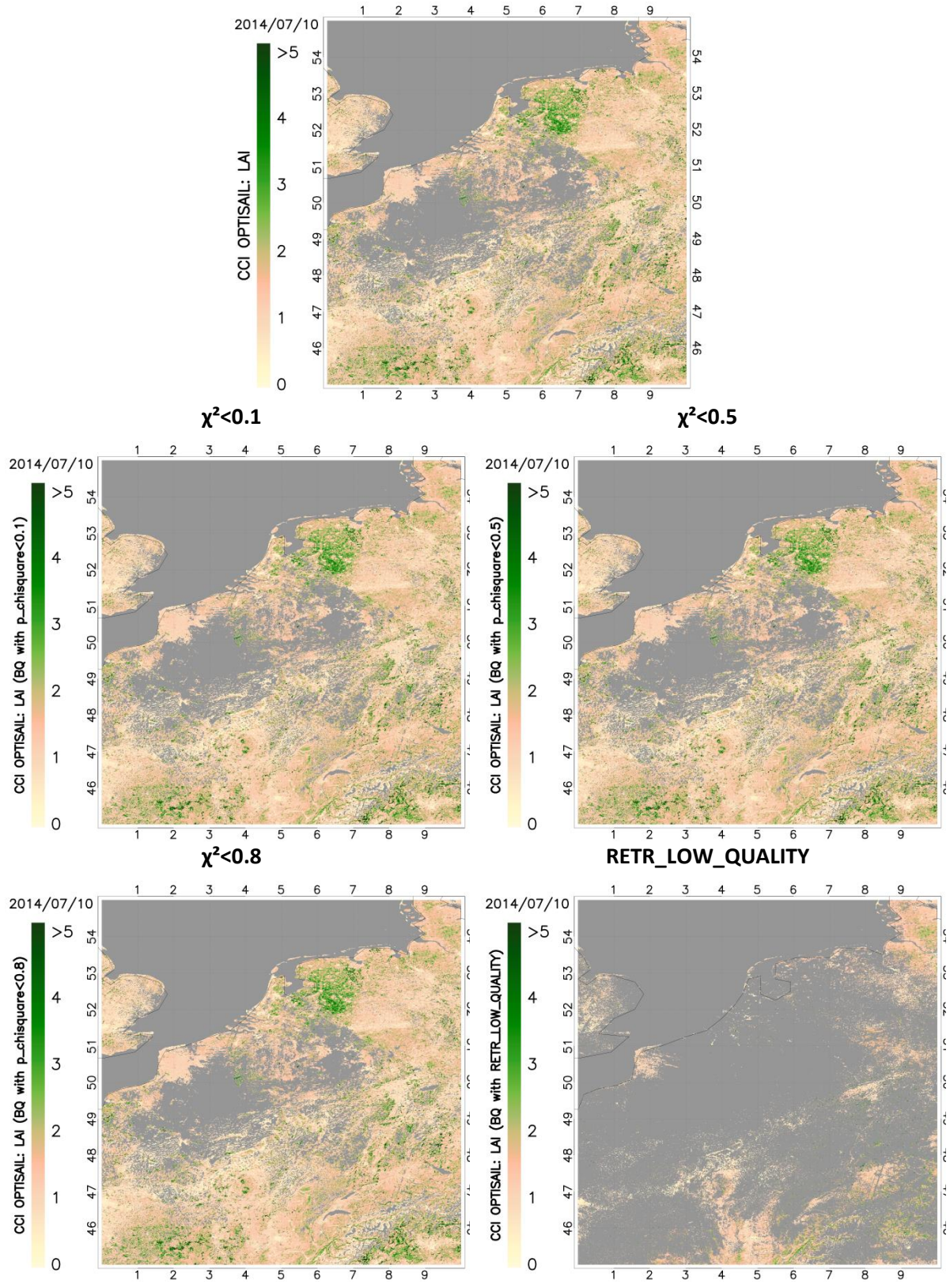

Figure 38: Maps over X18Y02 tile (2014.07.10) of VP_CCI (CCI OPTISAIL) LAI products best quality pixels (Top) and including additional flags: pixels with χ^2<0.1 (middle-left), χ^2<0.5 (middle-right), χ^2<0.8 (bottom-left) or RETR_LOW_QUALITY (bottom-right) were removed.

3.6.3 Impact on temporal consistency

In order to evaluate the utility of the additional flags in the removal of outliers, 50 sites for each biome type are analysed. The outlier classification is based on visual inspection. Figure 39 shows the number and percentage of sites affected by at least one outlier. The biome types more affected by outliers are NLF (>80% of sites) and SBA (about 60% of sites). The rest of biomes present outliers in around 50% of cases, except DBF where only 40% of sites are affected. In average, around 50% of sites present outliers.

Figure 40 shows the number and percentage of outliers that can be filtered using different additional quality layers: χ^2<0.1, χ^2<0.5, χ^2<0.8 or RETR_LOW_QUALITY.

- χ^2<0.1 removes between 30-60% of outliers.
- χ^2<0.5 removes between 60-85% of outliers.
- χ^2<0.8 removes between 70-90% of outliers.
- RETR_LOW_QUALITY removes between 45-95% of outliers.

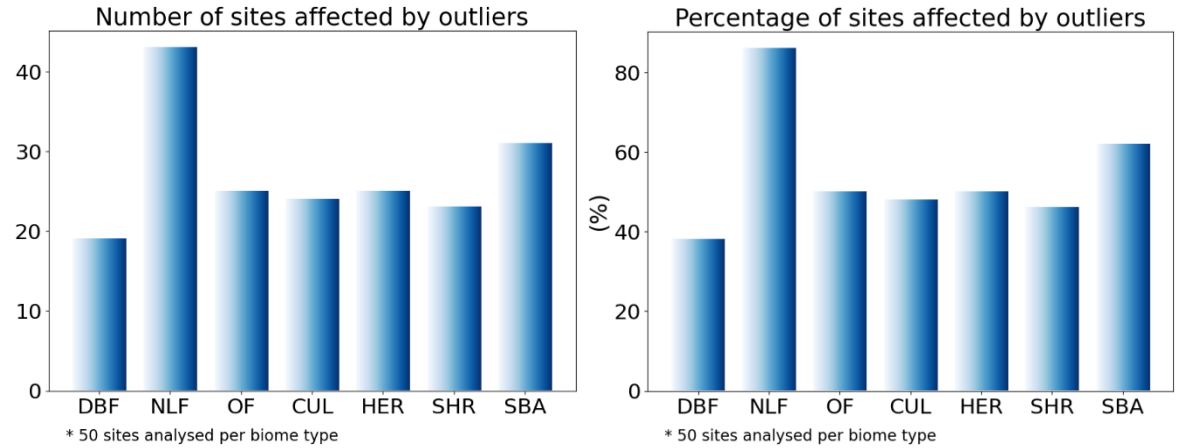

Figure 39: Number (left) and percentage (right) of sites affected by outliers based on qualitative evaluation of 50 sites for each biome type.

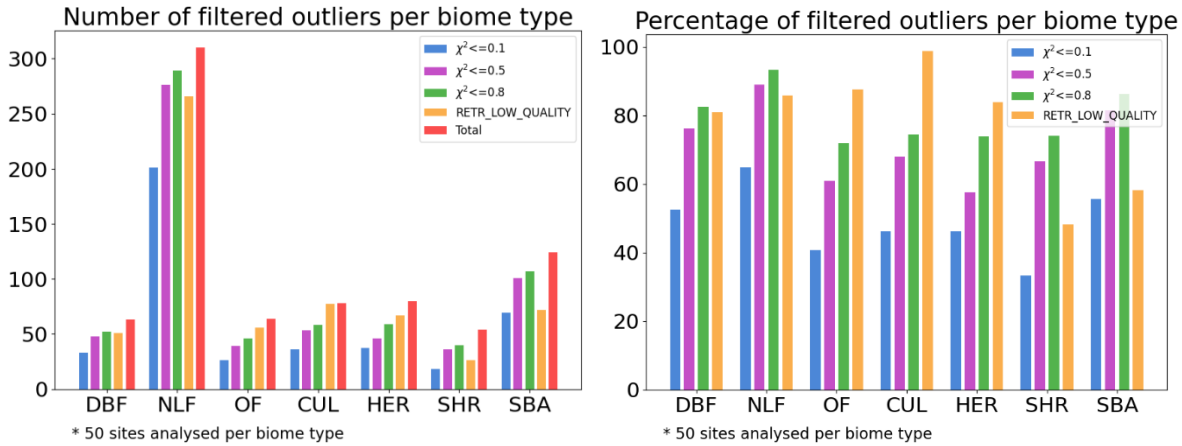

Figure 40: Number (left) and percentage (right) of outliers that can be filtered using different additional quality layers: χ^2<0.1 (blue), χ^2<0.5 (purple), χ^2<0.8 (green) or RETR_LOW_QUALITY (yellow).

Figure 41, Figure 42 and Figure 43 shows several examples of temporal trajectories for NLF, cultivated and SBA selected sites.

In case of χ^2, when the threshold turns more restrictive (χ^2<0.1, χ^2<0.5, χ^2<0.8), the outlier identification is better, but more valid data is also removed (see red crosses in temporal profiles).

RETR_LOW_QUALITY typically removes more valid data than χ^2 (in line to that found in previous sub-section 3.6.2). Most of the outliers can be identified using RETR_LOW_QUALITY but it detects lower number of outliers than χ^2 in some biomes such as NLF and SBA (the biomes which are more affected by outliers).

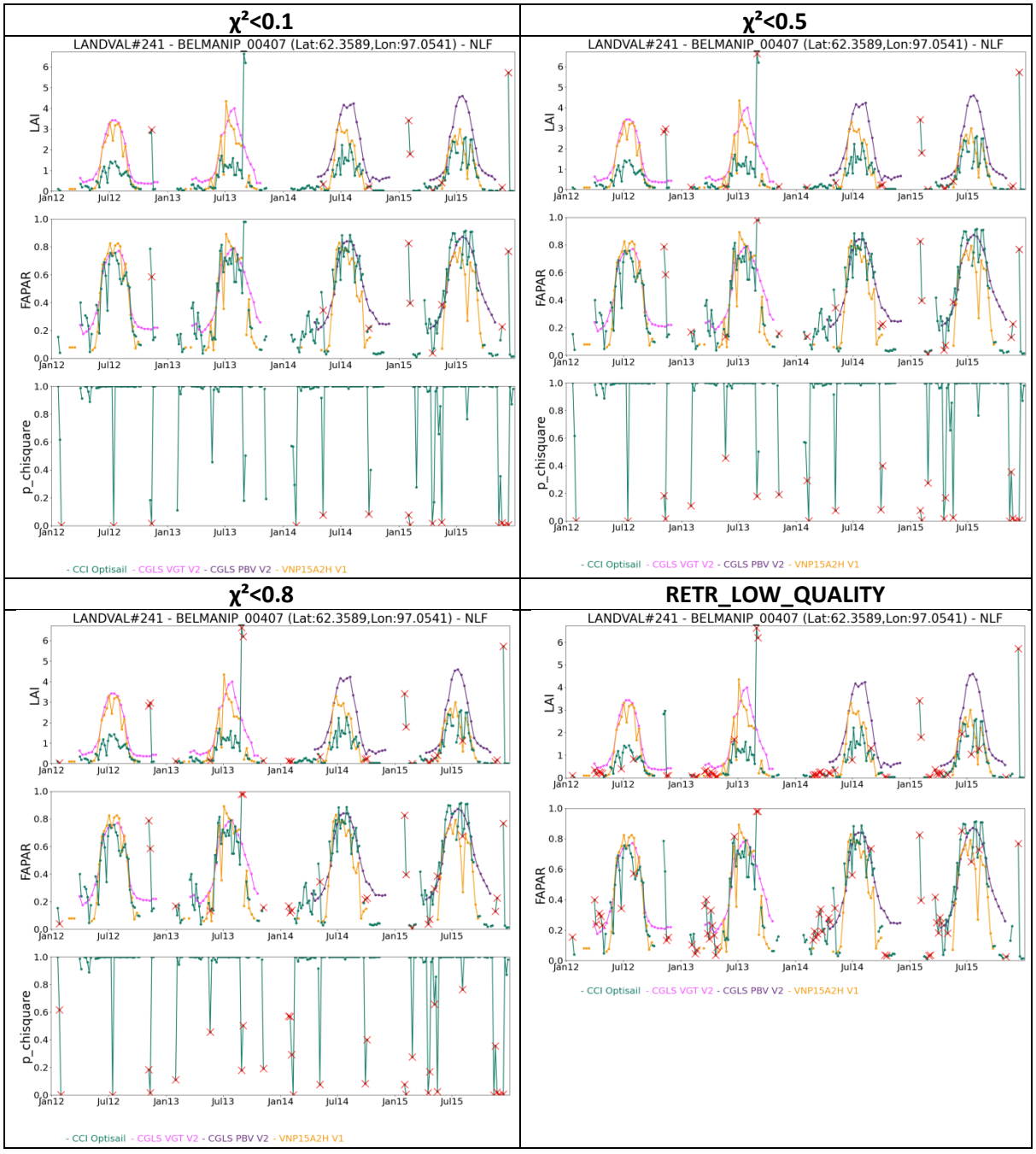

Figure 41: Temporal profiles over a selected NLF site of VP_CCI (CCI OPTISAIL) (green), CGLS (pink for SPOT/VGT and purple for PROBA-V) and VNP15A2H C6.1 (yellow). In case of VP_CCI the activation of additional flags is represented by red crosses: χ^2<0.1 (top-left), χ^2<0.5 (top-right), χ^2<0.8 (bottom-left) or RETR_LOW_QUALITY (bottom-right)

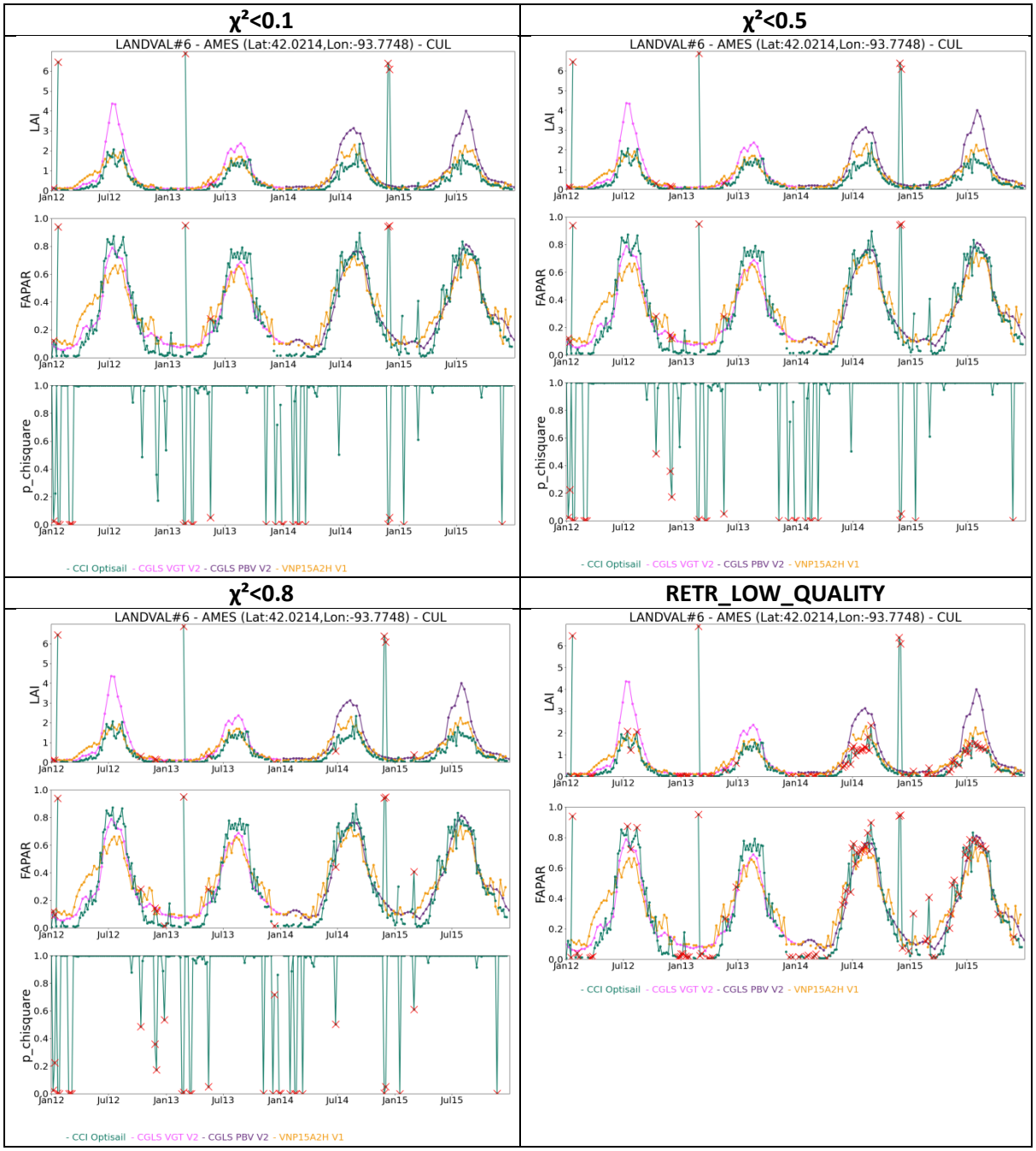

Figure 42: Temporal profiles over a selected cultivated site of VP_CCI (CCI OPTISAIL) (green), CGLS (pink for SPOT/VGT and purple for PROBA-V) and VNP15A2H C6.1 (yellow). In case of VP_CCI the activation of additional flags is represented by red crosses: χ²<0.1 (top-left), χ²<0.5 (top-right), χ²<0.8 (bottom-left) or RETR_LOW_QUALITY (bottom-right)

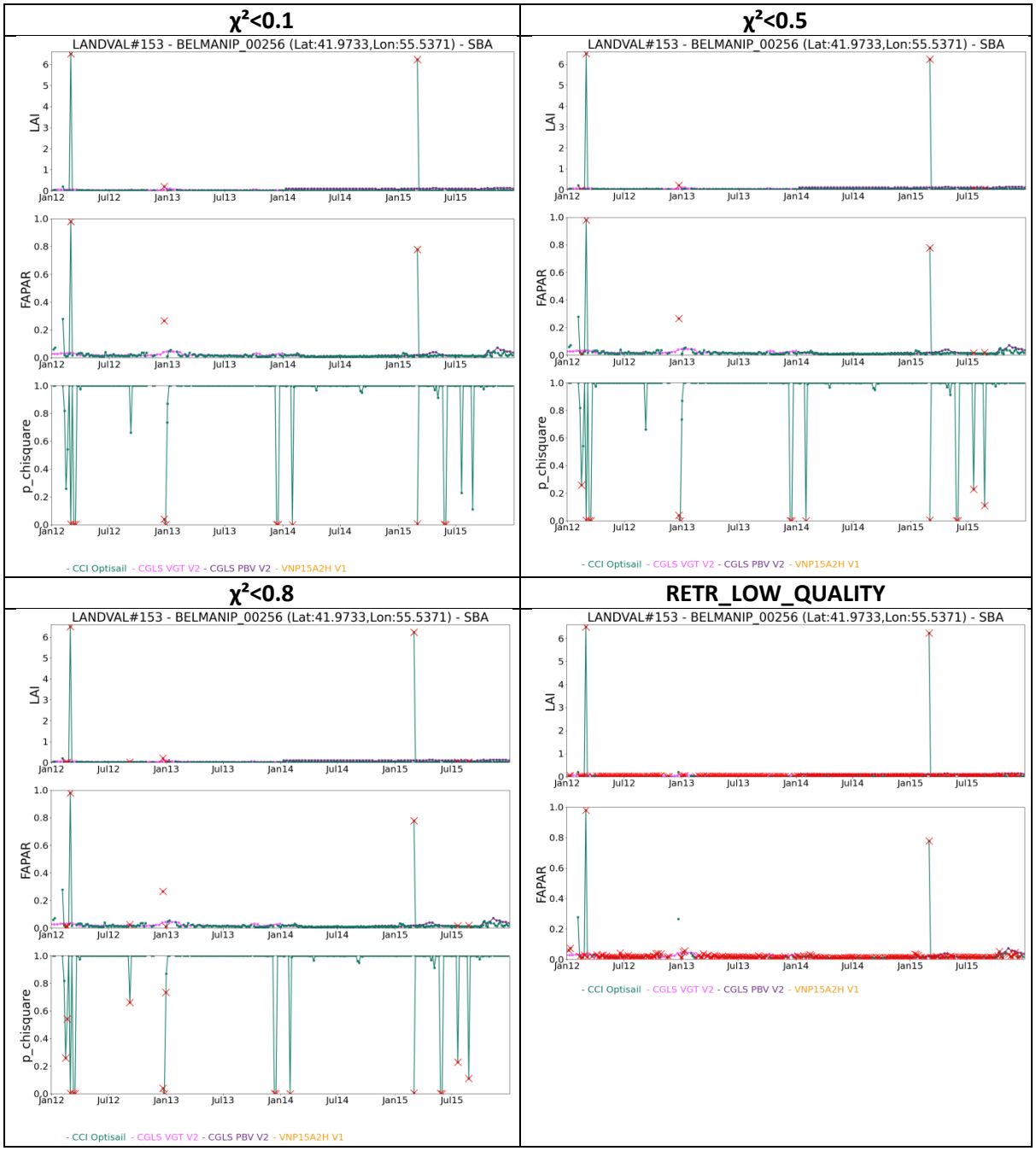

Figure 43: Temporal profiles over a selected SBA site of VP_CCI (CCI OPTISAIL) (green), CGLS (pink for SPOT/VGT and purple for PROBA-V) and VNP15A2H C6.1 (yellow). In case of VP_CCI the activation of additional flags is represented by red crosses: χ²<0.1 (top-left), χ²<0.5 (top-right), χ²<0.8 (bottom-left) or RETR_LOW_QUALITY (bottom-right)

4 Conclusions

The quality assessment of VP_CCI LAI and fAPAR products is conducted over a climate data record (2000-2020) dataset retrieved from SPOT/VGT and PROBA-V input data (CDRP-1). The dataset was generated over a latitudinal North-South transect and over a selection of sites for both product intercomparison (LANDVAL) and direct validation (DIRECT V2.1, GBOV, AMMA) purposes. The methodology is described in the product validation plan [VP-CCI_D1.3_PVP_V1.1], in agreement with the CEOS LPV best practices for validation of LAI products. Two main validation approaches are defined: direct validation (i.e., comparison of satellite products with in situ measurements) and indirect validation or product intercomparison. Several criteria of performance are evaluated, including completeness, spatial consistency, temporal consistency, error evaluation (Accuracy, Precision and Uncertainty) and conformity test regarding CGOS uncertainty requirements.

The summary of the validation results is provided in Table 7. Main conclusions for each quality criteria are:

Product completeness

- VP_CCI shows the expected spatial trend of missing data, which is mainly located over northern regions (wintertime) and the equatorial belt.
- Over areas typically affected by cloud/snow (northern regions in winter) and persistent cloud coverage (equatorial), VP_CCI shows better completeness than CGLS V2 non-filled and VNP15A2H C1, which could be indicative of less restrictive cloud/snow screening approach.

Spatial consistency

- VP_CCI LAI and fAPAR shows, generally, reliable spatial distributions. However, the spatial consistency needs to be improved as several inconsistencies are found:
    - Unrealistic high values over northern regions (Europe), showing abrupt changes (i.e., outliers) between consecutive dates for both local scale and larger areas.
    - Unrealistically low values for LAI over equatorial areas with noisy transitions between consecutive dates.
    - Stripes displaying different values over northern latitudes in winter and equatorial areas.
- VP_CCI and CGLS V2 are spatially consistent over large areas with most of residuals between ±0.5 LAI and ±0.1 fAPAR. Larger spatial inconsistencies are however observed over equatorial areas and Europe.

Temporal consistency

- VP_CCI temporal variations display good consistency with reference products over most of the 720 LANDVAL sites, as well as they are consistent with ground data showing similar temporal trajectories.
- The main limitations from the qualitative inspection of VP_CCI temporal trajectories are:
    - Noisy temporal variations mainly over EBF, probably due to cloud contamination.
    - Some outliers are found typically during wintertime.
- VP_CCI displays remarkably good temporal continuity when different data sources are used (SPOT/VGT, PROBA-V), improving that of other products (e.g., CGLS V2) over sparse vegetated and desert targets.

Error evaluation (Direct validation)

- Comparison with DIRECT V2.1:
    - For effective LAI, VP_CCI shows systematic lower values (mainly for forest higher values) (B=-0.6) and RMSD of 1.2. Around 16% and 26% of VP_CCI cases are within goal and threshold GCOS uncertainty requirements.
    - Satellite CGLS V2 and MOD15A2H C6.1 references show slightly better accuracy and only slightly higher number of cases within goal (~17-19%) and threshold (~28-30%) GCOS uncertainty requirements.
    - For fAPAR, VP_CCI shows systematic positive bias (0.07), linear relationship (slope~ 1) and RMSD of 0.15. Satellite references show better overall agreement for fAPAR.
    - VP_CCI provides lower number of samples within optimal (12%) and threshold (22%) GCOS uncertainty requirements than CGLS V2 (23% and 33%) and MOD15A2H C6.1 (22% and 30%).

- Comparison with GBOV V3:
    - VP_CCI shows large negative bias compared with GBOV V3 LAI for forest sites, as expected (LAIeff VP_CCI vs LAI true GBOV).
    - For non-forest sites VP_CCI shows better agreement with GBOV V3 LAI (B=0.1, RMSD= 0.29) than CGLS V2 and VNP15A2H C1. For non-forest sites, VP_CCI shows the higher number of samples within GCOS optimal (25%) and threshold (47%) uncertainty requirements.
    - For fAPAR, VP_CCI (B=0.02, RMSD=0.14) tends to provide higher values than GBOV V3 for non-forest sites and the opposite trend for forest cases. Both satellite references provide lower uncertainties around 0.1.
    - VP_CCI provides slightly lower cases within goal (18%) and threshold (33%) GCOS uncertainty requirements than reference products.
- Comparison with AMMA:
    - VP_CCI shows slight positive bias (0.05) and RMSD of 0.31 compared with AMMA LAIeff, with 18% and 38% of cases are within optimal and threshold GCOS levels. Reference satellite CGLS V2 and MOD15A2H C6.1 products show similar overall uncertainty in relative terms compared with LAI (RMSD~75%).
    - For fAPAR, VP_CCI shows a tendency to provide higher values than AMMA ground measurements (B=0.06, slope=1.3), with overall uncertainty (RMSD) of 0.15. CGLS V2 shows the best agreement (B~0, RMSD=0.12) and MOD15A2H C6.1 shows similar performance than VP_CCI.

Error evaluation (product intercomparison)

- VP_CCI shows, as expected, large differences (lower values) with CGLS V2, MOD15A2H C6.1 and VNP15A2H C1 due to the different LAI definitions (LAIeff vs true LAI). Slopes of MAR are typically around 0.5 compared with references. The comparison of VP_CCI fAPAR with reference satellite products shows:
    - VP_CCI vs CGLS V2 shows the better agreement (B=-4%, RMSD = 0.09). VP_CCI typically tends to provide slightly lower values than CGLS V2 for low values and high (EBF) values.
    - Worse agreement is found in the comparison of VP_CCI vs NASA MOD15A2H C6.1 and VNP15A2H C1 products (RMSD=0.13). The NASA product is higher than VP_CCI for low fAPAR values, expected due to known NASA products limitations.
    - Per biome type, larger discrepancies are found between VP_CCI and reference products for EBF and NLF.

- VP_CCI provides, in overall, better intra-annual precision than VNP15A2H C1 (i.e., high stability at short time scale) and worse than CGLS V2 (expected as it is a smoothed product).
- The inter-annual precision of VP_CCI (4.7% for LAI and 6.1% for fAPAR) is similar to that found for CGLS V2 and slightly better than VNP15A2H C1.

Summary and concluding remarks:

This validation exercise, performed over a limited dataset (global sampling of sites and latitudinal transect), demonstrated overall good quality of VP_CCI LAI and fAPAR product. The product completeness was better than other existing reference products, because of ingesting thin clouds in the OPTISAIL retrieval. A good spatial consistency is found in overall, however there are some spatial inconsistencies such as stripes or unrealistic high values that need to be improved at local scale. VP_CCI LAI and fAPAR temporal variations are consistent with reference products and ground observations. The direct validation using DIRECT V2.1, GBOV V3 and AMMA showed good correlations with only slightly worse accuracy and l uncertainty than other satellite references, except in the comparison with GBOV V3 for non-forest cases where VP_CCI shows the best agreement. The comparison with satellite references shows, as expected, lower values for LAI (VP_CCI provides LAIeff whilst references true LAI) and good agreement for FAPAR (RMSD=0.09 compared with CGLS V2 and RMSD=0.12 compared with MOD15A2H C6.1 and VNP15A2H C1). VP_CCI provides, in overall, better smoothness than VNP15A2H C1 (i.e., higher precision at short time scale) and worse than CGLS V2 (as expected as it is a smoothed product). The inter-annual precision of VP_CCI is similar to that found for CGLS V2 and slightly better than VNP15A2H C1.

The main limitations of the VP_CCI products are:

- Stripes artifacts and some spatial inconsistencies over northern regions (Europe, with abrupt changes showing unexpected high values) and equatorial areas (lower values), probably due to cloud/snow contamination.
- Noisy profiles (mainly for EBF) and some outliers for other biomes are found.

It should be noted that p_chisquare or RETR_LOW_QUALTY layers could be partly useful to identify (and filter) most of these outliers as a consequence of more restrictive screening (i.e., worse completeness). In case of χ^2, when the threshold turns more restrictive (i.e., greater χ^2), the outlier identification is better, but more valid data is also removed. RETR_LOW_QUALITY is also useful to identify most of the outliers, but the product completeness is considerably worse removing a large amount of valid retrievals. Consequently, based on our analysis, it is recommended to use χ^2 to filter outliers.

Table 7: Summary of VP_CCI validation results

Criteria	performance	Comments
Product completeness	+	- Gaps located in wintertime (northern) and equatorial areas. Better than reference products over these areas (probably cloud/snow contamination). VP_CCI quality flag is little restrictive.
Spatial consistency	±	- Relivable distributions and good spatial consistency with CGLS V2 over most areas. - Some stripe artefacts and spatial inconsistencies mainly over EBF and some areas over Europe.

Temporal consistency	±	- VP_CCI shows similar temporal trends than reference satellite products (CGLS V2, MOD15A2H C6.1, VNP15A2H C1) and ground observations (DIRECT V2.1, GBOV V3 and AMMA). - VP_CCI provides some outliers not identified by quality flags and noisy temporal trends over EBF.
Error evaluation: Direct validation vs DIRECT V2.1	±	LAI: - B=-0.6, RMSD=1.2, goal/threshold=16%/26%. VP_CCI<DIRECT V2.1 mainly for high values (forests). - References show improved results: CGLS V2 (19%/30% within optimal/target) and MOD15A2H C6.1 (17%/28%) fAPAR : - B=0.07, RMSD=0.15, goal/threshold=12%/22%. Linear relation (slope ~ 1). - References show improved results: CGLS V2 (23%/33% within optimal/target) and MOD15A2H C6.1 (22%/ 30%).
Error evaluation: Direct validation vs GBOV V3	±	LAI (forest): - VP_CCI (LAIeff) < GBO V3 (true LAI). LAI (non-forest): - B=0.01, RMSD=0.29, goal/threshold=25%/48%. - References show worse results: CGLS V2 (5%/10% within optimal/target) and VNP15A2H C1 (12%/ 22%). fAPAR: - B=0.02, RMSD=0.14, goal/threshold=18%/33%. VP_CCI > GBOV V3 for non-forest sites and < for forest cases. - References show better results: CGLS V2 (23%/38% within optimal/target) and VNP15A2H C1 (19%/ 38%).
Error evaluation: Direct validation vs AMMA	±	LAI: - B=0.05, RMSD=0.31, goal/threshold=18%/38%. - References show worse compliance: CGLS V2 (17%/30% within optimal/target) and MOD15A2H C6.1 (11%/30%). fAPAR: - B=0.06, RMSD=0.15, goal/threshold=7%/12%. - References show better results: CGLS V2 (8%/17% within optimal/target) and MOD15A2H C6.1 (10%/ 21%).
Error evaluation: Product intercomparison	±	LAI: - Large differences in both cases (LAIeff vs true LAIeff). fAPAR : - Vs. CGLS V2: B=-0.01, RMSD=0.09, goal/threshold=16%/30% - VS. NASA: B=-0.3, RMSD=0.13, % goal/threshold=12%/23% Analysis per biome: large differences for EBF and NLF.
Intra-annual precision	±	- VP_CCI better than VNP15A2H C1 and worse than CGLS V2 (smoothed)
Inter-annual precision	+	- VP_CCI (4.7% for LAI and 6.1% for fAPAR) is similar to that found for CGLS V2 and slightly better than VNP15A2H C1.

References

Asrar, G., Myneni, R.B., 1991. Applications of Radiative Transfer Models for Remote Sensing of Vegetation Conditions and States, in: Photon-Vegetation Interactions. Springer Berlin Heidelberg, pp. 537–558. https://doi.org/10.1007/978-3-642-75389-3_17

Baret, F., Weiss, M., Lacaze, R., Camacho, F., Makhmara, H., Pacholcyzk, P., Smets, B., 2013. GEOV1: LAI and FAPAR essential climate variables and FCOVER global time series capitalizing over existing products. Part1: Principles of development and production. Remote Sens. Environ. 137, 299–309. https://doi.org/10.1016/j.rse.2012.12.027

Blessing, S., Giering, R., 2021. Simultaneous Retrieval of Soil, Leaf, and Canopy Parameters from Sentinel-3 OLCI and SLSTR Multi-spectral Top-of-Canopy Reflectances. https://doi.org/10.20944/PREPRINTS202109.0147.V1

Brown, L.A., Camacho, F., García-Santos, V., Origo, N., Fuster, B., Morris, H., Pastor-Guzman, J., Sánchez-Zapero, J., Morrone, R., Ryder, J., Nightingale, J., Boccia, V., Dash, J., 2021a. Fiducial Reference Measurements for Vegetation Bio-Geophysical Variables: An End-to-End Uncertainty Evaluation Framework. Remote Sens. 2021, Vol. 13, Page 3194 13, 3194. https://doi.org/10.3390/RS13163194

Brown, L.A., Meier, C., Morris, H., Pastor-Guzman, J., Bai, G., Lerebourg, C., Gobron, N., Lanconelli, C., Clerici, M., Dash, J., 2020. Evaluation of global leaf area index and fraction of absorbed photosynthetically active radiation products over North America using Copernicus Ground Based Observations for Validation data. Remote Sens. Environ. 247, 111935. https://doi.org/10.1016/j.rse.2020.111935

Brown, L.A., Ogutu, B.O., Camacho, F., Fuster, B., Dash, J., 2021b. Deriving Leaf Area Index Reference Maps Using Temporally Continuous in Situ Data: A Comparison of Upscaling Approaches. IEEE J. Sel. Top. Appl. Earth Obs. Remote Sens. 14, 624–630. https://doi.org/10.1109/JSTARS.2020.3040080

Camacho, F., Cernicharo, J., Lacaze, R., Baret, F., Weiss, M., 2013. GEOV1: LAI, FAPAR essential climate variables and FCOVER global time series capitalizing over existing products. Part 2: Validation and intercomparison with reference products. Remote Sens. Environ. 137, 310–329. https://doi.org/10.1016/j.rse.2013.02.030

Camacho, F., Fuster, B., Li, W., Weiss, M., Ganguly, S., Lacaze, R., Baret, F., 2021. Crop specific algorithms trained over ground measurements provide the best performance for GAI and fAPAR estimates from Landsat-8 observations. Remote Sens. Environ. 260, 112453. https://doi.org/10.1016/J.RSE.2021.112453

Chen, J.M., Menges, C.H., Leblanc, S.G., 2005. Global mapping of foliage clumping index using multi-angular satellite data. Remote Sens. Environ. 97, 447–457. https://doi.org/10.1016/J.RSE.2005.05.003

D'Odorico, P., Gonsamo, A., Pinty, B., Gobron, N., Coops, N., Mendez, E., Schaepman, M.E., 2014. Intercomparison of fraction of absorbed photosynthetically active radiation products derived from satellite data over Europe. Remote Sens. Environ. 142, 141–154. https://doi.org/10.1016/j.rse.2013.12.005

Fang, H., 2021. Canopy clumping index (CI): A review of methods, characteristics, and applications. Agric. For. Meteorol. 303, 108374. https://doi.org/10.1016/J.AGRFORMET.2021.108374

Fang, H., Wei, S., Liang, S., 2012. Validation of MODIS and CYCLOPES LAI products using global field measurement data. Remote Sens. Environ. 119, 43–54. https://doi.org/10.1016/j.rse.2011.12.006

Fang, H., Zhang, Y., Wei, S., Li, W., Ye, Y., Sun, T., Liu, W., 2019. Validation of global moderate resolution leaf area index (LAI) products over croplands in northeastern China. Remote Sens. Environ. 233, 111377. https://doi.org/10.1016/J.RSE.2019.111377

Féret, J.B., Gitelson, A.A., Noble, S.D., Jacquemoud, S., 2017. PROSPECT-D: Towards modeling leaf optical properties through a complete lifecycle. Remote Sens. Environ. 193, 204–215.

https://doi.org/10.1016/J.RSE.2017.03.004

Fernandes, R.A., Plummer, S.E., Nightingale, J., Baret, F., Camacho, F., Fang, H., Garrigues, S., Gobron, N., Lang, M., Lacaze, R., Leblanc, S.G., Meroni, M., Martinez, B., Nilson, T., Pinty, B., Pisek, J., Sonnentag, O., Verger, A., Welles, J.M., Weiss, M., Widlowski, J.-L., Schaepman-Strub, G., Román, M.O., Nicheson, J., 2014. Global Leaf Area Index Product Validation Good Practices. Version 2.0. In G. Schaepman-Strub, M. Román, & J. Nickeson (Eds.), Best Practice for Satellite-Derived Land Product Validation (p. 76): Land Product Validation Subgroup (WGCV/CEOS), doi:10.5067/do [WWW Document]. https://doi.org/10.5067/doc/ceoswgcv/lpv/lai.002

Fuster, B., Sánchez-Zapero, J., Camacho, F., García-Santos, V., Verger, A., Lacaze, R., Weiss, M., Baret, F., Smets, B., 2020. Quality Assessment of PROBA-V LAI, fAPAR and fCOVER Collection 300 m Products of Copernicus Global Land Service. Remote Sens. 12, 1017. https://doi.org/10.3390/rs12061017

Garrigues, S., Lacaze, R., Baret, F., Morisette, J.T., Weiss, M., Nickeson, J.E., Fernandes, R., Plummer, S., Shabanov, N. V., Myneni, R.B., Knyazikhin, Y., Yang, W., 2008. Validation and intercomparison of global Leaf Area Index products derived from remote sensing data. J. Geophys. Res. Biogeosciences 113. https://doi.org/10.1029/2007JG000635

Harper, W. V., 2014. Reduced Major Axis regression: teaching alternatives to Least Squares. Proc. Ninth Int. Conf. Teach. Stat. 1–4. https://doi.org/10.1016/B978-0-12-420228-3.00013-0

Hiernaux, P., Diarra, L., Trichon, V., Mougin, E., Soumaguel, N., Baup, F., 2009a. Woody plant population dynamics in response to climate changes from 1984 to 2006 in Sahel (Gourma, Mali). J. Hydrol. 375, 103–113. https://doi.org/10.1016/J.JHYDROL.2009.01.043

Hiernaux, P., Mougin, E., Diarra, L., Soumaguel, N., Lavenu, F., Tracol, Y., Diawara, M., 2009b. Sahelian rangeland response to changes in rainfall over two decades in the Gourma region, Mali. J. Hydrol. 375, 114–127. https://doi.org/10.1016/J.JHYDROL.2008.11.005

Justice, C.O., Román, M.O., Csiszar, I., Vermote, E.F., Wolfe, R.E., Hook, S.J., Friedl, M., Wang, Z., Schaaf, C.B., Miura, T., Tschudi, M., Riggs, G., Hall, D.K., Lyapustin, A.I., Devadiga, S., Davidson, C., Masuoka, E.J., 2013. Land and cryosphere products from Suomi NPP VIIRS: Overview and status. J. Geophys. Res. Atmos. https://doi.org/10.1002/jgrd.50771

Knyazikhin, Y., Martonchik, J. V., Myneni, R.B., Diner, D.J., Running, S.W., 1998. Synergistic algorithm for estimating vegetation canopy leaf area index and fraction of absorbed photosynthetically active radiation from MODIS and MISR data. J. Geophys. Res. 103, 32257. https://doi.org/10.1029/98JD02462

Lacherade, S., Fougnie, B., Henry, P., Gamet, P., 2013. Cross calibration over desert sites: Description, methodology, and operational implementation. IEEE Trans. Geosci. Remote Sens. 51, 1098–1113. https://doi.org/10.1109/TGRS.2012.2227061

Leblanc, S.G., Fournier, R.A., 2014. Hemispherical photography simulations with an architectural model to assess retrieval of leaf area index. Agric. For. Meteorol. 194, 64–76. https://doi.org/10.1016/J.AGRFORMET.2014.03.016

Loew, A., Bennartz, R., Fell, F., Lattanzio, A., Doutriaux-Boucher, M., Schulz, J., 2016. A database of global reference sites to support validation of satellite surface albedo datasets (SAVS 1.0). Earth Syst. Sci. Data 8, 425–438. https://doi.org/10.5194/essd-8-425-2016

Miller, J.B., 1967. A formula for average foliage density. Aust. J. Bot. 15, 141–144. https://doi.org/10.1071/BT9670141

Morisette, J.T., Baret, F., Privette, J.L., Myneni, R.B., Nickeson, J.E., Garrigues, S., Shabanov, N. V., Weiss, M., Fernandes, R.A., Leblanc, S.G., Kalacska, M., Sánchez-Azofeifa, G.A., Chubey, M., Rivard, B., Stenberg, P., Rautiainen, M., Voipio, P., Manninen, T., Pilant, A.N., Lewis, T.E., Iiames, J.S., Colombo, R., Meroni, M., Busetto, L., Cohen, W.B., Turner, D.P., Warner, E.D., Petersen, G.W., Seufert, G., Cook, R., 2006. Validation of global moderate-resolution LAI products: A framework proposed within the CEOS land product validation subgroup. IEEE Trans. Geosci. Remote Sens. 44, 1804–1814. https://doi.org/10.1109/TGRS.2006.872529

Myneni, R.B., Hoffman, S., Knyazikhin, Y., Privette, J.L., Glassy, J., Tian, Y., Wang, Y., Song, X., Zhang,

Y., Smith, G.R., Lotsch, A., Friedl, M., Morisette, J.T., Votava, P., Nemani, R.R., Running, S.W., 2002. Global products of vegetation leaf area and fraction absorbed PAR from year one of MODIS data. Remote Sens. Environ. 83, 214–231. https://doi.org/10.1016/S0034-4257(02)00074-3

Myneni, R.B., Williams, D.L., 1994. On the relationship between FAPAR and NDVI. Remote Sens. Environ. 49, 200–211. https://doi.org/10.1016/0034-4257(94)90016-7

Nestola, E., Sánchez-Zapero, J., Latorre, C., Mazzenga, F., Matteucci, G., Calfapietra, C., Camacho, F., 2017. Validation of PROBA-V GEOV1 and MODIS C5 & C6 fAPAR Products in a Deciduous Beech Forest Site in Italy. Remote Sens. 9, 126. https://doi.org/10.3390/rs9020126

Nilson, T., 1971. A theoretical analysis of the frequency of gaps in plant stands. Agric. Meteorol. 8, 25–38. https://doi.org/10.1016/0002-1571(71)90092-6

Pinty, B., Lavergne, T., Dickinson, R.E., Widlowski, J.-L., Gobron, N., Verstraete, M.M., 2006. Simplifying the interaction of land surfaces with radiation for relating remote sensing products to climate models. J. Geophys. Res. 111, D02116. https://doi.org/10.1029/2005JD005952

Redelsperger, J.L., Thorncroft, C.D., Diedhiou, A., Lebel, T., Parker, D.J., Polcher, J., 2006. African Monsoon Multidisciplinary Analysis: An International Research Project and Field Campaign. Bull. Am. Meteorol. Soc. 87, 1739–1746. https://doi.org/10.1175/BAMS-87-12-1739

Ross, J., 1981. The radiation regime and architecture of plant stands, The radiation regime and architecture of plant stands. Springer Netherlands. https://doi.org/10.1007/978-94-009-8647-3

Sánchez-Zapero, J., Camacho, F., Martínez-Sánchez, E., Lacaze, R., Carrer, D., Pinault, F., Benhadj, I., Muñoz-Sabater, J., 2020. Quality Assessment of PROBA-V Surface Albedo V1 for the Continuity of the Copernicus Climate Change Service. Remote Sens. 2020, Vol. 12, Page 2596 12, 2596. https://doi.org/10.3390/rs12162596

Sánchez-Zapero, J., Martínez-Sánchez, E., Camacho, F., Wang, Z., Carrer, D., Schaaf, C., García-Haro, F.J., Nickeson, J., Cosh, M., 2023. Surface ALbedo VALidation (SALVAL) Platform: Towards CEOS LPV Validation Stage — Application to Three Global Albedo Climate Data Records. Remote Sens. 2023, Vol. 15, Page 1081 15, 1081. https://doi.org/10.3390/RS15041081

Skiles, S.M.K., Painter, T.H., 2019. Toward Understanding Direct Absorption and Grain Size Feedbacks by Dust Radiative Forcing in Snow With Coupled Snow Physical and Radiative Transfer Modeling. Water Resour. Res. 55, 7362–7378. https://doi.org/10.1029/2018WR024573

Song, B., Liu, L., Du, S., Zhang, X., Chen, X., Zhang, H., 2021. ValLAI_Crop, a validation dataset for coarse-resolution satellite LAI products over Chinese cropland. Sci. Data 2021 81 8, 1–16. https://doi.org/10.1038/s41597-021-01024-4

Verger, A., Baret, F., Weiss, M., 2008. Performances of neural networks for deriving LAI estimates from existing CYCLOPES and MODIS products. Remote Sens. Environ. 112, 2789–2803. https://doi.org/10.1016/j.rse.2008.01.006

Verger, A., Baret, F., Weiss, M., Kandasamy, S., Vermote, E., 2013. The CACAO method for smoothing, gap filling, and characterizing seasonal anomalies in satellite time series. IEEE Trans. Geosci. Remote Sens. 51, 1963–1972. https://doi.org/10.1109/TGRS.2012.2228653

Verger, A., Sánchez-Zapero, J., Weiss, M., Descals, A., Camacho, F., Lacaze, R., Baret, F., 2023. GEOV2: Improved smoothed and gap filled time series of LAI, FAPAR and FCover 1 km Copernicus Global Land products. Int. J. Appl. Earth Obs. Geoinf. 123, 103479. https://doi.org/10.1016/J.JAG.2023.103479

Verhoef, W., Jia, L., Xiao, Q., Su, Z., 2007. Unified optical-thermal four-stream radiative transfer theory for homogeneous vegetation canopies. IEEE Trans. Geosci. Remote Sens. 45, 1808–1822. https://doi.org/10.1109/TGRS.2007.895844

Wang, Y., Tian, Y., Zhang, Y., El-Saleous, N., Knyazikhin, Y., Vermote, E., Myneni, R.B., 2001. Investigation of product accuracy as a function of input and model uncertainties: Case study with SeaWiFs and MODIS LAI/FPAR algorithm. Remote Sens. Environ. 78, 299–313. https://doi.org/10.1016/S0034-4257(01)00225-5

Wang, Z., Schaaf, C., Lattanzio, A., Carrer, D., Grant, I., Roman, M., Camacho, F., Yang, Y., Sánchez-Zapero, J., 2019. Global Surface Albedo Product Validation Best Practices Protocol. Version 1.0.

In Z. Wang, J. Nickeson & M. Román (Eds.), Good Practices for Satellite-Derived Land Product Validation (p. 45): Land Product Validation Subgroup (WGCV/CEOS). [WWW Document]. https://doi.org/doi: 10.5067/DOC/CEOSWGCV/LPV/ALBEDO.001

Weiss, M., Baret, F., Block, T., Koetz, B., Burini, A., Scholze, B., Lecharpentier, P., Brockmann, C., Fernandes, R., Plummer, S., Myneni, R., Gobron, N., Nightingale, J., Schaepman-Strub, G., Camacho, F., Sanchez-Azofeifa, A., 2014. On line validation exercise (OLIVE): A web based service for the validation of medium resolution land products. application to FAPAR products. Remote Sens. 6, 4190–4216. https://doi.org/10.3390/rs6054190

Weiss, M., Baret, F., Garrigues, S., Lacaze, R., 2007. LAI and fAPAR CYCLOPES global products derived from VEGETATION. Part 2: validation and comparison with MODIS collection 4 products. Remote Sens. Environ. 110, 317–331. https://doi.org/10.1016/j.rse.2007.03.001

Wilson, J.W., 1963. Estimation of foliage denseness and foliage angle by inclined point quadrats. Aust. J. Bot. 11, 95–105. https://doi.org/10.1071/BT9630095

Xu, B., Park, T., Yan, K., Chen, C., Zeng, Y., Song, W., Yin, G., Li, J., Liu, Q., Knyazikhin, Y., Myneni, R., 2018. Analysis of Global LAI/FPAR Products from VIIRS and MODIS Sensors for Spatio-Temporal Consistency and Uncertainty from 2012–2016. Forests 9, 73. https://doi.org/10.3390/f9020073

Yan, K., Park, T., Chen, C., Xu, B., Song, W., Yang, B., Zeng, Y., Liu, Z., Yan, G., Knyazikhin, Y., Myneni, R.B., 2018. Generating global products of LAI and FPAR from SNPP-VIIRS data: Theoretical background and implementation. IEEE Trans. Geosci. Remote Sens. 56, 2119–2137. https://doi.org/10.1109/TGRS.2017.2775247

Yan, K., Park, T., Yan, G., Chen, C., Yang, B., Liu, Z., Nemani, R., Knyazikhin, Y., Myneni, R., 2016a. Evaluation of MODIS LAI/FPAR Product Collection 6. Part 1: Consistency and Improvements. Remote Sens. 8, 359. https://doi.org/10.3390/rs8050359

Yan, K., Park, T., Yan, G., Liu, Z., Yang, B., Chen, C., Nemani, R., Knyazikhin, Y., Myneni, R., 2016b. Evaluation of MODIS LAI/FPAR Product Collection 6. Part 2: Validation and Intercomparison. Remote Sens. 8, 460. https://doi.org/10.3390/rs8060460

Yang, W., Huang, D., Tan, B., Stroeve, J.C., Shabanov, N. V., Knyazikhin, Y., Nemani, R.R., Myneni, R.B., 2006. Analysis of leaf area index and fraction of PAR absorbed by vegetation products from the terra MODIS sensor: 2000-2005. IEEE Trans. Geosci. Remote Sens. 44, 1829–1841. https://doi.org/10.1109/TGRS.2006.871214

Annex I: Scatterplots between VP_CCI and CGLS V2 per biome

LAI

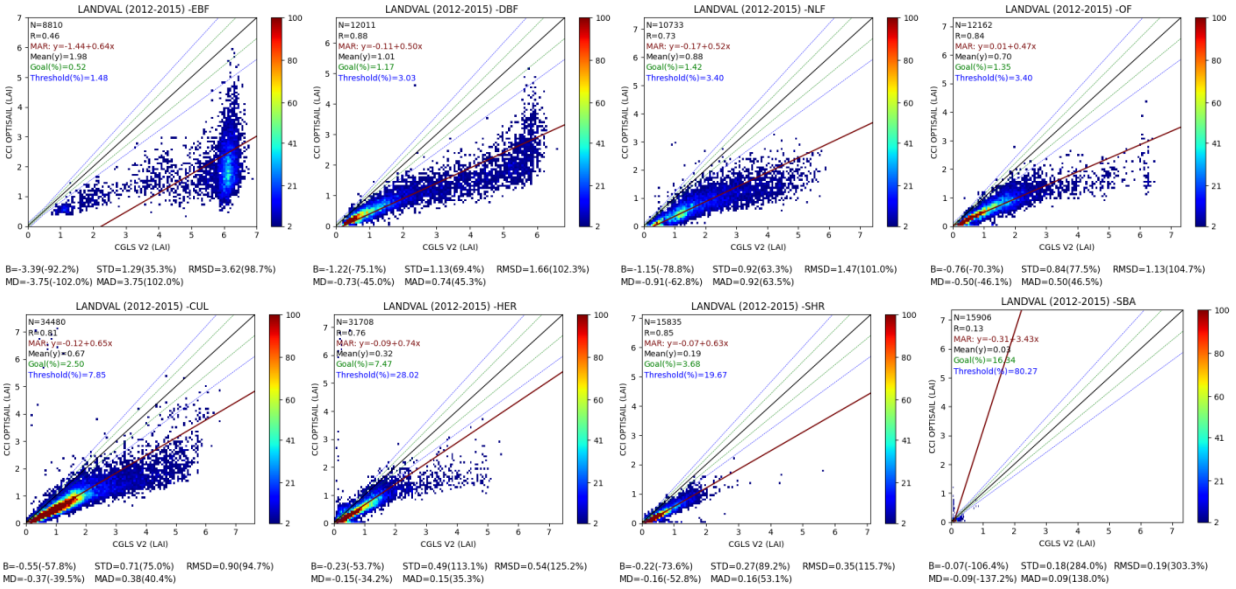

fAPAR

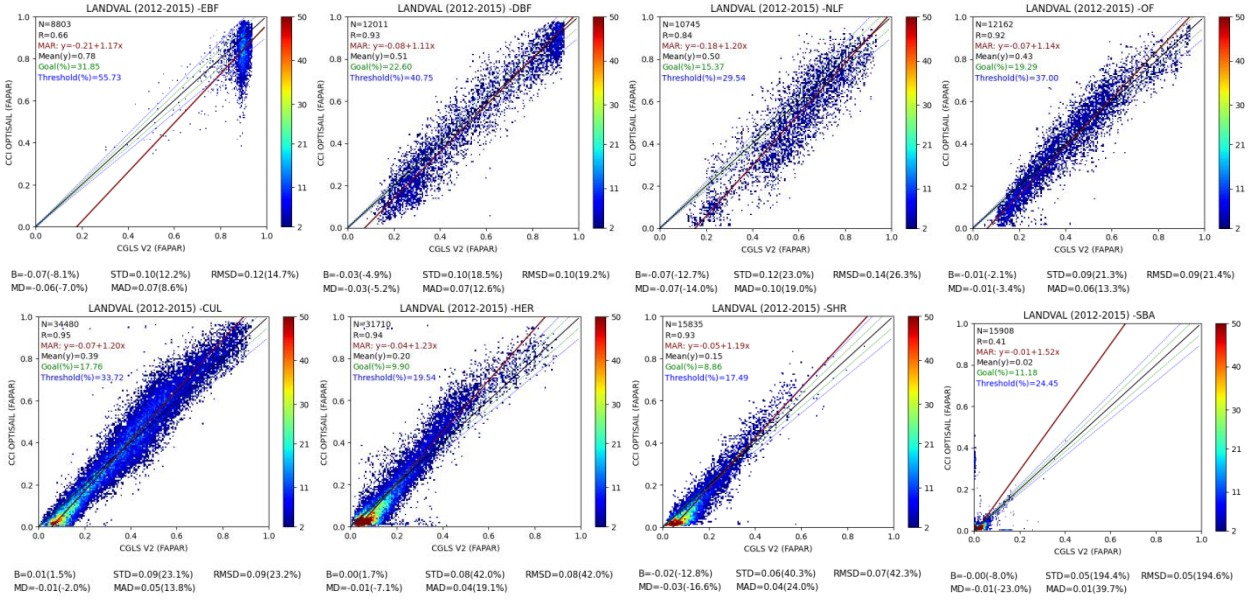

Annex II: Scatterplots between OPTISAIL and VNP15A2H C1 per biome

LAI

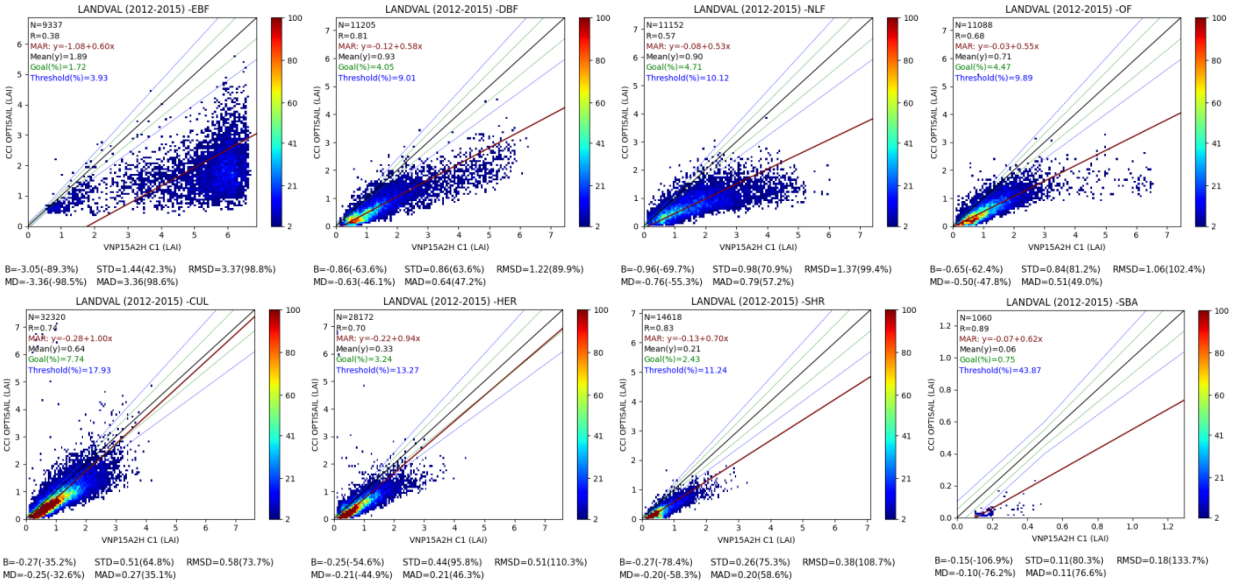

fAPAR